UNIVERSITY OF CALIFORNIA SAN DIEGO

Regulation of $CD8^+$ T Lymphocyte Fate Specification by the lncRNA Malat1

A dissertation submitted in partial satisfaction of the requirements

for the degree Doctor of Philosophy

in

Biomedical Sciences

by

Jad Nabih Kanbar

Committee in charge:

Professor John Chang, Chair
Professor Ananda Goldrath
Professor Stephen Hedrick
Professor Wendy Huang
Professor Gene Yeo

2022

The Dissertation of Jad Nabih Kanbar is approved, and it is acceptable in quality and form for publication on microfilm and electronically.

University of California San Diego

2022

DEDICATION

To my wife, son, mom, dad, brother, and that one there is my other brother

EPIGRAPH

DNA, you know, is Midas' gold. Everyone who touches it goes mad.

Maurice Wilkins

TABLE OF CONTENTS

DISSERTATION APPROVAL PAGE……..……..……..…..iii

TABLE OF CONTENTS…….……..……...……vi

LIST OF ABBREVIATIONS…….……..…..……..…vii

LIST OF FIGURES…….viii

ACKNOWLEDGEMENTS……...ix

VITA……..xii

ABSTRACT OF THE DISSERTATION……...xiii

INTRODUCTION……..…1

CHAPTER 1: MALAT1 LNCRNA REGULATES $CD8^+$ T CELL DIFFERENTIATION…….....8

CHAPTER 2: MALAT1 INTERACTS WITH EZH2 TO MAINTAIN H3K27ME3 DEPOSITION ON MEMORY-ASSOCIATED GENES…….……31

CHAPTER 3: CONCLUSIONS……....50

APPENDIX A: MATERIALS AND METHODS…….……...54

APPENDIX B: SUPPLEMENTAL TABLES……..……67

REFERENCES……89

LIST OF ABBREVIATIONS

ChIP-seq	Chromatin immunoprecipitation sequencing
FACS	Fluorescence activated cell sorting
gMFI	Geometric mean fluorescence intensity
GO	Gene Ontology
GRID-seq	Global RNA Interactions with DNA by Deep sequencing
LCMV-Arm	Lymphocytic choriomeningitis-Armstrong
lncRNA	long noncoding RNA
$Malat1^{KD}$	Malat1 knockdown shRNA
MP	Memory Precursor
NT	non-target shRNA
PCA	Principal Component Analysis
RNA-seq	RNA sequencing
S.E.M.	Standard error of the mean
shRNA	Short hairpin RNA
siIEL	Small Intestine Intraepithelial
T_{CM}	T central memory
T_{EM}	T effector memory
t-T_{EM}	terminal-T effector memory
TE	Terminal Effector
t-SNE	t-distributed stochastic neighbor embedding
UMAP	uniform manifold approximation and projection
WGCNA	Weighted gene co-expression network analyses

LIST OF FIGURES

Figure 1.1 in vivo shRNA screen reveals lncRNA Malat1 as critical regulator of $CD8^+$ T cell differentiation……..……..20

Figure 1.2 lncRNA Malat1 regulates effector $CD8^+$ T cell differention……..……..…21

Figure 1.3 lncRNA Malat1 regulates early effector $CD8^+$ T cell differention……..…..22

Figure 1.4 Transcription factors associated with memory differention are upregulated in $KLRG1^{hi}$ effector cells…….…...24

Figure 1.5 lncRNA Malat1 regulates memory $CD8^+$ T cell differention…….……...25

Figure 1.6 lncRNA Malat1 knockdown reduces siIEL T_{RM} cell differention……26

Figure 1.7 Single-Cell RNA-seq reveals that Malat1 depletion upregulates memory associated factors…….....27

Figure 1.8 WGCNA reveals distinct gene modules differentially regulated by Malat1……...…29

Figure 1.9 Malat1 represses generation of secondary T_{EM} cells……..……30

Figure 2.1 Replicate GRID-seq libraries generated reproducible RNA chromatin interaction patterns……..……...…40

Figure 2.2 lncRNAs in activated $CD8^+$ T cells are a substational portion of all RNA chromatin interactions……...…….41

Figure 2.3 Malat1 clusters with *trans* lncRNAs that focus chromatin interactions on gene promoters and gene bodies……...……..…..42

Figure 2.4 Malat1 enriches on chromatin marked by the epigentic repressive histone mark H3K27me3…….……44

Figure 2.5 Malat1 preferentially interacts on genes assoicated with memory differentiation…….....46

Figure 2.6 Malat1 maintain H3K27me3 deposition on memory-associated genes……..….....47

Figure 2.7 Malat1 interacts with Ezh2 to maintain H3K27me3 deposition……...…49

ACKNOWLEDGMENTS

I would like to acknowledge first my mentor John T. Chang for his guidance, support, patience, and encouragement as I cleared hurdles along the way in graduate school. John always had my best interest in mind and if I ever needed any help on any matter, he was always there to provide it. My time under John has taught me how to think critically about my work and how to effectively use my time to achieve the goals. I am forever fortunate that John took me in his lab when I needed a fresh start at the start of graduate school. It has been an incredibly fulfilling time.

I would like to thank various members of the Chang Lab. Chistella Widjaja helped get me started with mouse work and techniques I would need to study the immune system. Jane Klann for being generous with her time showing me how to dissect mice and properly compensate samples for flow. Daniel Garcia and Nadia Kurd for letting me bounce ideas off them no matter how off course I might have gotten with them. Lab managers Justine Lopez, Tiffani Tysl, and Cynthia Indralingam for seemingly always having reagents and mice ready the day of experiment like magicians. Matthew Tsai, Brigid Boland, Jocelyn Olvera, Lauren Quezada, Tiani Louis, Paul Hsu, Elena Lim, Eleanor Kim, Han Duong, Abigail Limary Shefai Patel, and William Wong for helpful discussions, commraderie, and lots of troubleshooting.

I would like to thank my committee Dr. Ananda Goldrath, Dr. Stephen Hedrick, Dr. Gene Yeo, and Dr. Wendy Huang for helpful feedback, support, and the positivity I needed to keep making strides in graduate school to finish. I lucked out with a great committee.

I would like to thank Zhaoren He, Brian Yee, and Yajing Hao for help with all things computational. Their interest and expertise in teaching me how to analyze my datasets helped transform my project.

I would like to thank past mentors Dr. Yishi Jin, my undergraduate mentor that let me in her lab many years ago because I did not want to let go of a project I had started in her upper division genetics lab course. It was with that opportunity, guidance and support I was able to pursue science as career. And I would like to thank Dr. Stephen Quake where I spent several years working on cutting edge work with the most talented people I had ever met. It was like drinking out of a fire hose and loved every minute.

Lastly, I would like to thank my family starting with my wife Alicia Kanbar. When we met, I was a technician trying to get my graduate applications in order. With your help I buckled down, got into graduate school, got in my thesis lab, and got my Ph.D. Along the way we married and had a beautiful son that has made the last years of graduate school both a challenge and the best distraction. To my parents Hiam and Nabih Kanbar that from my first day in undergrad till today always believed that I could do this. My parents are my foundation and they never let me give up. Lastly to Al and Arminda Grosnick that were just as supportive and helpful as my own parents with my journey in graduate school. It takes many people to finish this endeavor and family provides unending support that is so important when times get hard.

Chapters and 1 and 2, in full, are adapted version of the material that has been submitted for publication. Jad N. Kanbar, Shengyun Ma, Nadia S. Kurd, Matthew S. Tsai, Tiffani Tysl, Christella E. Widjaja, Eleanor S. Kim, Abigail E. Limary, Brian Yee, Zhaoren He, Yajing Hao, Xiang-Dong Fu, Gene Yeo, Wendy J. Huang, John T. Chang

(2022). The long noncoding RNA Malat1 regulates $CD8^+$ T cell differentiation by mediating epigenetic repression. In revision. The dissertation was the primary author of all material.

VITA

2007 B.S., Neuroscience and Behaviour, University of California Santa Cruz

2012 M.S., Biomedical Engineering, Cal Poly San Luis Obispo

2022 Ph.D., Biomedical Sciences, University of California San Diego

ABSTRACT OF THE DISSERTATION

Regulation of $CD8^+$ T Lymphocyte Fate Specification by the lncRNA Malat1

by

Jad Nabih Kanbar

Doctor of Philosophy in Biomedical Sciences

University of California San Diego 2022

Professor John T. Chang, Chair

During an immune response to microbial infection, $CD8^+$ T cells give rise to short-lived effector cells and memory cells that provide long-lived protection. Although the transcriptional programs regulating $CD8^+$ T cell differentiation have been extensively characterized, the role of long noncoding RNAs (lncRNAs) in this process remains poorly understood. Using a functional genetic knockdown screen, we identified the

lncRNA Malat1 as a regulator of terminal effector cells and the terminal effector memory (t-T_{EM}) subset of circulating memory $CD8^+$ T cells. Evaluation of chromatin-enriched lncRNAs revealed that Malat1 clustered with *trans* lncRNAs that exhibit increased RNA interactions at gene promoters and gene bodies. Moreover, we observed that Malat1 is associated with increased H3K27me3 deposition at a number of memory cell-associated genes through a direct interaction with Ezh2, thereby promoting terminal effector and t-T_{EM} cell differentiation. Our findings suggest an important functional role of MALAT1 in regulating $CD8^+$ T cell differentiation and broaden the knowledge base of lncRNAs in $CD8^+$ T cell biology.

INTRODUCTION

The $CD8^+$ *T Cell Response and Differentiation to Microbial Infection*

Naive antigen-specific $CD8^+$ T cells are part of the adaptive branch of the immune system that have completed development in the thymus. Once a naive $CD8^+$ T cell has recognized its cognate antigen, an acute response to a foreign antigen or microbial infection follows a distinct pattern of response. For full activation, a $CD8^+$ T cell must be presented with three distinct signals. The initial interaction between the antigen-specific T cell and antigen presenting cell (APC) provides the first (signal 1). A co-stimulatory signal through the CD28 receptor which interacts with CD80 (B7.1) and CD81 (B7.2) on APCs provides the second (signal 2). Lastly, pro-inflammatory cytokines such as IL-12 and type I interferons (IFNs) enhance expansion of $CD8^+$ T cells (signal 3). $CD8^+$ T cells then rapidly expand, acquire anti-microbial effector function, and produce cytokines. Lastly, $CD8^+$ T cells migrate to sites of infection and clear pathogen-infected cells providing cell mediated immunity.

Following viral clearance, $CD8^+$ T cells begin to contract and the majority die via apoptosis, however approximately 5-10% survive to mature long-lived protective memory $CD8^+$ T (Joshi et al., 2007). Long-lived memory cells survive in the absence of antigen stimulation through homeostatic proliferation and by receiving interleukin-7 and interleukin-15 (Kaech and Wherry, 2007). Memory cells are then maintained in a poised multipotent state to provide immunity against secondary encounters. The differentiation pathways that govern immunological memory have significant implications in the effective design of vaccines. Heterogeneity exists within the memory subset that include

conventional effector memory (T_{EM}), terminal-Effector Memory (t- T_{EM}), central memory (T_{CM}), and resident memory (T_{RM}) cells. T_{EM} are characterized through low expression of CD62L, recirculate in the blood, localize to non-lymphoid structures, and provide immediate effector function upon antigen rechallenge. t- T_{EM} compared to T_{EM} have reduced proliferative potential but more robust cytotoxicity on a per cell basis (Milner et al., 2020; Renkema et al., 2020). T_{CM} are characterized by higher expression of CD62L, home to secondary lymphoid structures, and can rapidly proliferate upon antigen rechallenge, and can provide robust protection against chronic infections and malignant cancers (Klebanoff et al., 2005; Nolz and Harty, 2011). Lastly, T_{RM} have low expression of CD62L, do not circulate, and localize to peripheral organs and tissues including liver, lung, gut, and brain (Mueller and Mackay, 2015).

An ongoing question in the field is how does functional heterogeneity in activated $CD8^+$ T cells arise from a single naive activated $CD8^+$ T lymphocyte? Phenotypic surface markers have been used to distinguish terminal effector cells and memory precursor cells during later stages of infection. These include KLRG1 (killer cell lectin-like receptor subfamily G, member 1, KLRG1), and IL-7R (interleukin-7 receptor, CD127), where $KLRG1^{hi}IL\text{-}7R^{lo}$ and $KLRG1^{lo}IL\text{-}7R^{hi}$ subsets distinguish terminal effector and putative memory precursors respectively (Joshi et al., 2007). However, these markers themselves do not always predict functional capacity of these populations. Recent work using fate mapping strategies demonstrated that a subset of $KLRG1^{hi}$ cells lose expression of KLRG1 (ex-KLRG1 cells) during the contraction phase and differentiative into T_{EM} and T_{CM} cells (Herndler-Brandstetter et al., 2018). Additionally, a $KLRG1^{hi}$ effector population remains into memory with characteristic features of memory

cells forming t-T_{EM} cells (Milner et al., 2020; Renkema et al., 2020). This underscores the importance of finding alternative phenotypic and functional markers that help distinguish early fate decisions in the immune response. Single-cell analysis has been instrumental in helping reveal cell-to-cell differences through gene expression in an unbiased way.

To this end prior work in our lab demonstrated that following acute infection, $CD8^+$ T cells that have undergone their first division cluster into two populations that may be precursors to the terminal effector vs. memory fates, which we term Div_{TE} and Div_{MEM} cells (Kakaradov et al., 2017). Early transcriptional burst featured key genes that promoted effector and memory fates, including upregulation of the chromatin regulator Ezh2, the catalytic subunit of the polycomb repressive complex 2 (Prc2). Furthermore, prior research has characterized critical regulators of $CD8^+$ T cell differentiation, with transcription factors *T-bet*, *Blimp1*, *Zeb2*, and Id2 promoting the formation of effector cells, and *Tcf7*, *Eomes*, Foxo1, and *Id3* regulating memory cell formation (Joshi et al., 2007; Kallies et al., 2009; Omilusik et al., 2015, 2018; Zhou and Xue, 2012; Banerjee et al., 2010; Michelini et al., 2013; Ji et al., 2011). However, the role of other potential mechanisms regulating $CD8^+$ T cell differentiation, such as DNA methylation, post-translational modifications, and noncoding RNAs, remain poorly understood.

The role of lncRNAs in $CD8^+$ *T cell differentiation*

Upon the completion of the human genome project a surprising finding was only ~2% coded for proteins, leaving much of the genome noncoding (Kopp and Mendell, 2018). The advent of next generation (NGS) sequencing technologies has revealed pervasive transcription with estimates of up to 75% of the human genome transcribed.

The list of long non-coding RNAs (lncRNAs), a class of pervasively transcribed noncoding molecules keeps growing with every new genome annotation, and as of 2019, there were 29,566 lncRNA transcripts documented compared to 19,940 protein coding transcripts (Hadjicharalambous and Lindsay, 2019). lncRNAs are a class of RNA molecules longer than 200 base pairs that are not translated into protein, but are transcribed by RNA Polymerase II, capped at the 5' end, and polyadenylated (Kopp and Mendell, 2018). Generally, except for a few exceptions, lncRNAs are transcribed at lower copy numbers than protein coding genes but are highly cell type and differentiation state specific (Plasek and Valadkhan, 2021). Loss or gain of function of lncRNAs have been shown to disrupt cellular processes, development, and disease projection (Rinn et al., 2020). Broadly their function can be characterized by the nature of their genomic interactions either close to their site of transcription (in *cis*) or distally (in *trans*) to other genomic locations (Morrison et al., 2021). The low copy numbers of lncRNAs favor a model of *cis* lncRNA regulating gene expression of their nearby genes (Wilusz et al., 2009). On the other hand, *trans* lncRNAs are generally expressed higher and play a role in transcriptional regulation by influencing nuclear structure and organization.

It has been estimated in mouse and human $CD8^+$ T cells that 25% of the transcriptome encodes for lncRNAs (Hudson et al., 2019). To date, few lncRNAs have been functionally characterized in $CD8^+$ T cells despite published observations that lncRNA expression profiles can distinguish naive, effector, and memory subsets, suggesting that lncRNAs may play important roles in $CD8^+$ T cell fate decisions (Hudson et al., 2019; Kotzin et al., 2019; Wang et al., 2015; Sharma et al., 2011). Analyses of

various subtypes of human lymphocytes including $CD4^+$ and $CD8^+$ T cells naïve, effector, and memory cells demonstrated that 73% of the 4,764 lncRNAs detected could uniquely cluster each cell type (Ranzani et al., 2015). Using lncRNAs to cluster each human lymphocyte populations was more cell type specific than using protein coding genes alone where only 31% of the 15,911 protein coding genes could unbiasedly cluster $CD4^+$ and $CD8^+$ T cells (Ranzani et al., 2015). In mouse and human $CD8^+$ T cells responding to acute infections, LCMV and Yellow fever vaccine respectively, ~800 overlapping lncRNAs were differentially expressed from naïve to memory differentiation, highlighting homologous roles for lncRNAs in $CD8^+$ T cell differentiation (Hudson et al., 2019). This underscores the importance in studying this class of molecules in $CD8^+$ T cells in the context of microbial infection. NeST, one of the first identified lncRNA in T cells, was shown to promote expression of *Ifnγ* through an interaction of the MLL/SET1 H3K4 Methylase Complex, thereby conferring resistance to *Salmonella* (Gomez et al., 2013). The lncRNA244, through its interactions with Ezh2, epigenetically represses IFNγ and TNFα, leading to $CD8^+$ T cell dysfunction and increased susceptibility to *Mycobacterium tuberculosis* infection (Wang et al., 2015). In LCMV infection, the lncRNA Morrbid was specifically induced following Type 1 IFNγ stimulation, which in turn promoted the expression of the proapoptotic factor *Bcl2l1*, thereby negatively regulating $CD8^+$ T cell expansion (Kotzin et al., 2019).

Our previous work raised the possibility that the lncRNA Malat1 might be involved in $CD8^+$ T cell differentiation in response to acute infection (Kakaradov et al., 2017). Malat1 was first identified in a screen for markers of early-stage non-small cell lung cancer (NSCLC) metastasis, with mutations in Malat1 and transcriptional

dysregulation subsequently confirmed in various cancer types (Ji et al., 2003; Kim et al., 2018; Gutschner et al., 2013). Malat1 localizes to nuclear speckles which sequester various proteins involved in RNA processing, transcription, and epigenetic regulation (Spector and Lamond, 2011). Nuclear speckles also contain a high density of RNA Polymerase II that associates with multiple DNA regions forming inter-chromosomal contacts at sites of active transcription (West et al., 2014; Quinodoz et al., 2018). In germline knockout models, Malat1 has been shown to be dispensable for normal mouse development and physiology (Zhang et al., 2012; Eißmann et al., 2012; Nakagawa et al., 2012; Yao et al., 2018). By contrast, acute knockdown of Malat1 has resulted in significant functional changes affecting cellular proliferation, motility, and differentiation (Tripathi et al., 2010; Tano et al., 2010; Bernard et al., 2010), suggesting that genetic and acute knockdown models may yield disparate phenotypes.

In this dissertation, we performed a functional genetic knockdown screen that suggested Malat1 as a regulator of $CD8^+$ T cell differentiation. Malat1 knockdown significantly reduced terminal effector cell differentiation at the peak of infection and t-T_{EM} memory cell formation by 30 days post-infection. Analyses of secondary recall immune responses revealed that t-T_{EM} cells were not dependent on Malat1 to give rise to secondary t-T_{EM} cells; by contrast, T_{EM} and T_{CM} cells were dependent on Malat1 to give rise to secondary t-T_{EM} and T_{EM} cells. Malat1 knockdown resulted in increased expression of a number of memory cell-associated. Examination of chromatin interactions with Malat1 revealed significant enrichment at gene promoters and gene bodies indicating an active role in transcription; furthermore, Malat1-interacting regions were correlated with a selective accumulation of the epigenetic repressive mark

H3K27me3 compared to the epigenetic activation marks H3K4me3, H3K4me1, and H3K27ac. Malat1, in part through an interaction with Ezh2, significantly increased H3K27me3 deposition on many genes associated with memory cell differentiation. Together, these findings suggest an important functional role of Malat1 in promoting terminal differentiation in $CD8^+$ T cells and broaden the knowledge base of lncRNAs in $CD8^+$ T cell biology.

CHAPTER 1: MALAT1 LNCRNA REGULATES CD8$^+$ T CELL DIFFERENTIATION

1.1: Introduction

The role of other potential mechanisms regulating CD8$^+$ T cell differentiation, such as DNA methylation, post-translational modifications, and noncoding RNAs, remain poorly understood. Our previous work raised the possibility that the lncRNA Malat1 might be involved in CD8$^+$ T cell differentiation in response to acute infection (Kakaradov et al., 2017). To date, few lncRNAs have been functionally characterized in CD8$^+$ T cells despite published observations that lncRNA expression profiles can distinguish naive, effector, and memory subsets, suggesting that lncRNAs may play important roles in CD8$^+$ T cell fate decisions (Hudson et al., 2019; Kotzin et al., 2019; Wang et al., 2015; Sharma et al., 2011). In this chapter we performed a functional genetic knockdown screen that suggested Malat1 as a regulator of CD8$^+$ T cell differentiation. We validated and characterized the phenotypic role of Malat1 in response to acute infection and in a rechallenge context. We highlighted phenotypic differences in effector and memory CD8$^+$ T cell subsets as result of Malat1 depletion by utilizing protein and gene expression data. We conclude that Malat1 governs a regulatory role in CD8$^+$ T cells, and depletion of Malat1 has important functional consequences in effector differentiation.

1.2: Results

1.2.1: In vivo functional genetic knockdown screen reveals the lncRNA Malat1 as a regulator of CD8$^+$ *T cell differentiation*

We previously observed a striking transcriptional divergence among $CD8^+$ T cells that had undergone their first division in response to viral infection and identified a number of putative regulators of $CD8^+$ T cell differentiation (Kakaradov et al., 2017). We therefore conducted a pooled shRNA screen of 365 shRNAs against 102 of these gene targets in order to assess their possible functional significance (**Fig. 1.1 A),** using a previously published approach (Chen et al., 2014; Milner et al., 2017). We transduced P14 $CD8^+$ $CD45.1^+$ T cells, which have transgenic expression of a T cell receptor (TCR) recognizing an immunodominant epitope of lymphocytic choriomeningitis virus (LCMV), with a pool of shRNA retroviruses. These cells were adoptively transferred into congenic CD45.2+ wild-type mice that were subsequently infected with the Armstrong strain of LCMV. At day 7 post-infection, terminal effector ("TE," $KLRG1^{hi}CD127^{lo}$) and memory precursor ("MP," $KLRG1^{lo}CD127^{hi}$) $CD8^+$ T cells were isolated by FACS (fluorescence-activated cell sorting). Non-targeting shRNAs were included as a negative control and shRNAs targeting *Tbx21*, the gene encoding the T-box transcription factor T-bet, were included as positive controls (**Supplementary Table 1).** Using a Z-score cutoff of $\pm$ 3, three Malat1 shRNAs were observed to be differentially enriched in $KLRG1^{lo}CD127^{hi}$ MP cells compared to $KLRG1^{hi}CD127^{lo}$ TE cells (**Fig. 1.1 B**). The knockdown efficiencies of each Malat1 shRNA were verified using multiple qPCR primers tiling the Malat1 locus with 83.1%, 69.4%, and 82.2% average knockdown (**Fig. 1.1 B**). Taken together, we identified three Malat1 shRNAs with effective knockdown to assess the role of Malat1 in $CD8^+$ T cell differentiation.

1.2.2: lncRNA Malat1 is a critical regulator of $CD8^+$ *TE differentiation*

We next evaluated the functional consequences of Malat1 knockdown during $CD8^+$ T cell differentiation. Congenically distinct P14 $CD8^+$ T cells were transduced with Malat1 shRNA (*Malat1^{KD}*, CD45.1) or Nontarget shRNA (*NT*, CD45.1.2) and adoptively co-transferred into CD45.2 recipient mice (**Fig. 1.2 A**). At day 7 after infection, *Malat1^{KD}* cells showed a marked numerical decrease as compared to *NT* cells (**Fig. 1.2 B, D, and F**). Moreover, *Malat1^{KD}* TE cells were decreased relative to *NT* TE cells, whereas *Malat1^{KD}* MP cells were increased relative to *NT* MP cells (**Fig. 1.2 C, E and G**). Relative to control cells, *Malat1^{KD}* TE cells exhibited decreased expression of KLRG1 and CX3CR1, phenotypic markers associated with terminal effector cells, whereas *Malat1^{KD}* MP cells exhibited increased expression of CD127 and CD27, phenotypic markers associated with memory cells (**Fig. 1.2 H**). Taken together, Malat1 knockdown dramatically decreases TE cells in response to infection.

1.2.3: lncRNA Malat1 regulates early effector $CD8^+$ *T cell differentiation*

Given the observed numerical deficiency of *Malat1^{KD}* $CD8^+$ T cells, we next sought to assess if Malat1 impaired effector differentiation before day 7 of infection. Congenically distinct P14 $CD8^+$ T cells were transduced with Malat1 shRNA (*Malat1^{KD}*, CD45.1) or Nontarget shRNA (*NT*, CD45.1.2) and adoptively co-transferred into CD45.2 recipient mice and evaluated on days 3, 5, and 7 after infection (**Fig. 1.3 A).** On day 3 after infection, there were equivalent numbers of *Malat1^{KD}* and *NT* cells, however by days 5 and 7 *Malat1^{KD}* cells showed a marked numerical decrease (**Fig. 1.3 B**). Characterizing TE differentiation on the basis of KLRG1 expression demonstrated that as early as day 3, $KLRG1^{hi}$ *Malat1^{KD}* cells were proportionally and numerically reduced,

with a corresponding increase in KLRG1^{lo} *Malat1^{KD}* cells (**Fig 1.3 C-E**). Additionally, assessing CX3CR1 expression, a marker that delineates degree of TE differentiation, revealed that CX3CR1^{hi}KLRG1^{hi} *Malat1^{KD}* cells were dramatically reduced compared to CX3CR1^{lo}KLRG1^{lo} *Malat1^{KD}* cells. Taken together, as early as day 3 after infection Malat1 depletion impacted cellular differentiation resulting in a specific numerical reduction of TE cells.

KLRG1^{hi} and KLRG1^{lo} *Malat1^{KD}* and *NT* cells exhibited similar expression of the proliferation marker Ki-67, suggesting that Malat1 knockdown did not affect proliferation several days after T cell activation (**Fig. 1.3 I**). However, expression for the membrane-bound apoptotic marker Annexin V was increased only in KLRG1^{hi} *Malat1^{KD}* cells at both days 5 and 7 suggesting the numerical deficiency observed in KLRG1^{hi} *Malat1^{KD}* cells may be partly attributed to an increased frequency of apoptotic cells. Lastly, functional characterization demonstrated *Malat1^{KD}* cells expressed more IL-2 promoting homeostatic proliferation; however, *Malat1^{KD}* and *NT* cells were similarly polyfunctional with equivalent frequencies of IFNγ^{hi}TNFα^{hi} cells (**Fig. 1.3 H**).

Flow cytometry analyses on days 5 and 7 demonstrated distinct expression levels of known determinants of CD8^{+} T cell differentiation in KLRG1^{hi} and KLRG1^{lo} *Malat1^{KD}* cells. Determinants of memory differentiation *Eomes*, *Tcf7*, *Zeb1*, *Lef1*, *Foxo1*, and *Bcl2* were consistently upregulated only in *Malat1^{KD}* KLRG1^{hi} cells, while determinants of terminal effector differentiation *Tbx21*, *Id2*, *Gzma* were consistently downregulated in KLRG1^{hi} *Malat1^{KD}* cells and unchanged in KLRG1^{lo} *Malat1^{KD}* cells (**Fig 1.4**). Interestingly *Gzmb* expression level was upregulated only in KLRG1^{hi} *Malat1^{KD}* cells, in line with our pooled shRNA screen observation that demonstrated *Gzmb*

knockdown led to enrichment of TE cells, suggesting a role for *Gzmb* in suppression of TE differentiation (**Fig 1.1 B**). Malat1 may play a role in suppressing levels of *Gzmb* promoting the differentiation of TE cells. Taken together, early after infection on day 3, total number of effector cells were equivalent between *Malat1*^{KD} and *NT* cells, however by days 5 and 7 there was a dramatic reduction in *Malat1*^{KD} cells with preferential impact on the differentiation of terminal effector cells.

1.2.4: lncRNA Malat1 is a critical regulator of CD8^{+} *t-*T_{EM} *differentiation*

Assessment of total circulating memory cells at 35 days after infection revealed decreased proportions of *Malat1*^{KD} cells compared to *NT* cells (**Fig. 1.5 A, C and E).** No changes were observed in the proportion or absolute number of *Malat1*^{KD} CD62L^{hi}CD127^{hi} T_{CM} cells. However, compared to control cells, the proportion and absolute number of *Malat1*^{KD} CD62L^{lo}CD127^{lo} (t-T_{EM}) cells were decreased, with a corresponding increase in the proportion, but not absolute number, of *Malat1*^{KD} CD62L^{lo}CD127^{hi} T_{EM} cells (**Fig. 1.5, B, D, and F**). Moreover, *Malat1*^{KD} t-T_{EM}, cells exhibited decreased expression of effector cell-associated markers KLRG1 and CX3CR1, along with increased expression of memory cell-associated markers CD127 and CD27 (**Fig 1.5 G**). Compared to control cells, *Malat1*^{KD} T_{EM} and T_{CM} cells also exhibited increased expression of CD127 and CD27 (**Fig 1.5 G**). In addition to effects on circulating memory subsets, knockdown of Malat1 resulted in a defect in tissue-resident memory cell differentiation. Compared to control cells at days 7 and 35 after infection, *Malat1*^{KD} CD8^{+} T cells were reduced in the small intestine epithelial (siIEL) compartment, both in terms of total cells as well as the proportion of CD69^{+}CD103^{+} cells

(**Fig. 1.6**). Taken together, these results demonstrate that Malat1 plays a critical role in the differentiation of effector and memory $CD8^+$ T cell subsets including dramatic reduction in t-T_{EM} upon depletion.

1.2.6: Single-cell RNA-seq analyses reveal that Malat1 depletion upregulates factors associated with memory cell differentiation

In order to begin to investigate the mechanisms underlying the role of Malat1 in $CD8^+$ T cell differentiation, we performed single-cell RNA-sequencing (scRNA-seq) of *Malat1^{KD}* and *NT* cells responding to viral infection. P14 $CD8^+$ T cells were transduced with Malat1 shRNA (*Malat1^{KD}*, CD45.1) or Nontarget shRNA (*NT*, CD45.1.2), adoptively co-transferred into CD45.2 recipient mice, and isolated at day 7 post-infection. Unsupervised t-distributed stochastic neighborhood embedding (tSNE) analysis revealed separation of the majority of *Malat1^{KD}* and *NT* cells (**Fig. 1.7 A**). Clustering analysis yielded three distinct clusters, with 76% of *Malat1^{KD}* cells in Cluster 0 and the remaining *Malat1^{KD}* cells distributed between Clusters 1 (10%) and 2 (14%) (**Fig. 1.7 B and C**). *NT* cells were distributed in nearly equal proportions among Clusters 0 (30%), 1 (37%), and 2 (33%).

Evaluating the transcriptional profile of each cluster revealed Cluster 1 *NT* cells expressed lowest levels of Klrg1, highest levels of Malat1 while enriching for the MP gene signature (**Fig. 1.7 F, G, H, and I**). In contrast, Clusters 0 and 2 *NT* cells expressed higher levels of Klrg1, lower levels of Malat1 and enrichment for the TE gene signature (**Fig. 1.7 D, E, F, H, and I**). We confirmed lower Malat1 expression in bulk TE relative MP cells (**Fig. 1.7 J**). Interestingly in Clusters 0 and 2 cells, a marked reduction

in Malat1 led to a subsequent enrichment of an MP gene signature (**Fig. 1.7 D, H, and I**). In all *Malat1*^{KD} cells, reduction of Malat1 corresponded to TE gene signature diminishment (**Fig. 1.7 G**). These results demonstrate the heterogeneity of effector cells at day 7, where we annotated two clusters of single cells (Clusters 0 and 2,) that enriched for a TE gene signature and subsequent Malat1 reduction led MP signature enrichment (**Fig. 1.7 H and I**). This contrasts with Cluster 1 cells which were already enriched for an MP gene signature, and Malat1 reduction subtly augmented MP gene expression (**Fig. 1.7 F and G**).

Differential gene expression analysis of known determinants of memory differentiation and function including *Tcf7*, *Eomes*, *Foxo1*, *Zeb1*, *Lef1*, *Bcl2*, *Myc*, *Il7r*, *Cd27*, *Cxcr3* were upregulated in Cluster 0 and to a lesser extent Cluster 2 *Malat1*^{KD} cells as compared to Cluster 1 *Malat1*^{KD} cells (**Fig. 1.7 K and L**). Characteristic phenotypic and functional markers of terminal effector differentiation *Tbx21*, *Zeb2*, Gzma, *Gzmb*, *Klrg1*, and *Cx3cr1* were downregulated in Cluster 0 and 1 *Malat1*^{KD} cells, and to a lesser extent Cluster 2 *Malat1*^{KD} cells (**Fig. 1.7 K and L**). This again highlights the heterogeneity of *Malat1*^{KD} cells where the transcriptional consequence of Malat1 depletion altered each cell cluster to varying degree with Cluster 0 *Malat1*^{KD} cells impacted to considerable effect through both upregulation of memory-associated genes and downregulated terminal effector-associated genes.

1.2.7: Single-cell weighted gene co-expression network analyses reveals distinct gene modules differentially regulated by Malat1

To elucidate genes with similar expression patterns upon Malat1 depletion, we performed weighted gene co-expression network analyses on all cells. Analyses revealed five distinct gene modules of which three modules were differentially expressed between *Malat1*^{KD} and *NT* cells (**Fig 1.8 A and B**). Module 1 genes were downregulated in all *Malat1*^{KD} cells, while Modules 3 and 4 genes were upregulated in all *Malat1*^{KD} cells (**Fig 1.8 B**). Biological gene ontology analysis revealed that both Modules 1 and 3 enriched in genes associated with T cell activation, while only Module 3 enriched for T lymphocyte differentiation (**Fig 1.8 C**). Module 4 enriched for genes associated with proteasomal and nucleotide processing (**Fig 1.8 C**). Module 3 had the highest frequency of differentially expressed genes at (728 of 1,856 genes; 39.2%), indicating Malat1 depletion significant upregulates similar genes involved in T cell differentiation (**Table 1).** Differentially expressed Module 3 genes included key memory-associated factors that were all upregulated in Cluster 0 and to lesser extent Cluster 2 *Malat1*^{KD} cells (**Fig 1.8 D**). Taken together, Malat1 negatively regulates a module of co-expressed genes associated with T lymphocyte differentiation, including key memory-associated genes, suggesting Malat1 may play a role in repressing their expression.

1.2.8: Malat1 plays a role in the generation of secondary memory T cells

Having established a role for Malat1 in differentiation of CD8^{+} T cells during primary infection, we next sought to determine whether Malat1 also plays a role in the generation of circulating memory T cell subsets upon infectious rechallenge. Thirty-five days after primary LCMV infection, *Malat1*^{KD} and *NT* t-T_{EM}, T_{EM}, or T_{CM} cells were

FACS-sorted, mixed in equal proportions, and transferred into new naive recipient mice which were then infected with LCMV (**Fig. 1.9 A**). Thirty-five days later, the number and proportion of secondary circulating memory T subsets were assessed (**Fig. 1.9 B and C**). Donor *Malat1*^{KD} and *NT* t-T_{EM}, cells gave rise to equal numbers of secondary t-T_{EM}, cells in *Malat1*^{KD} and *NT* cells (**Fig. 1.9 B and C**), suggesting that Malat1 does not play a critical role in the ability of primary t-T_{EM}, cells to give rise to secondary t-T_{EM}, cells upon rechallenge. By contrast, compared to donor *NT* cells, donor *Malat1*^{KD} t-T_{EM}, cells gave increased numbers and proportions of secondary T_{EM} cells. Moreover, compared to donor *NT* cells, donor *Malat1*^{KD} T_{EM} and T_{CM} cells gave rise to reduced numbers and proportions of secondary t-T_{EM}, cells, but increased numbers and proportions of secondary T_{EM} cells (**Fig. 1.9 B and C**). Secondary memory T cells derived from donor *Malat1*^{KD} and *NT* cells were similarly polyfunctional with equivalent frequencies of IFNγ^{hi}TNFα^{hi} cells (**Fig. 1.9 D**), though secondary memory cells derived from *Malat1*^{KD} T_{EM} and T_{CM} donors tended to express more IL-2 compared to those derived from *NT* donors (**Fig. 1.9 E**). Taken together, these results suggest that Malat1 plays a role in repressing the generation of secondary T_{EM} cells derived from t-T_{EM}, T_{EM}, and T_{CM} cells, in addition to its role in regulating primary t-T_{EM} cell differentiation.

1.3: Discussion

The molecular regulation of memory CD8$^+$ T cell differentiation has been an area of intense investigation. Prior work in this field has focused primarily on protein-coding genes, while the role of the noncoding portion of the transcriptome in this process remains poorly understood. Here we performed a functional genetic knockdown screen

suggesting lncRNA Malat1 as a regulator of $CD8^+$ T cell differentiation. We provide functional evidence that Malat1 plays a critical role in the formation of terminally differentiated cells and t-T_{EM} circulating memory subset during primary infection. Malat1 depletion as early as day 3 of infection negatively impacted the differentiation and accumulation of $KLRG1^{hi}$ cells, precursors to terminally differentiated cells. While $KLRG1^{lo}$ *Malat1*^{KD} cells accumulated by day 3, the total pool of effector cells by day 5 was dramatically reduced due to extensive loss of cells with a terminal fate. Therefore, the predominate phenotype upon Malat1 depletion is loss of terminal effector cells and accumulation of cells with memory potential.

Evaluating expression levels of key molecular drivers of $CD8^+$ T cell differentiation revealed Malat1 depletion in $KLRG1^{hi}$ cells consistently upregulated memory-associated genes *Eomes*, *Tcf7*, Zeb1, *Lef1*, *Foxo1*, and *Bcl2* and downregulated determinants of terminal effector differentiation *Tbx21*, *Id2*, *Gzma*. $KLRG1^{lo}$ *Malat1*^{KD} cells demonstrated varying expression levels of memory-associated genes with some factors upregulated including *Lef1* and *Bcl2* and others unchanged or even reduced including *Eomes*, *Zeb1*, *Tcf7*, and *Foxo1*. Additionally, expression level of factors associated with terminal differentiation remained unchanged in $KLRG1^{lo}$ *Malat1*^{KD} cells. These findings suggest that Malat1 regulates $CD8^+$ T cell differentiation in a subset specific manner whereby depletion diminishes accumulation of $KLRG1^{hi}$ cells to greater affect than cells that have already acquired phenotypic characteristics of memory cells. While $KLRG1^{hi}$ *Malat1*^{KD} exhibited increased Annexin V expression indicating apoptosis as contributing factor to numeric loss, cellular proliferation as

measured by Ki-67 was not altered demonstrating all *Malat1*^{KD} cells maintained an ability to proliferate normally.

Our single-cell analyses revealed three clusters of effector cells at day 7 with differing transcriptional profiles. Annotating each single-cell cluster by enrichment of TE and MP gene signatures as well as KLRG1 and Malat1 expression allowed us to characterize two clusters (Clusters 0 and 2) that enriched for a TE gene profile and one cluster (Cluster 1) that enriched for MP gene profile. Interestingly Clusters 0 and 2 cells that expressed lower levels of Malat1 were sensitive to its depletion and in turn promoted enrichment of the MP signature. Cluster 1 cells in contrast were transcriptionally similar to MP cells and knockdown of Malat1 only marginally promoted expression of MP genes. Our single cell data revealed a heterogenous population of cells with higher KLRG1 expression (Clusters 0 and 2), where depletion of Malat1 most impacted Clusters 0 *Malat1*^{KD} cells at key memory and terminal-effector associated genes. It is interesting to speculated if these Cluster 0 cells may constitute a KLRG1^{hi} population of cells that downregulate KLRG1 expression contributing to the ex-KLRG1 pool of cells which populate all circulating memory subsets (Herndler-Brandstetter et al., 2018).

Notably, we observed that once t-T_{EM} cells had formed, Malat1 did not play a critical role in the ability of primary t-T_{EM} cells to give rise to secondary t-T_{EM} cells upon infectious rechallenge, in contrast to primary T_{EM} and T_{CM} cells, which were dependent on Malat1 to give rise to secondary t-T_{EM} cells. This suggests that multipotent CD8^{+} naive and memory T_{EM} and T_{CM} cells are dependent on Malat1, whereas more differentiated t-T_{EM} cells may be less so. In total, these results demonstrate that Malat1

has a selective effect in promoting certain circulating memory cell subsets (t-T_{EM}) but not others (T_{EM} and T_{CM}). To our knowledge, this is the one of few examples in which a regulator of $CD8^+$ T cell differentiation selectively affects only certain circulating memory subsets. Genetic deletions of known regulators of $CD8^+$ T cell differentiation, such as *Foxo1*, *Bcl6*, and *T-bet,* reduced t-T_{EM} cell formation in response to LCMV infection, but also led to reductions in both T_{EM} and T_{CM} cells, effectively diminishing the entire pool of circulating memory cells (Milner et al., 2020).

Chapter 1, in full, is an adapted version of the material that has been submitted for publication. Jad N. Kanbar, Shengyun Ma, Nadia S. Kurd, Matthew S. Tsai, Tiffani Tysl, Christella E. Widjaja, Eleanor S. Kim, Abigail E. Limary, Brian Yee, Zhaoren He, Yajing Hao, Xiang-Dong Fu, Gene Yeo, Wendy J. Huang, John T. Chang (2022). The long noncoding RNA Malat1 regulates $CD8^+$ T cell differentiation by mediating epigenetic repression. In revision. The dissertation was the primary author of all material.

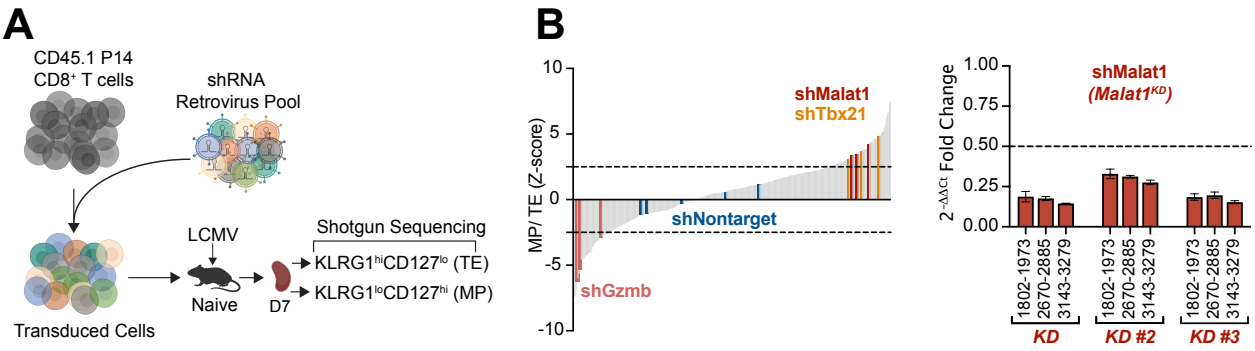

Figure 1.1. *in vivo* shRNA screen reveals lncRNA Malat1 as a critical regulator of CD8⁺ T cell differentiation (A) CD45.1⁺ P14 T cells were transduced with a shRNA pool; 7 days after infection TE- (KLRG1^{hi}CD127^{lo}) and MP-phenotype (KLRG1^{lo}CD127^{hi}) cells were isolated by FACS. **(B)** Enrichment of shRNA constructs in MP cells relative to TE cells, reported as the average Z-score from two independent screens, n = 20 mice per screen (left). Validation of three *Malat1^{KD}* shRNAs in activated CD8⁺ T cells with locus coordinates for each Malat1 primer set (right).

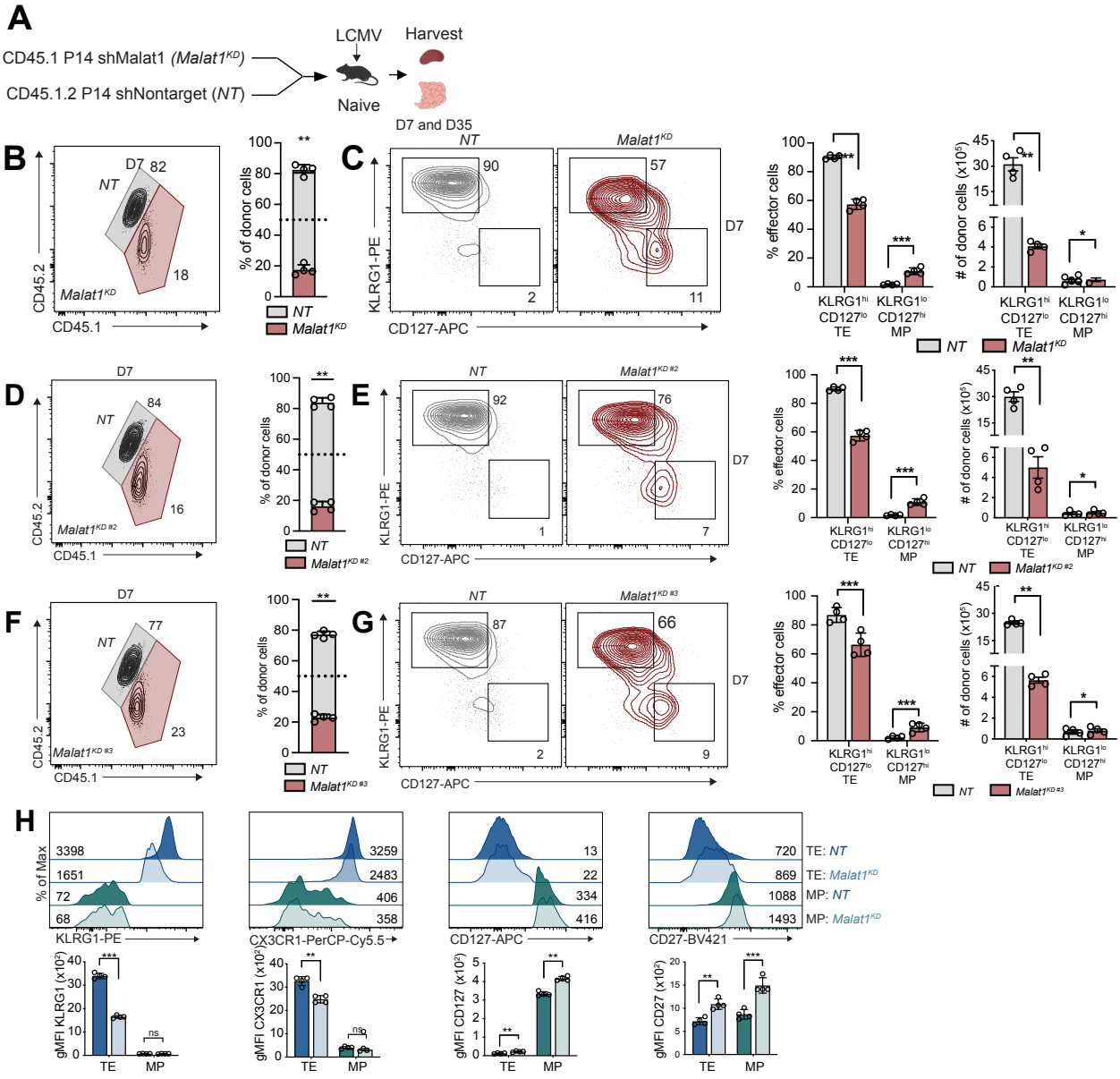

Figure 1.2 lncRNA Malat1 regulates effector CD8⁺ T cell differentiation. (A) P14 CD8⁺ T cells were transduced with Malat1 shRNA (*Malat1^{KD} or Malat1$^{KD\ \#2}$* or *Malat1$^{KD\ \#3}$*, CD45.1) or Nontarget shRNA (*NT,* CD45.1.2); cells were adoptively co-transferred at a 1:1 ratio into CD45.2 recipient mice that were subsequently infected with LCMV. Splenocytes or SI IE were harvested on Days 7 and 35 for analysis. (**B, D and F**) Quantification of splenic *NT* and *Malat1^{KD}* (B) or *Malat1$^{KD\ \#2}$* (D) or *Malat1$^{KD\ \#3}$* (F) ratios at day 7 after infection. (**C, E, and G**) Representative flow cytometry plots of TE- and MP-phenotype cells (left) and quantification (right) among co-transferred cells. **(H)** Representative flow cytometry plots and quantification of key TE- and MP-associated molecules. All data are from one representative experiment out of two independent experiments with n = 4 to 5 per group; *P < 0.05, ***P < 0.005. Graphs indicate mean ± SEM, symbols represent individual mice.

Figure 1.3 lncRNA Malat1 regulates early effector CD8$^+$ T cell differentiation. (A) P14 CD8$^+$ T cells were transduced with Malat1 shRNA (*Malat1^{KD},* CD45.1) or Nontarget shRNA (*NT,* CD45.1.2); cells were adoptively co-transferred at a 1:1 ratio into CD45.2 recipient mice that were subsequently infected with LCMV. Spleenocytes were harvested on Days 3, 5, and 7. **(B)** Quantification of spleenic *NT* and *Malat1^{KD}* ratios at days 3, 5 and 7 after infection. **(C, D, and E)** Representative flow cytometry plots of Klrg1- and CD127-phenotype cells (C) and quantification of frequencies (D) and numeric ratio of cells (E) of Klrg1^{hi} and Klrg1^{lo} cells. (**F, G, and H)** Representative flow cytometry plots of Klrg1- and CX3CR1-phenotype cells (F) and quantification of frequencies (G) and numeric ratio of cells (H) of Klrg1^{hi}CX3CR1^{hi} and Klrg1^{lo} CX3CR1^{lo} cells. **(I)** Quantification of frequency of Ki67$^+$ cells in Klrg1^{hi} and Klrg1^{lo} on Day 7. **(J).** Quantification of frequency of AnnexinV$^+$ cells in Klrg1^{hi} and Klrg1^{lo} on Days 5 and 7. **(K)** *Malat1^{KD}* and *NT* cells on day 7 after infection were cultured *ex vivo* in the presence of cognate gp33-41 peptide for 5 hours and proportion of IL-2$^+$ (top) or IFN-γ^+ and TNF-α^+ (bottom). All data are from one representative experiment out of two independent experiments with n = 4 to 7 mice per group; *P < 0.05, ***P < 0.005, paired *t* test. Graphs indicate mean ± SEM, symbols represent individual mice.

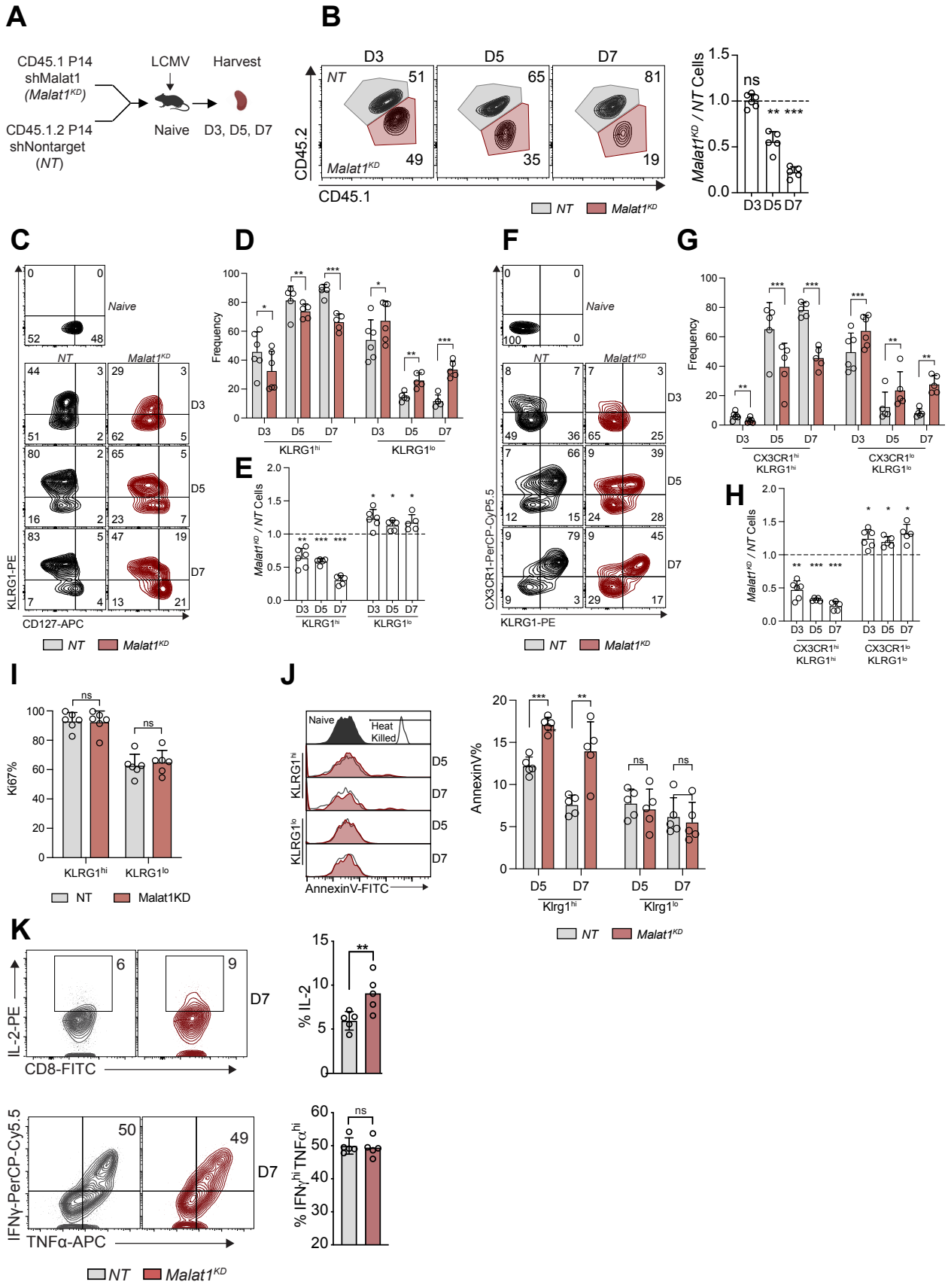
A
CD45.1 P14
shMalat1
(Malat1KD)
CD45.1.2 P14
shNontarget
(NT)
LCMV
Naive
Harvest
D3, D5, D7
B
D3
D5
D7
NT
Malat1KD
CD45.2
CD45.1
Malat1KD / NT Cells
ns
C
Naive
KLRG1-PE
CD127-APC
D
Frequency
KLRG1hi
KLRG1lo
E
Malat1KD / NT Cells
F
CX3CR1-PerCP-CyP5.5
KLRG1-PE
G
CX3CR1hi KLRG1hi
CX3CR1lo KLRG1lo
H
I
Ki67%
KLRG1hi
KLRG1lo
NT
Malat1KD
J
Naive
Heat Killed
KLRG1hi
KLRG1lo
AnnexinV-FITC
AnnexinV%
Klrg1hi
Klrg1lo
K
IL-2-PE
CD8-FITC
% IL-2
IFNγ-PerCP-Cy5.5
TNFα-APC
% IFNγhiTNFαhi

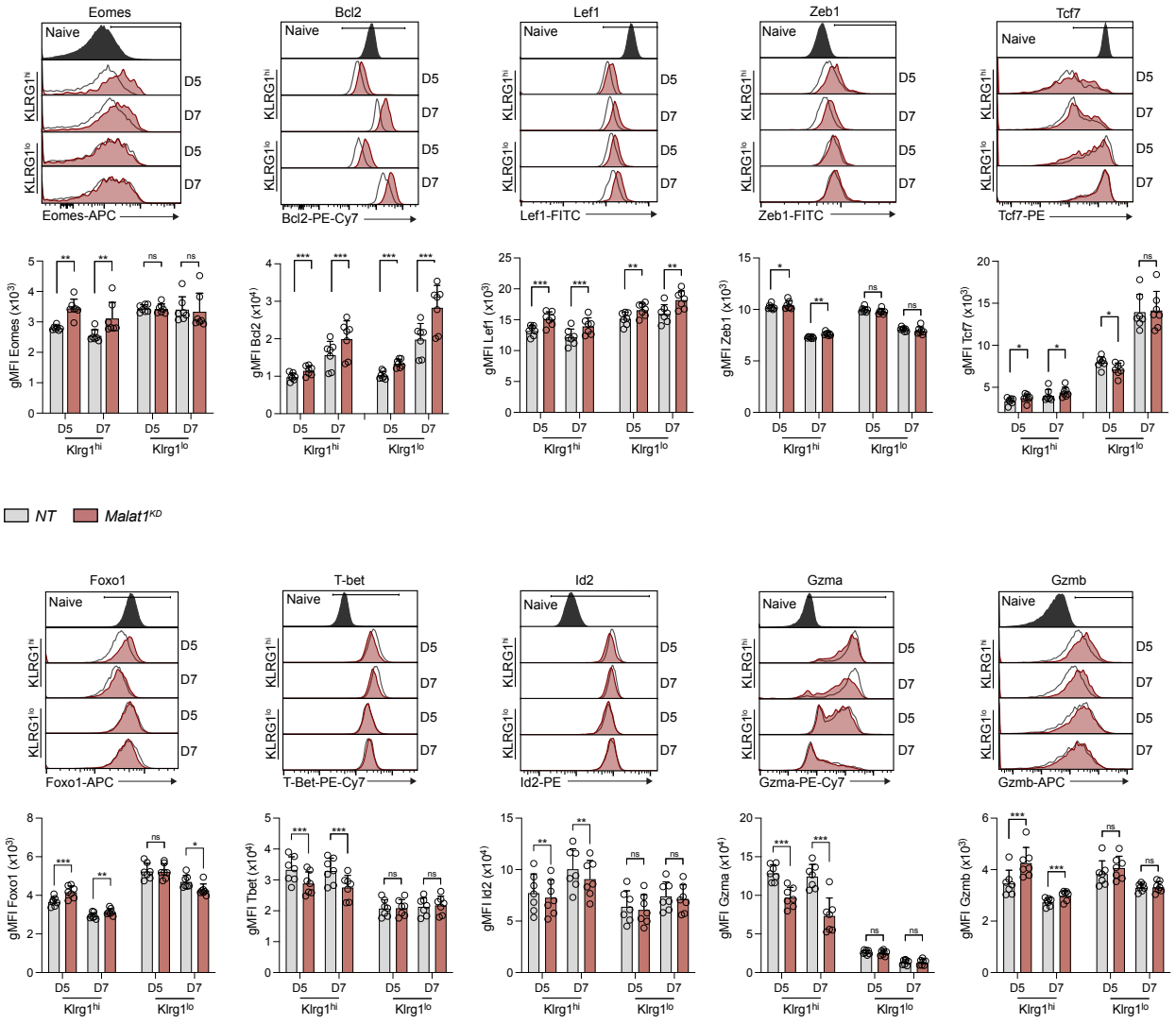

Figure 1.4 Transcription factors associated with memory differentiation are upregulated in KLRG1^{hi} effector cells. Representative flow cytometry plots and quantification of protein expression of memory-associated genes: *Eomes*, *Bcl2*, *Zeb1*, *Lef1*, *Tcf7*, and *Foxo1* and terminal effector-associated genes: *T-bet*, *Id2*, *Gzma*, and *Gzmb* in *Malat1^{KD}* and *NT* Klrg1^{hi} and Klrg1^{lo} cells at days 5 and 7 after infection. All data are from one representative experiment out of two independent experiments with n = 5 to 7 mice per group; *P < 0.05, ***P < 0.005, paired *t* test. Graphs indicate mean ± SEM, symbols represent individual mice.

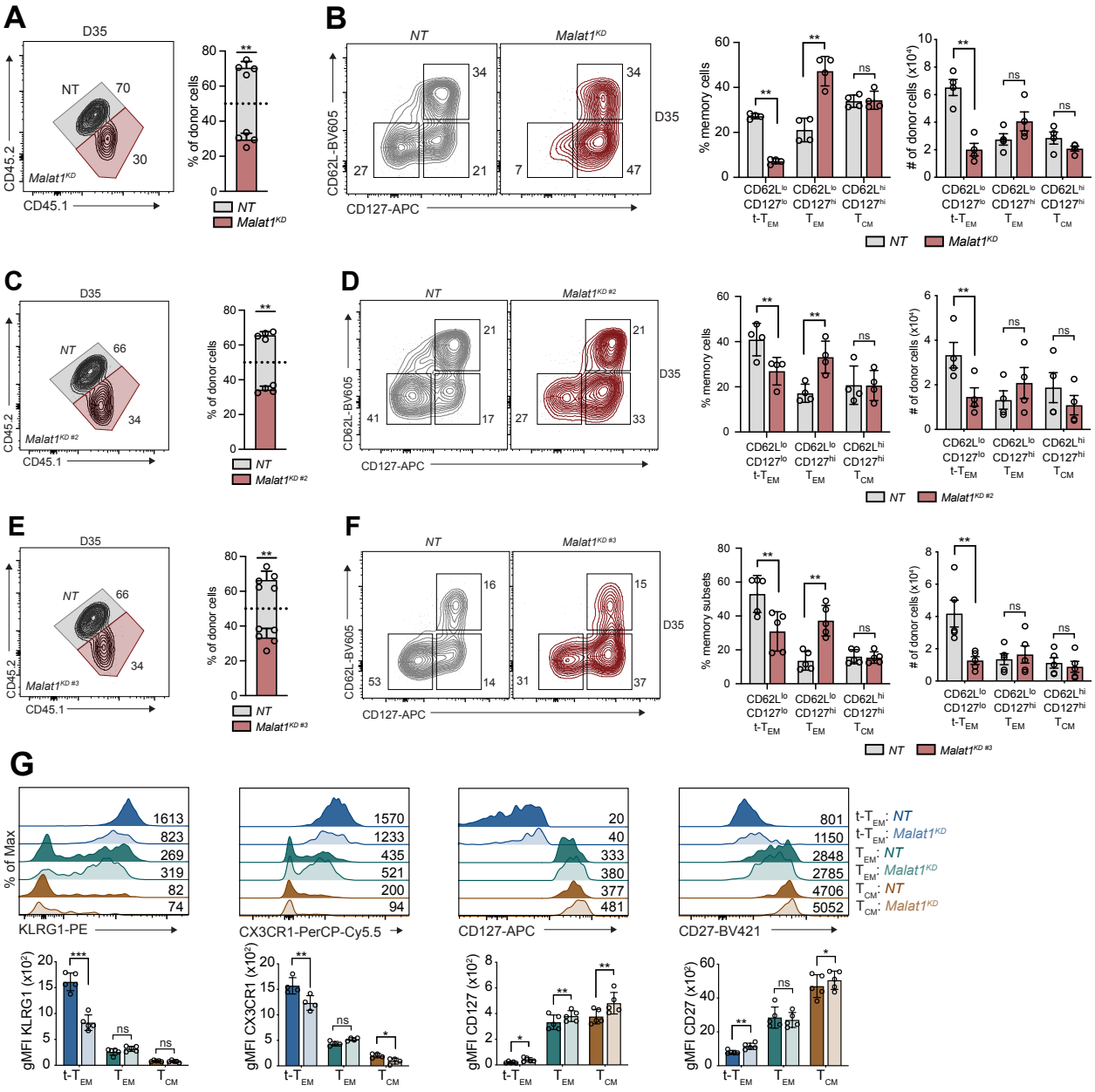

Figure 1.5 lncRNA Malat1 regulates memory CD8⁺ T cell differentiation. P14 CD8⁺ T cells were transduced with Malat1 shRNA (*Malat1^{KD} or Malat1$^{KD\ \#2}$* or *Malat1$^{KD\ \#3}$*, CD45.1) or Nontarget shRNA (*NT,* CD45.1.2); cells were adoptively co-transferred at a 1:1 ratio into CD45.2 recipient mice that were subsequently infected with LCMV (see also experimental setup in Fig. 1.2 A). (**A, C and E**) Quantification of splenic *NT* and *Malat1^{KD}* (A) or *Malat1$^{KD\ \#2}$* (C) or *Malat1$^{KD\ \#3}$* (E) ratios at day 35 after infection (**B, D and F**). Representative flow cytometry plots and quantification of *NT* and *Malat1^{KD}* t-T_{EM}, T_{EM}, and T_{CM} cells. **(G)** Representative flow cytometry plots and quantification of t-T_{EM}, T_{EM}, and T_{CM} molecules. All data are from one representative experiment out of two independent experiments with n = 4 to 5 per group; *P < 0.05, ***P < 0.005. Graphs indicate mean ± SEM, symbols represent individual mice.

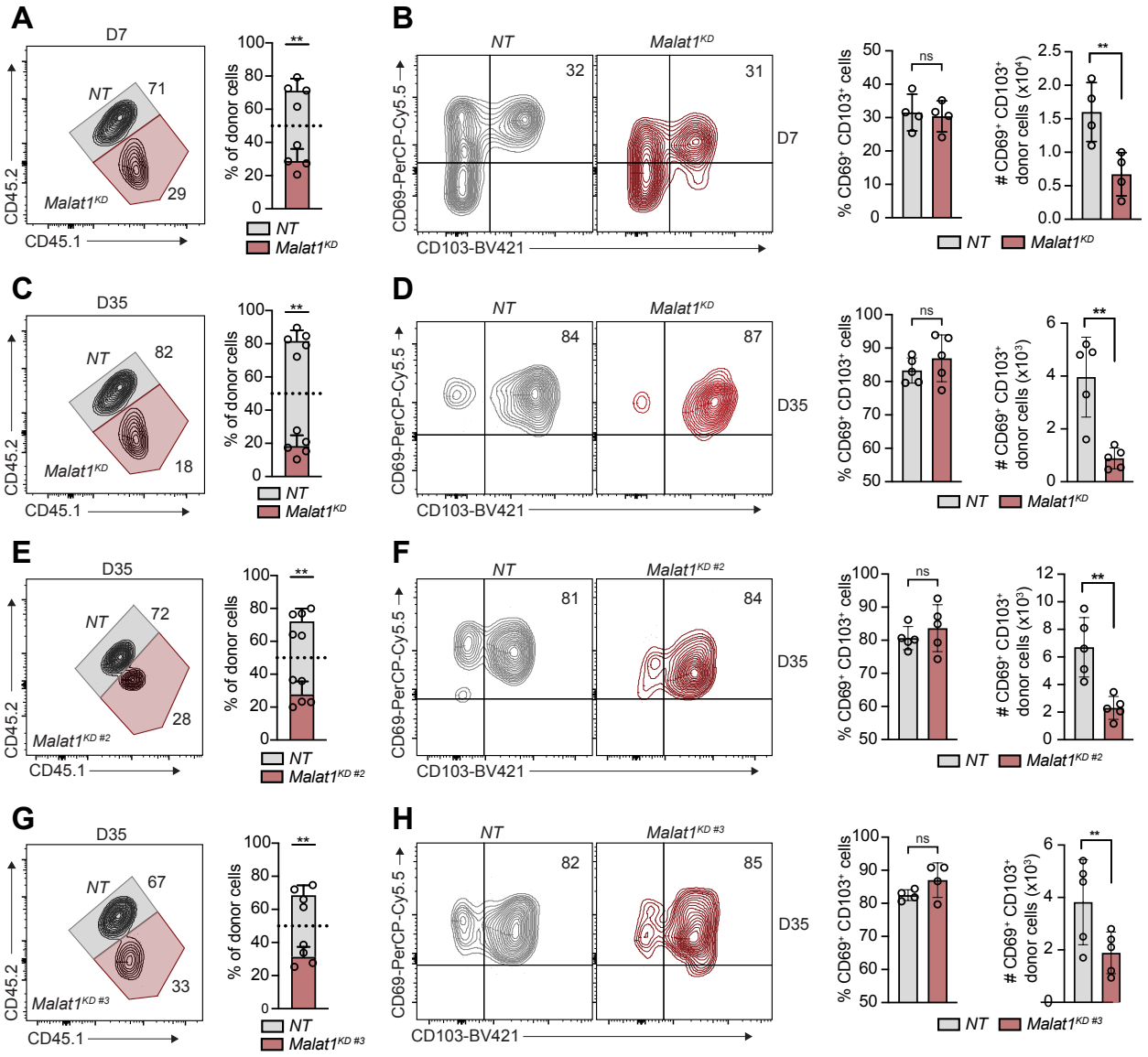

Figure 1.6. lncRNA Malat1 knockdown reduces siIEL T_{RM} cell differentiation. P14 $CD8^+$ T cells were transduced with Malat1 shRNA (*Malat1*$^{KD\ \#2}$, *Malat1*$^{KD\ \#3}$ or *Malat1*$^{KD\ \#3}$, CD45.1) or Nontarget shRNA (*NT,* CD45.1.2) (see also experimental setup in Fig. 1.2 A) and adoptively co-transferred at 1:1 ratio into CD45.2 recipient mice that were subsequently infected with LCMV. **(A)** Quantification of siIEL *NT* and *Malat1*^{KD} ratios at day 7 after infection. **(B)** Representative flow cytometry plots of $CD69^+CD103^+$ cells (left) and quantification (right) at day 7 after infection among co-transferred cells. **(C, E,** and **G)** Quantification of siIEL *NT* and *Malat1*^{KD} (C), *Malat1*$^{KD\ \#2}$ (E), or *Malat1*$^{KD\ \#3}$ (G) ratios at day 35 after infection. **(D, F,** and **H)** Representative flow cytometry plots of T_{RM} cells (left) and quantification (right) at day 35 among co-transferred cells. All data are from one representative experiment out of two independent experiments with n = 4 to 5 mice per group; *P < 0.05, ***P < 0.005, paired *t* test. Graphs indicate mean ± SEM, symbols represent individual mice.

Figure 1.7. Single-Cell RNA-Seq reveals that Malat1 depletion upregulates memory associated factors. (A) tSNE analysis of *Malat1*^{KD} and *NT* cells on day 7 after LCMV infection. **(B)** Clustering analysis of *Malat1*^{KD} and *NT* cells as one plot (left) or separated by sample type (right). **(C)** Bar graph quantifying proportion of *Malat1*^{KD} and *NT* cells among each cluster type. (**D, E)** tSNE analysis of TE gene signature enrichment split by *Malat1*^{KD} and *NT* cells (D) and TE gene signature enrichment for each cluster split by *Malat1*^{KD} and *NT* cells (E). (**F, G)** tSNE analysis of MP gene signature enrichment split by *Malat1*^{KD} and *NT* cells (D) and MP gene signature enrichment for each cluster split by *Malat1*^{KD} and *NT* cells (E). (**H, I)** Relative expression profile of Klrg1 (H) and Malat1 (I) for each cluster split by *Malat1*^{KD} and *NT* cells. **(J)** Normalized bulk RNA-seq expression of Malat1 from TE and MP subsets. **(K, L)** Single cells gene expression profiles (J) and average expression (K) of genes relevant to CD8^{+} T cell differentiation, cytotoxicity, and trafficking for each cluster split by *Malat1*^{KD} and *NT* cells.

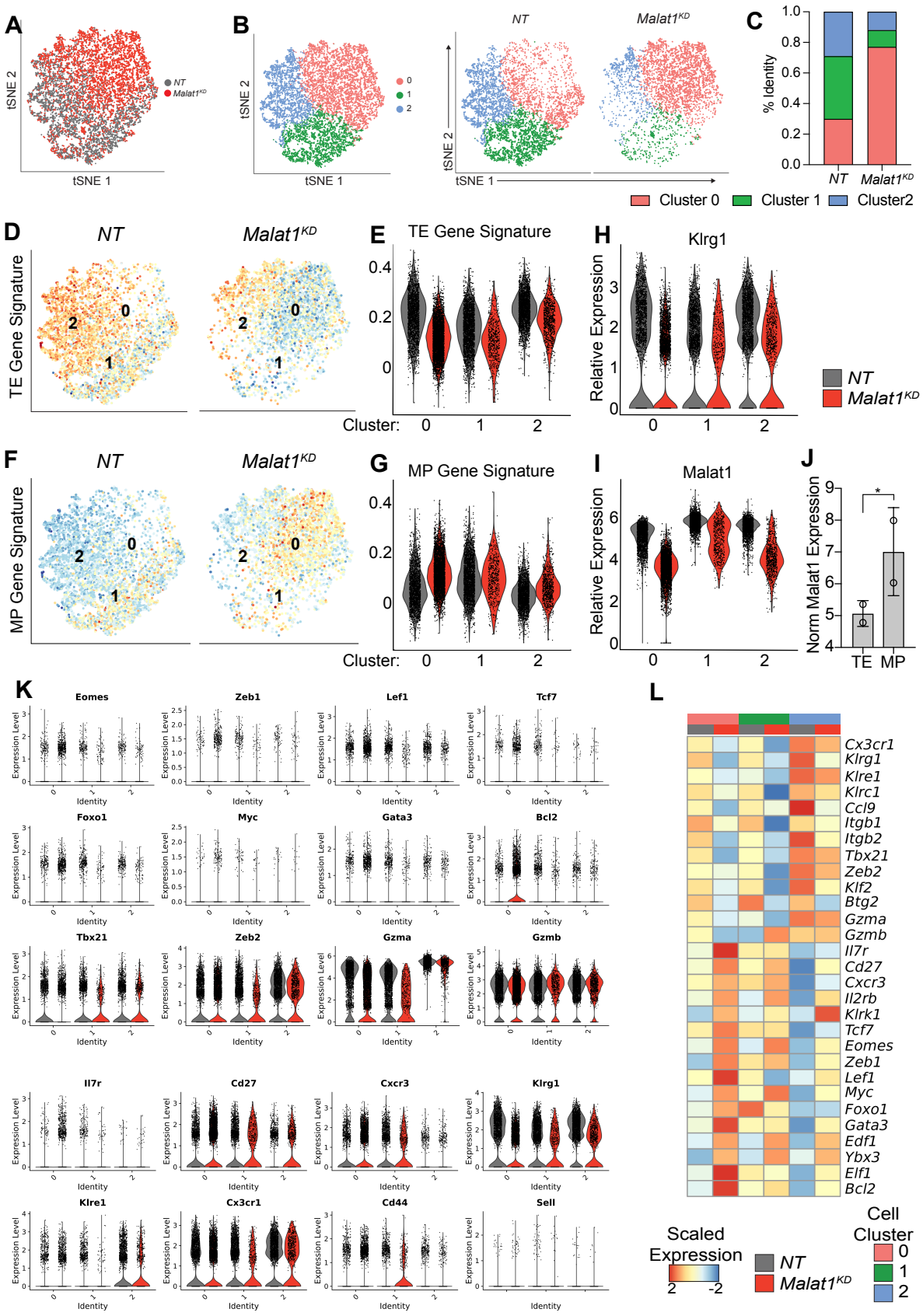
A
tSNE 2
tSNE 1
NT
Malat1KD
B
tSNE 2
tSNE 1
0
1
2
NT
Malat1KD
C
% Identity
1.0
0.8
0.6
0.4
0.2
0.0
NT
Malat1KD
Cluster 0
Cluster 1
Cluster2
D
NT
Malat1KD
TE Gene Signature
E
TE Gene Signature
Cluster: 0 1 2
H
Klrg1
Relative Expression
NT
Malat1KD
F
NT
Malat1KD
MP Gene Signature
G
MP Gene Signature
Cluster: 0 1 2
I
Malat1
Relative Expression
J
Norm Malat1 Expression
TE MP
K
Eomes
Zeb1
Lef1
Tcf7
Foxo1
Myc
Gata3
Bcl2
Tbx21
Zeb2
Gzma
Gzmb
Il7r
Cd27
Cxcr3
Klrg1
Klre1
Cx3cr1
Cd44
Sell
Expression Level
Identity
L
Cx3cr1
Klrg1
Klre1
Klrc1
Ccl9
Itgb1
Itgb2
Tbx21
Zeb2
Klf2
Btg2
Gzma
Gzmb
Il7r
Cd27
Cxcr3
Il2rb
Klrk1
Tcf7
Eomes
Zeb1
Lef1
Myc
Foxo1
Gata3
Edf1
Ybx3
Elf1
Bcl2
Scaled Expression
2
-2
NT
Malat1KD
Cell Cluster
0
1
2

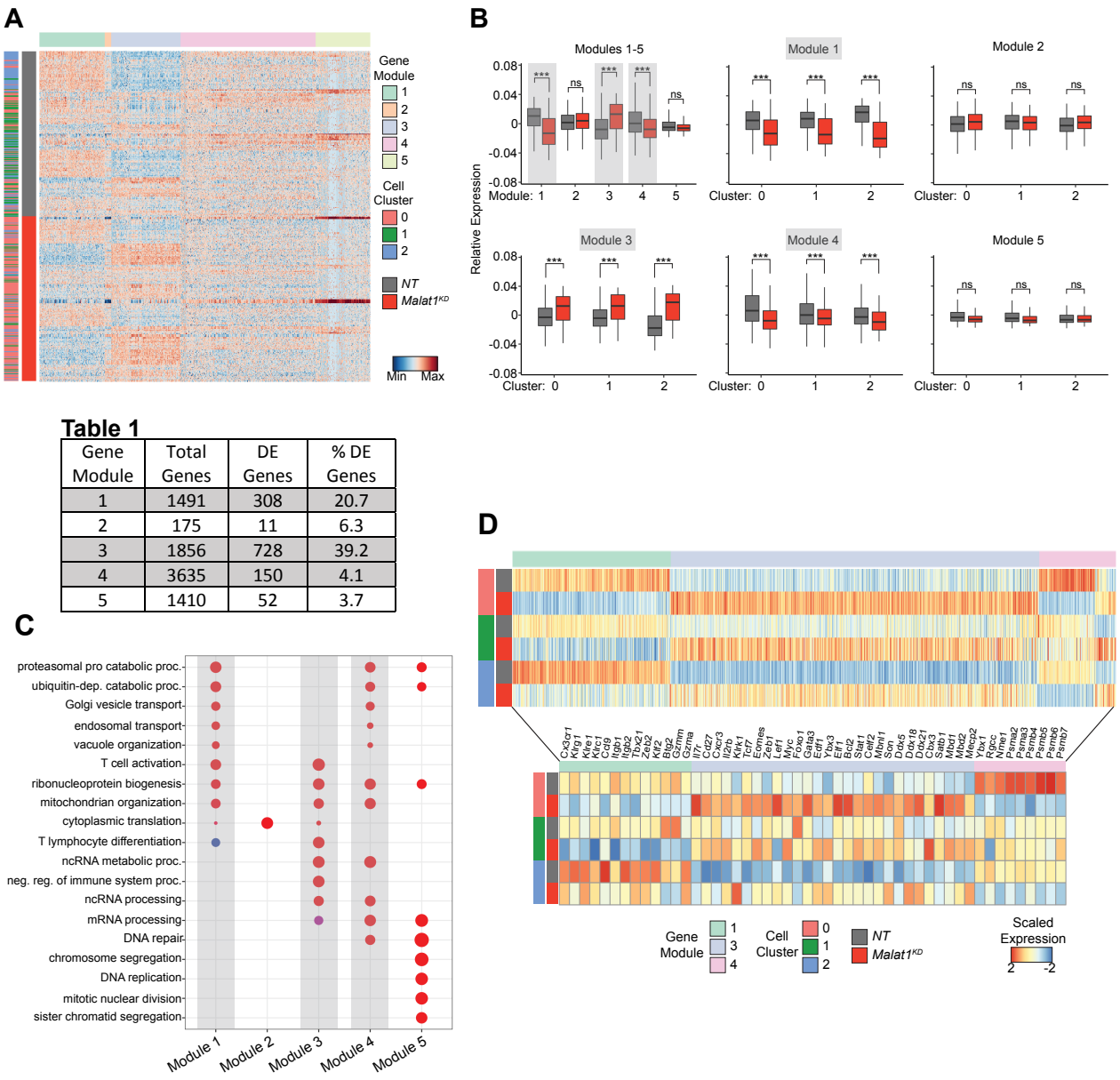

Table 1

Gene Module	Total Genes	DE Genes	% DE Genes
1	1491	308	20.7
2	175	11	6.3
3	1856	728	39.2
4	3635	150	4.1
5	1410	52	3.7

Figure 1.8. WGCNA reveals distinct gene modules differentially regulated by Malat1. (A) Weighted gene coexpression network analyses where each row represents a single cell grouped by *NT* and *Malat1*^{KD} cells within each cluster and each column represents a single gene grouped by module. **(B)** Box plot analysis of relative expression of each gene module for each cluster split by *NT* and *Malat1*^{KD} cells. **(C)** Biological gene ontology analyses of each gene module. **(D)** Mean expression of differentially expressed genes for gene modules 1, 3, and 4 within *NT* and *Malat1*^{KD} cells grouped by clusters and highlighting some key genes associated with TE and MP differentiation. Statistical significance was determined by Student's *t* test, *P < 0.05, ***P < 0.005 (B).

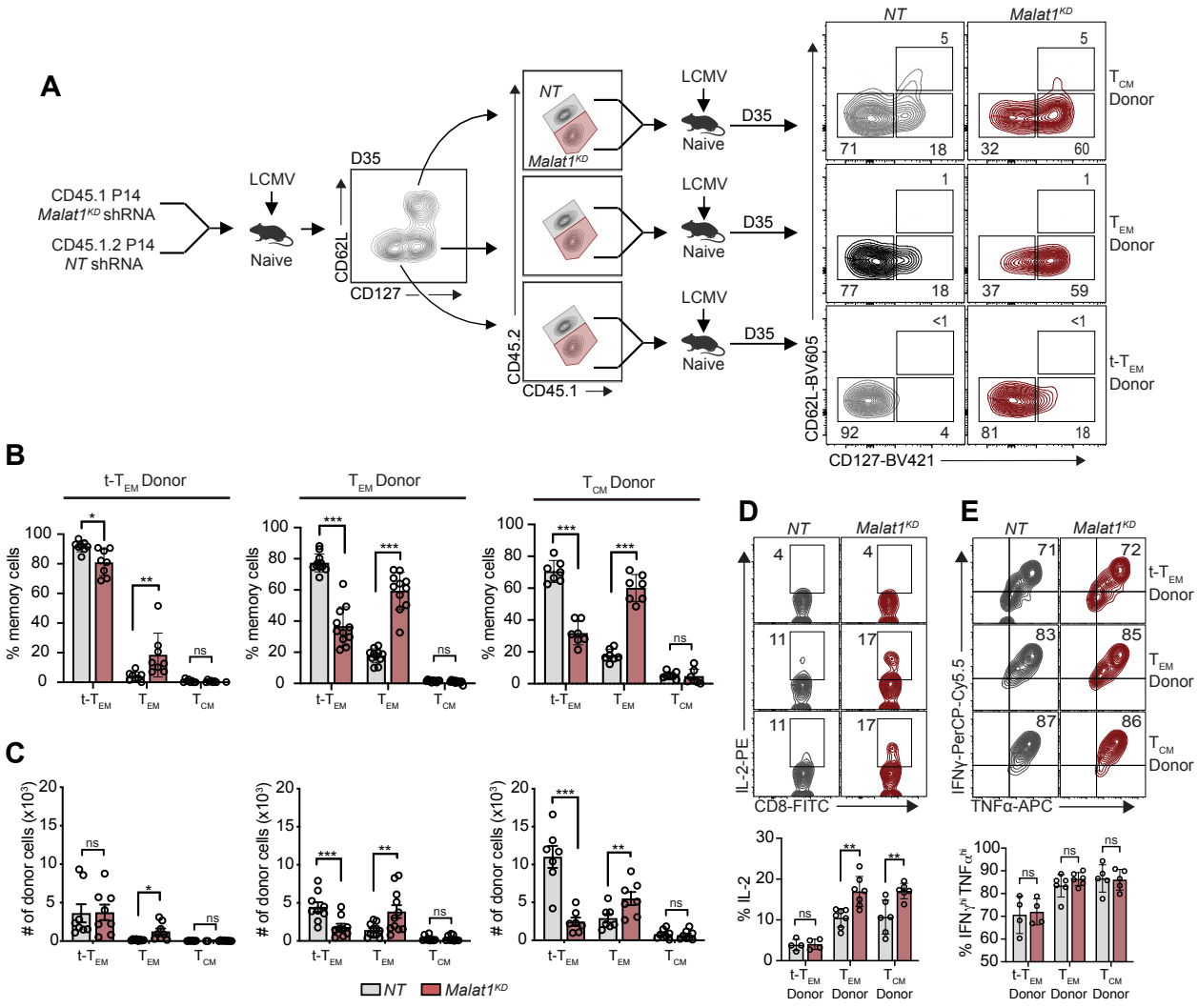

Figure 1.9 Malat1 represses generation of secondary T_{EM} cells (A) P14 $CD8^+$ T cells were transduced with Malat1 shRNA (*Malat1^{KD},* CD45.1) or Nontarget shRNA (*NT,* CD45.1.2) and adoptively co-transferred at a 1:1 ratio into CD45.2 recipient mice, which were then infected with LCMV. Thirty-five days after primary infection, *Malat1^{KD}* and *NT* cells were sorted from t-$T_{EM,}$ T_{EM}, or T_{CM} subsets, mixed at a 1:1 (5,000 *Malat1^{KD}* cells/5,000 *NT* cells) ratio, and adoptively transferred into naïve CD45.2 recipient followed by infectious challenge with LCMV (secondary infection). **(B)** Frequency of secondary memory populations derived from transferred t-T_{EM} (left), T_{EM} (middle), and T_{CM} (right) donor cells was assessed at 30 days after secondary LMCV infection. **(C)** Quantification of secondary memory subsets derived from t-T_{EM} (left), T_{EM} (middle), and T_{CM} (right) donor populations. **(D)** Frequency of IL-2^+ cells among secondary t-T_{EM}, T_{EM}, and T_{CM} cells cultured *ex vivo* in the presence of cognate gp33-41 peptide for 5 hours. **(E)** Frequency of IFNγ^{hi}TNFα^{hi} cells among secondary t-T_{EM}, T_{EM}, and T_{CM} cells, as in Fig. 3 D. All data are from one representative experiment out of two independent experiments with n = 9 to 10 mice per group (B, C) or n = 4 to 6 mice per group (D, E); *P < 0.05, ***P < 0.005, paired *t* test. Graphs indicate mean ± SEM, symbols represent individual mice.

CHAPTER 2: MALAT1 INTERACTS WITH EZH2 TO MAINTAIN H3K27ME3 DEPOSITION ON MEMORY-ASSOCIATED GENES

2.1: Introduction

It has been estimated in mouse and human $CD8^+$ T cells that 25% of the transcriptome encodes for lncRNAs (Hudson et al., 2019). To date, few lncRNAs have been functionally characterized in $CD8^+$ T cells despite published observations that lncRNA expression profiles can distinguish naive, effector, and memory subsets. Having noted that Malat1 may influence the repression of memory-associated genes, in this chapter we aimed to assess the mechanism to which Malat1 may regulate transcription. We first explored Malat1 interaction patterns on chromatin and correlated these interactions to both repressive and activating epigenetic marks. Owing to the previously reported association of Malat1 and Ezh2, the functional enzymatic component of the Polycomb Repressive Complex 2 (PRC2) which deposits repressive methyl groups to histone H3 at lysine 27 (Wang et al., 2015), we explored if Malat1 was necessary to maintain repressive marks on key memory-associated genes.

2.2: Results

2.2.1: A substantial portion of RNA chromatin interactions are represented by lncRNAs

To begin to elucidate the transcriptional influence of Malat1 on gene expression, we performed GRID-seq (Global RNA Interactions with DNA by Deep sequencing) with a specific focus on lncRNAs. Replicate libraries of P14 $CD8^+$ T cells were cultured in the presence of cognate gp33-41 peptide for 5 days in vitro (**Fig. 2.1 A and B**). Evaluation

of the $CD8^+$ T cell transcriptome revealed that a substantial proportion of RNA chromatin interactions were represented by lncRNAs (15.4%), in line with previous reports of lncRNA abundance in activated $CD8^+$ T cells (Hudson et al., 2019).

Chromatin-enriched lncRNAs analysis revealed that a majority of lncRNAs interact within their chromosome of origin and a separate subset of lncRNAs that engage in highly trans interactions throughout the mouse genome (**Fig. 2.2 B**). Increased representation of lncRNAs originating from chromosomes 19 and X validated a high level of XIST enrichment over chromosome X (**Fig. 2.2 C**). Malat1 and NEAT1 both enriched over chromosome 19; however, in contrast to NEAT1, Malat1 engaged in trans interactions beyond its chromosome of origin (**Fig. 2.2 C**). Principal component analysis (PCA) and k-means clustering of 66 chromatin-enriched lncRNAs resulted in 3 clusters of lncRNAs separated on the first principal component by genomic coverage (**Fig. 2.2 B and D**). Clusters 1 and 2 separated 11 highly trans-interacting lncRNAs each with genomic coverage greater than 20%, grouping Malat1 with the Cluster 2 lncRNAs (**Fig. 2.2 B and D**). Cluster 3 grouped all lncRNAs with less than 12% genomic coverage with interactions predominantly within their chromosome of origin (**Fig. 2.2 B and D**). We further evaluated the 11 highly trans-interacting lncRNAs by performing Spearman pairwise correlation analyses and hierarchical clustering, which again separated these lncRNAs into two clusters, suggesting distinct genomic interaction features between these two groups of trans-interacting lncRNAs (**Fig. 2.2 E**). Taken together, this data suggests lncRNAs uniquely interact throughout the genome in activate $CD8^+$ T cells.

2.2.2: Malat1 groups with a cluster of highly trans-lncRNAs that interact at promoters and gene bodies

To test the hypothesis that clusters of lncRNAs have unique interaction patterns, we analyzed differential RNA chromatin interactions and found that compared to Cluster 1 lncRNAs, Cluster 2 lncRNAs exhibited greater interaction levels (**Fig. 2.3 A**) on genomic regions annotated to genes (**Fig 2.3 B**). This trend was similarly observed when comparing Cluster 2 and Cluster 3 lncRNAs (**Fig. 2.3 D and E**). Genomic feature annotation of differential RNA chromatin interactions demonstrated that Cluster 2 lncRNAs were associated with promoters and gene bodies with greater frequency, whereas Cluster 1 lncRNAs were associated with distal intergenic regions with greater frequency, highlighting the distinct interaction features of these two clusters of highly trans-interacting lncRNAs (**Fig. 2.3 C and Fig 2.3 F**). Taken together, these results indicate that Malat1 associates with a cluster of trans-interacting lncRNAs that have RNA interactions preferentially at promoters and gene bodies.

2.2.3: Malat1-chromatin enrichment correlates with high coverage of H3K27me3 marks from terminal effector cells

Owing to the previously reported association of Malat1 and Ezh2, the functional enzymatic component of the Polycomb Repressive Complex 2 (PRC2) which deposits repressive methyl groups to histone H3 at lysine 27 (Wang et al., 2015), we explored epigenetic regulation at Malat1-interacting regions, utilizing publicly available ChIP-seq (chromatin immunoprecipitation) datasets in terminal effector (TE) and memory precursor (MP) $CD8^+$ T cells for several histone marks (Yu et al., 2017; Gray et al.,

2017). In TE cells, the repressive histone mark H3K27me3 demonstrated the highest proportions of coverage and covered regions at Malat1 interaction regions, as compared to active histone marks H3K4me3, H3K27ac, and H3K4me1 (**Fig. 2.4 A, C, and E**). We next tested if Malat1 displayed preferential interaction on H3K27me3 marks from either TE or MP cells. Malat1 demonstrated higher coverage on H3K27me3 marks from TE cells as compared to MP cells (**Fig. 2.4 B and D**) Moreover, uniform manifold approximation and projection (UMAP) analyses of all RNA chromatin interactions demonstrated that 96.7% of all Malat1 interaction sites were also marked by H3K27me3 deposition from TE cells (**Fig 2.4 F and G**). Taken together, this data suggests a subset specific interaction pattern for Malat1 in TE cells, in line our previous data demonstrating phenotypic and transcriptional roles for Malat1 in the differentiation of TE cells.

2.2.4: Malat1-chromatin enrichment correlates genes associated with memory cell differentiation

Focusing on genes known to play a role in $CD8^+$ T cell differentiation, we next evaluated Malat1 interaction levels at genes harboring H3K27me3 (Yu et al., 2017), and found increased Malat1 enrichment at genes associated with memory precursor cells as compared to those associated with terminal effector cells (**Fig. 2.5 A and B**). Furthermore, Malat1 enrichment was increased at genes unique to Cluster 0 as compared to all other clusters (**Fig. 2.5 C**) including memory cell-associated genes *Tcf7*, *Eomes*, *Zeb1*, *Lef1*, and Bcl2, which were all upregulated as a consequence of Malat1 knockdown (**Fig 2.5 D**) again raising the possibility of Malat1-mediated

transcriptional suppression. Taken together, these results suggest that Malat1 may play a role in repressing genes associated with memory cell differentiation.

2.2.5 Malat1 maintains H3K27me3 deposition at genes associated with memory cell differentiation

Having observed upregulated expression of memory cell-associated genes in *Malat1^{KD}* cells, we aimed to explore if H3K27me3-mediated epigenetic suppression was coordinately attenuated in *Malat1^{KD}* cells. We performed H3K27me3, H3K4me3, and Ezh2 ChIP-seq on *Malat1^{KD}* and *NT* cells isolated 7 days after infection. Analyses identified 5,012 differentially modified regions (DMRs) due to loss of H3K27me3 deposition (**Fig. 2.6 A**); by contrast, H3K4me3 DMRs were not found at these regions. In concordance with reduced H3K27me3 deposition, Ezh2 deposition was also reduced in H3K27me3 DMRs indicating reduced PRC2 activity at these regions (**Fig. 2.6 A**).

Genomic annotation of H3K27me3 DMRs revealed that greater than 85% of these DMRs were located within 2-3 Kb of transcription start sites and gene bodies, strengthening the notion of transcriptional dysregulation in *Malat1^{KD}* cells (**Fig. 2.7 B**). Consistent with a Malat1-mediated role in transcriptional repression, correlation of RNA-seq data with H3K27me3 DMRs demonstrated H3K27me3 loss with concurrent upregulation in gene expression (**Fig. 2.7 C**). Several memory cell-associated genes *Tcf7*, *Eomes*, *Zeb1*, *Lef1*, Id3, and *Bcl2* displayed H3K27me3 and Ezh2 loss at transcription start sites in *Malat1^{KD}* cells with associated increases in gene expression (**Fig. 2.7 D**). Together, these results suggest that Malat1 maintains H3K27me3 deposition at a number of memory cell-associated genes.

2.2.5: Malat1 interacts with Ezh2 to maintain H3K27me3 deposition

Having established the impact of Malat1 depletion in the deposition of H3K27me3, we next explored the ability of Malat1 to directly interact with Ezh2. Flow cytometry analyses of H3K37me3 expression levels at day 7 after infection confirmed global decreases within *Malat1*^{KD} TE and MP subsets compared to their *NT* counterparts, while H3K4me3 levels remained unchanged, consistent with ChIP-seq data (**Fig. 2.7 A**). However, no changes in protein expression or nuclear localization pattern of Ezh2 in *Malat1*^{KD} cells were observed, indicating that Malat1 does not regulate expression or localization of Ezh2.

We then assessed Malat1 interaction with Ezh2 using RNA-Binding Protein Immunoprecipitation (RIP) qPCR using in vitro activated CD8^{+} T cells. We observed enrichment for Malat1 as compared to housekeeping genes (*Gapdh* and *Actb*) upon Ezh2 pulldown (**Fig. 2.7 C**). Notably, knockdown of Malat1 did not impact Ezh2 interaction with other lncRNAs Xist and Neat1, demonstrating that knockdown of Malat1 specifically disrupted Ezh2-Malat1 interactions (**Fig. 2.7 D**). Together, with our Ezh2 ChiP-seq results suggest that Malat1 through direct interactions with Ezh2 is necessary to maintain H3K27me3 deposition at a number of memory cell-associated genes.

2.3: Discussion

Although a significant fraction of the CD8^{+} T cell coding genome is represented by lncRNAs, their roles remain poorly understood. We determined that over 15% of chromatin-enriched RNAs are engaged by lncRNAs, in line with previous data showing

that 25% of total poly-A captured RNAs are represented by lncRNAs in both mouse and human CD8$^+$ T cells (Hudson et al., 2019). This underscores the importance in studying this class of molecules in CD8$^+$ T cells in the context of microbial infection. Studies investigating mechanistic roles for Malat1 in transcriptional regulation have focused on interactions with various RNA processing enzymes, transcription factors, and epigenetic modifiers (Arun et al., 2018). Malat1 localizes to nuclear speckles which contain a large density of RNA Polymerase II and forms inter-chromosomal contacts, placing Malat1 in trans at regions of active transcription (Mao et al., 2011; West et al., 2014; Quinodoz et al., 2018). Our GRID-seq analysis allowed for an unbiased view of all chromatin-enriched RNAs and a direct comparison of Malat1 chromatin enrichment patterns relative to all other lncRNAs in activated CD8$^+$ T cells. We found two clusters (Clusters 1 and 2) of highly enriched trans lncRNAs; Malat1 grouped with Cluster 2 lncRNAs, which were more highly associated with gene promoters and gene bodies, whereas Cluster 1 lncRNAs were more highly associated with distal intergenic sites. While our analysis explored highly trans-interacting lncRNAs, further investigation into locally interacting lncRNAs may shed light into functional mechanisms of these classes of lncRNAs, many of which remain unexplored.

Moreover, our GRID-seq analysis focused on lncRNAs and their genomic enrichment sites, but future studies may benefit by taking the reverse approach, focusing on genomic regions with high levels of RNA interaction and then identifying unifying groups of chromatin-enriched RNAs that contribute to these high level interaction regions. In our work, we focused on known drivers of effector and memory CD8$^+$ T cell differentiation and found that Malat1 has higher levels of interactions with

genes associated with memory cell differentiation relative to those associated with terminal effector cell differentiation. Extension of this analysis to our single-cell data analysis demonstrated that genes upregulated in Cluster 0 cells also exhibited higher levels of Malat1 interaction. Many memory-associated genes in this cluster were upregulated upon Malat1 knockdown, raising the possibility that Malat1 influences transcriptional regulation through epigenetic repression, potentially through a direct interaction with Ezh2. Indeed, Malat1-interaction sites had higher levels of H3K27me3 coverage as compared to other epigenetic markers H3K27ac, H3K4me4, and H3K4me1; moreover, H3K27me3 deposition was dramatically reduced upon Malat1 depletion. We note that Malat1-interaction at H3K27me3 marks derived from TE cells than MP cells reinforcing the conclusion that Malat1 has a subset specific role in TE cells during $CD8^+$ T cell differentiation.

In concordance with increased Malat1 interactions at gene bodies and gene promoters, 86.8% at DMRs were within the transcription start sites of gene promoters, providing further evidence of Malat1 transcriptional regulation in $CD8^+$ T cells. Reduced H3K27me3 deposition on, and coordinately increased expression of, numerous memory cell-associated genes were reminiscent of the changes previously observed in Ezh2-deficient $CD8^+$ T cells (Kakaradov et al., 2017; Gray et al., 2017), consistent with the idea that Malat1 acts, in part, through its actions on Ezh2. We note that *Malat1*^{KD} cells exhibited upregulation of memory-associated genes along with downregulation of genes associated with terminal effector differentiation. Since we did not observe changes in the epigenetic activation mark H3K4me3 upon Malat1 depletion, it remains possible that Malat1 depletion promotes the activity of another epigenetic repressor acting on genes

associated with terminal effector cell differentiation. Taken together, these findings demonstrate that Malat1 may promote TE and t-T_{EM}, cell formation by repressing a transcriptional program that promotes T_{EM} cell differentiation and advance our understanding of the functional role and underlying mechanisms by which lncRNAs may influence $CD8^+$ T cell memory differentiation.

Chapter 2, in full, is an adapted version of the material that has been submitted for publication. Jad N. Kanbar, Shengyun Ma, Nadia S. Kurd, Matthew S. Tsai, Tiffani Tysl, Christella E. Widjaja, Eleanor S. Kim, Abigail E. Limary, Brian Yee, Zhaoren He, Yajing Hao, Xiang-Dong Fu, Gene Yeo, Wendy J. Huang, John T. Chang (2022). The long noncoding RNA Malat1 regulates $CD8^+$ T cell differentiation by mediating epigenetic repression. In revision. The dissertation was the primary author of all material.

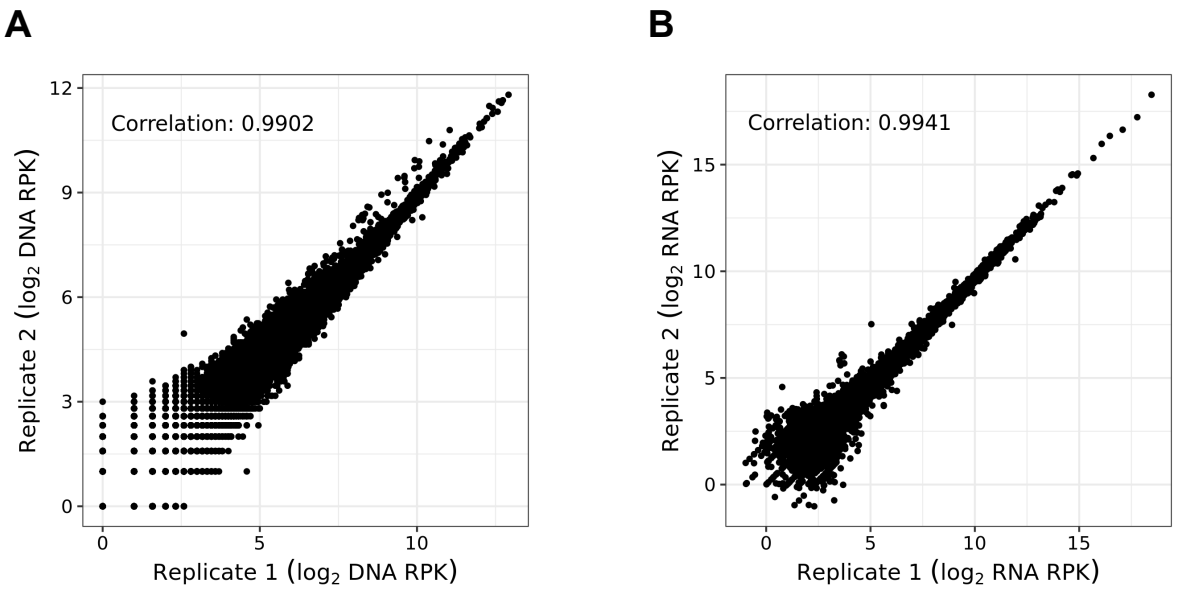

Figure 2.1. Replicate GRID-seq libraries generated repoducible RNA chromatin interaction patterns. (A) Reproducibility of GRID-seq libraries for expression of all RNA enriched chromatin (reads per kilobase, 1-Kb binned genome) and **(B)** DNA interaction level of all chromatin-interacting RNAs (reads per kilobase, 1-Kb binned genome).

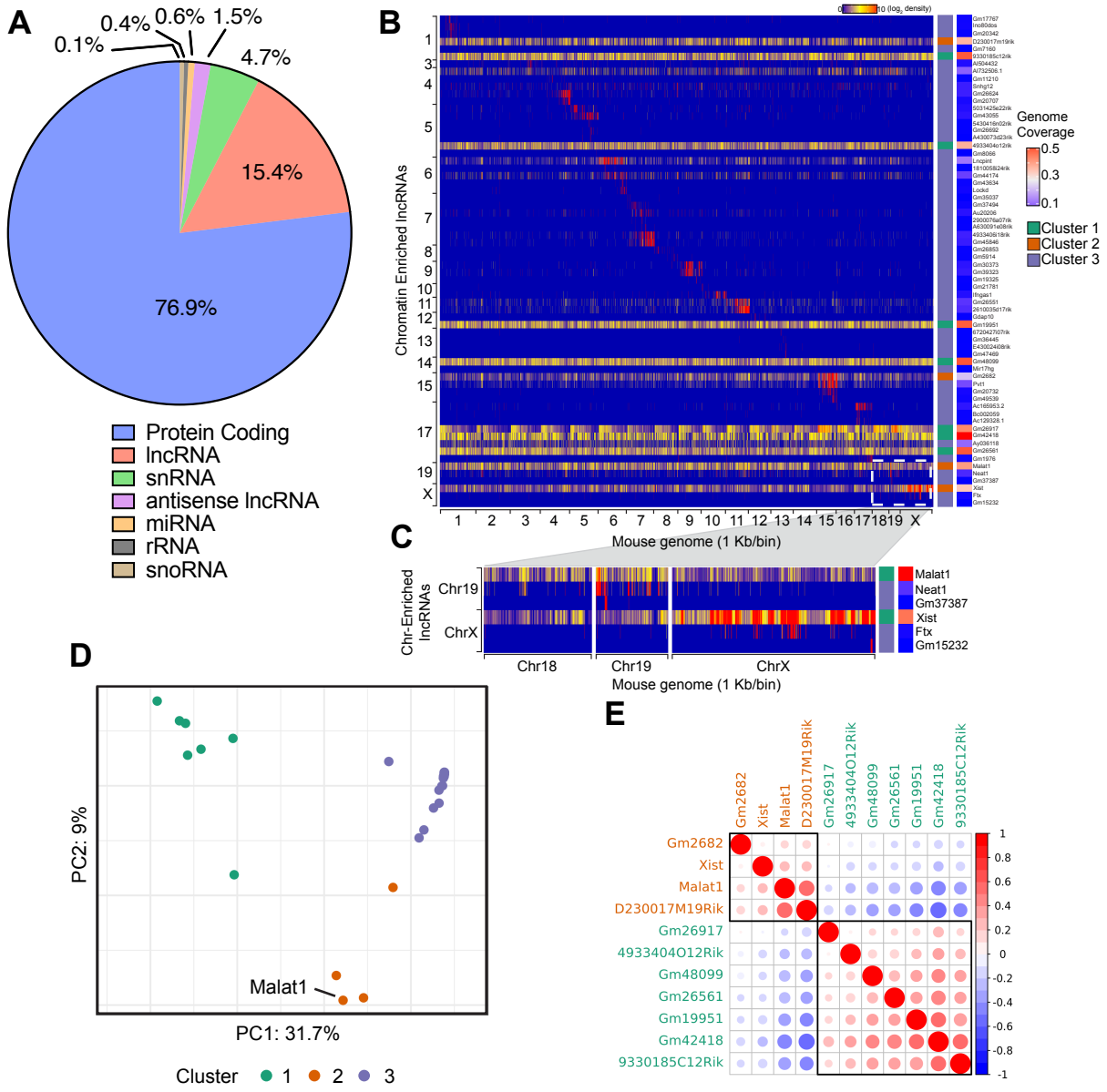

Figure 2.2. lncRNAs in activated CD8⁺ T cells are a substantial portion of all RNA chromatin interactions. (A) Distribution of genome-wide RNA chromatin interactions in P14 CD8⁺ T cells 4 days after activation. GRID-seq analyses was performed in duplicate and samples pooled together for analysis. **(B)** Heatmap of chromatin-enriched lncRNA across the murine genome. Rows represent chromatin-enriched lncRNAs and columns represent the murine genome at 1-Kb resolution. Row annotations display genome coverage of each lncRNA, and clusters colored to match those from (D). **(C)** Enlarged representative region of lncRNAs from chromosomes 19 and X and their chromatin interactions on chromosomes 18, 19, and X at 1-Kb resolution. **(D)** PCA plot and k-means clustering of lncRNAs colored by cluster groups. **(E)** Spearman correlation matrix plot and hierarchical clustering of 11 highly-*trans* lncRNAs with rectangles surrounding each cluster. lncRNA gene names are color-coded to match colors of k-means clusters in (B and C).

Figure 2.3. Malat1 clusters with *trans* lncRNAs that focus chromatin interactions on gene promoters and gene bodies. **(A)** Differential lncRNA chromatin interaction regions between Cluster 2 and 1 lncRNAs, displayed by direct comparison (box-plot; left) or genome-wide (circos-plot; right). **(B)** Number of unique gene interactions between Cluster 2 and 1 lncRNAs. **(C)** Distribution of genomic annotations from differential lncRNA chromatin interaction regions between Cluster 2 and 1. **(D)** Differential lncRNA chromatin interaction regions between Clusters 2 and 3 lncRNAs displayed by direct comparison (box-plot; left) or genome-wide (circos-plot; right). **(E)** Number of unique gene interactions between Clusters 2 or 3 lncRNAs. **(D)** Distribution of genomic annotations from differential lncRNA chromatin interaction regions between Clusters 2 and 3. Statistical significance was determined in by Student's *t* test, ***P < 0.005 (A, D) and Pearson's Chi-squared test, ***P < 0.005 (C, G). Statistical significance was determined by Student's *t* test, ***P < 0.005 (A) and Pearson's Chi-squared test, ***P < 0.005 (C).

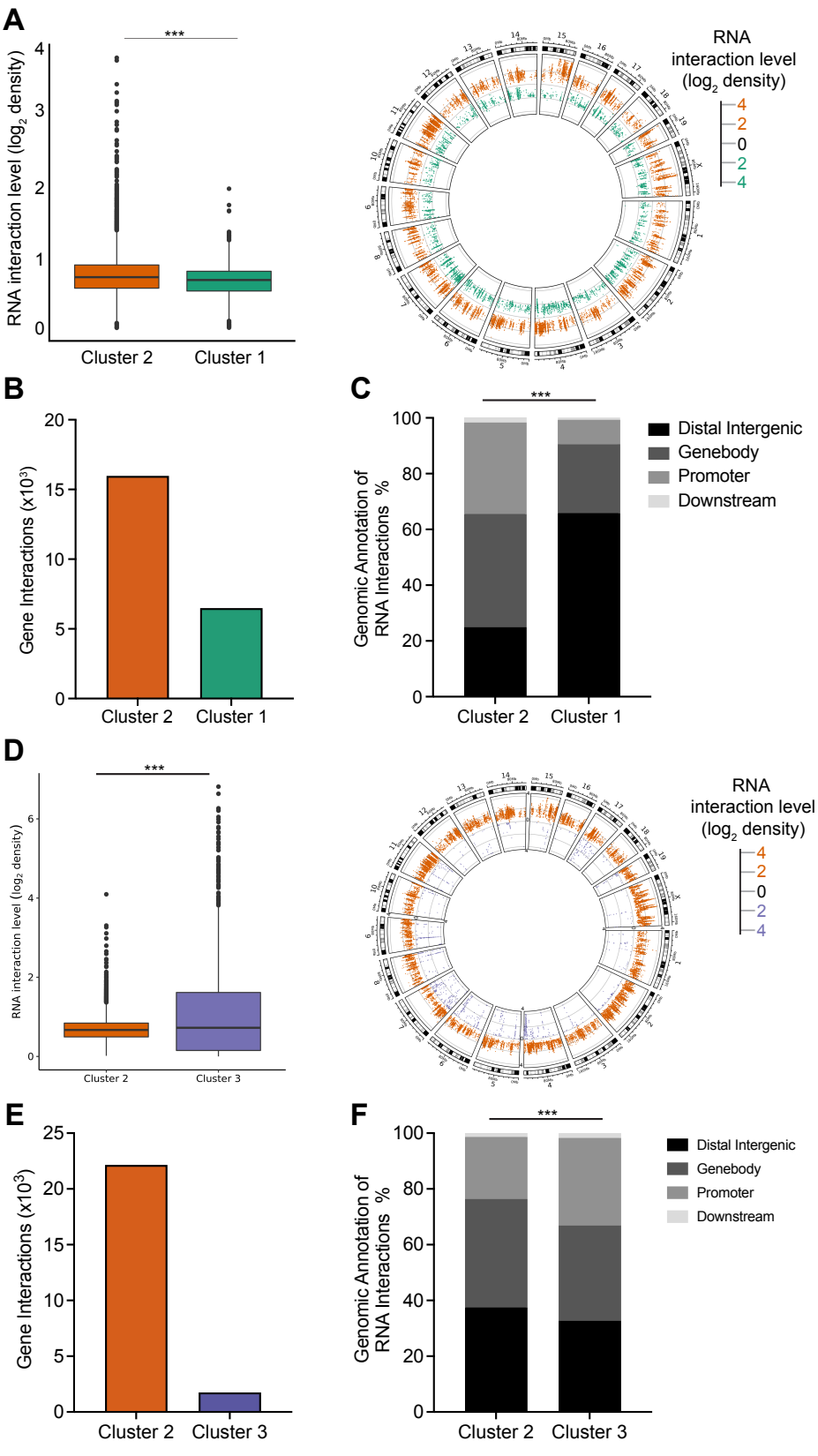
A
***
RNA interaction level (log2 density)
0
1
2
3
4
Cluster 2
Cluster 1
RNA
interaction level
(log2 density)
4
2
0
2
4
B
Gene Interactions (x10³)
0
5
10
15
20
Cluster 2
Cluster 1
C
***
Genomic Annotation of
RNA Interactions %
0
20
40
60
80
100
Cluster 2
Cluster 1
Distal Intergenic
Genebody
Promoter
Downstream
D
***
RNA interaction level (log2 density)
0
2
4
6
Cluster 2
Cluster 3
RNA
interaction level
(log2 density)
4
2
0
2
4
E
Gene Interactions (x10³)
0
5
10
15
20
25
Cluster 2
Cluster 3
F
***
Genomic Annotation of
RNA Interactions %
0
20
40
60
80
100
Cluster 2
Cluster 3
Distal Intergenic
Genebody
Promoter
Downstream

Figure 2.4. Malat1 enriches on chromatin marked by the epigenetic repressive histone mark H3K27me3. (A) Coverage heatmap of H3K27me3, H3K27ac, H4K3me3, and H3K4me1 epigenetic marks from terminal effector cells at Malat1-interacting genomic regions ± 25 Kb. **(B)** Coverage heatmap of H3K27me3 from memory precursor cells at Malat1-interacting genomic regions ± 25 Kb. **(C)** Cumulative distribution of coverage of epigenetic mark from terminal effector cells within Malat1-interacting regions at 100-Kb resolution. **(D)** Cumulative distribution of coverage of H3K27me3 marks from terminal effector and memory precursor cells within Malat1-interacting regions at 100-Kb resolution. **(E)** Normalized covered regions per 1000 bp of each epigenetic mark at Malat1-interacting genomic regions. **(F)** UMAP of all RNA chromatin interactions at 100-Kb resolution with chromosomal regions labeled (top left), Malat1-interacting regions (top right), H3K27me3-interacting regions (bottom left), and overlap interactions (bottom right). **(G)** Quantification of overlap with Malat1-interacting regions with coverage of H3K27me3. Statistical significance was determined in by Student's *t* test, ***P < 0.005 (B and C).

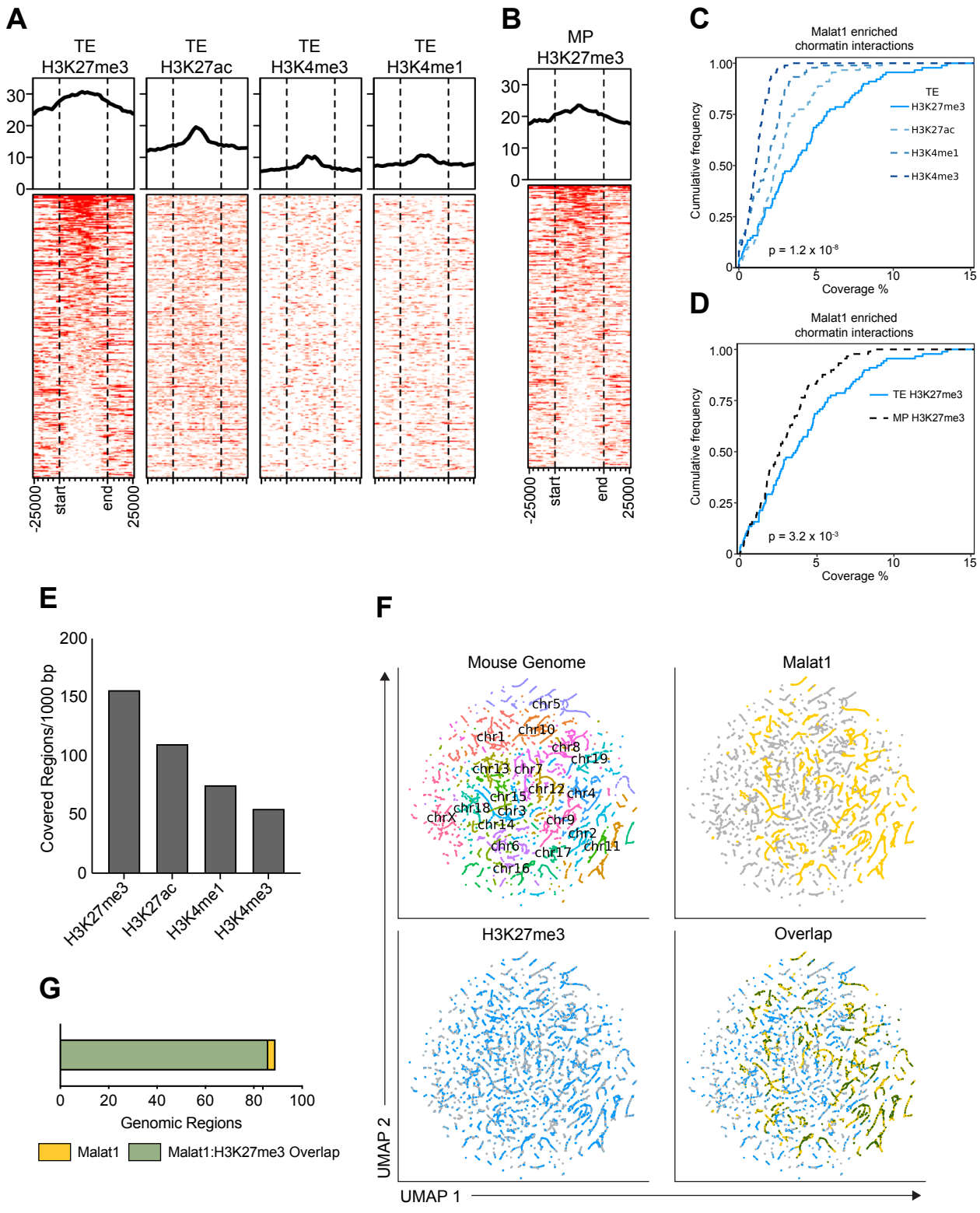
A
TE H3K27me3
TE H3K27ac
TE H3K4me3
TE H3K4me1
30
20
10
0
-25000
start
end
25000
B
MP H3K27me3
C
Malat1 enriched chromatin interactions
Cumulative frequency
Coverage %
TE H3K27me3
H3K27ac
H3K4me1
H3K4me3
p = 1.2 x 10-8
D
Malat1 enriched chromatin interactions
TE H3K27me3
MP H3K27me3
p = 3.2 x 10-3
E
Covered Regions/1000 bp
H3K27me3
H3K27ac
H3K4me1
H3K4me3
F
Mouse Genome
Malat1
H3K27me3
Overlap
UMAP 2
UMAP 1
G
Genomic Regions
Malat1
Malat1:H3K27me3 Overlap

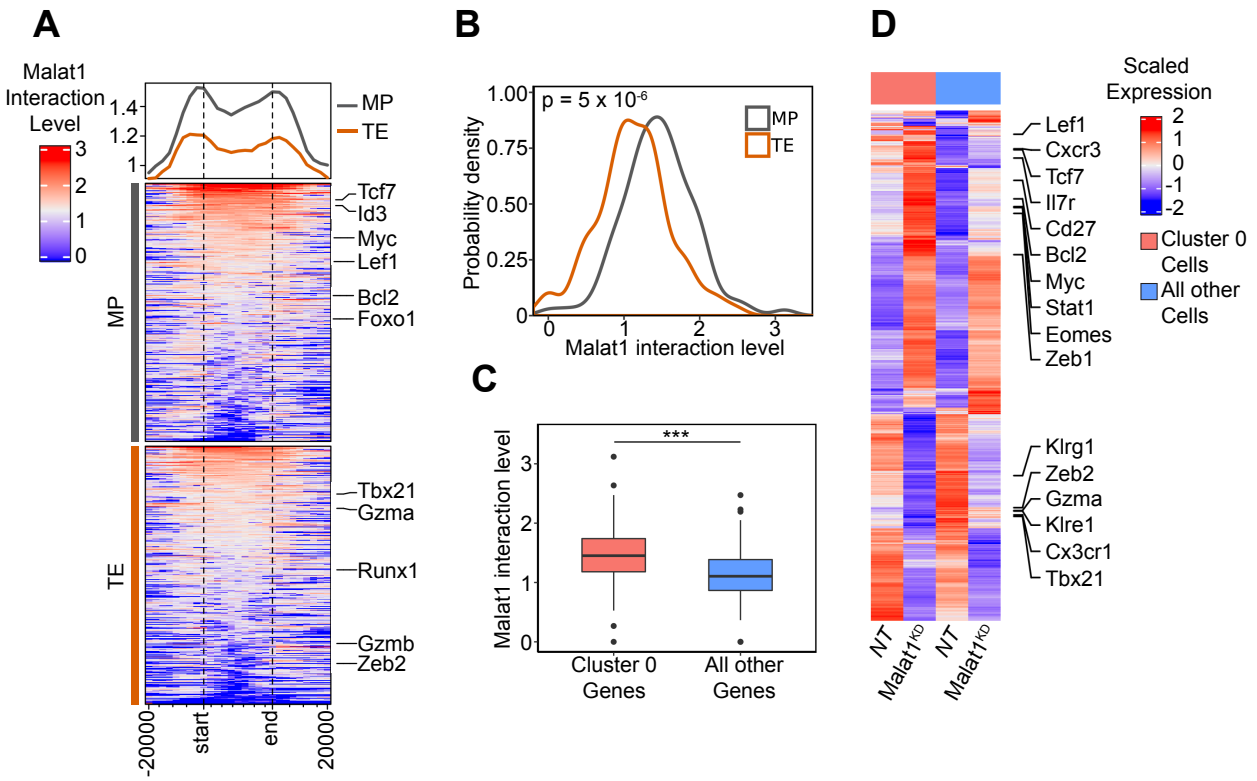

Figure 2.5. Malat1 preferentially interacts on genes associated with memory differentiation. (A) Heatmap of Malat1 interaction level on gene bodies of TE- and MP-associated genes. **(B)** Probability density distribution of Malat1 interactions from (A). **(C)** Malat1 RNA interaction level of differentially expressed genes between unique to Cluster 0 cells compared to all other cells. **(D)** Heatmap of highlighting key differentially expressed genes from (C) in Cluster 0 *Malat1*^{KD} and *NT* cells compared to all other *Malat1*^{KD} and *NT* cells. Statistical significance was determined in by Student's *t* test, ***P < 0.005 (B and C).

Figure 2.6. Malat1 maintains H3K27me3 deposition on memory-associated genes. **(A)** Deposition of H3K27me3, H3K4me3, and Ezh2 centered on H3K27me3 differentially methylated regions (DMRs) ± 2 Kb in *Malat1*^{KD} and *NT* cells at day 7 after infection. **(B)** Genomic annotations of DMRs from A. **(C)** Log fold change of H3K27me3 deposition as a function of log fold change gene expression in *Malat1*^{KD} versus *NT* cells at day 7 after infection. **(D)** Alignment tracks of H3K27me3 (*Malat1*^{KD} and *NT*), H3K4me3 (*Malat1*^{KD} and *NT*), Ezh2 (*Malat1*^{KD} and *NT*), and RNA expression (*Malat1*^{KD} and *NT*) for key genes associated with memory cells. Gray highlight and blue arrow denote H3K27me3 DMR regions.

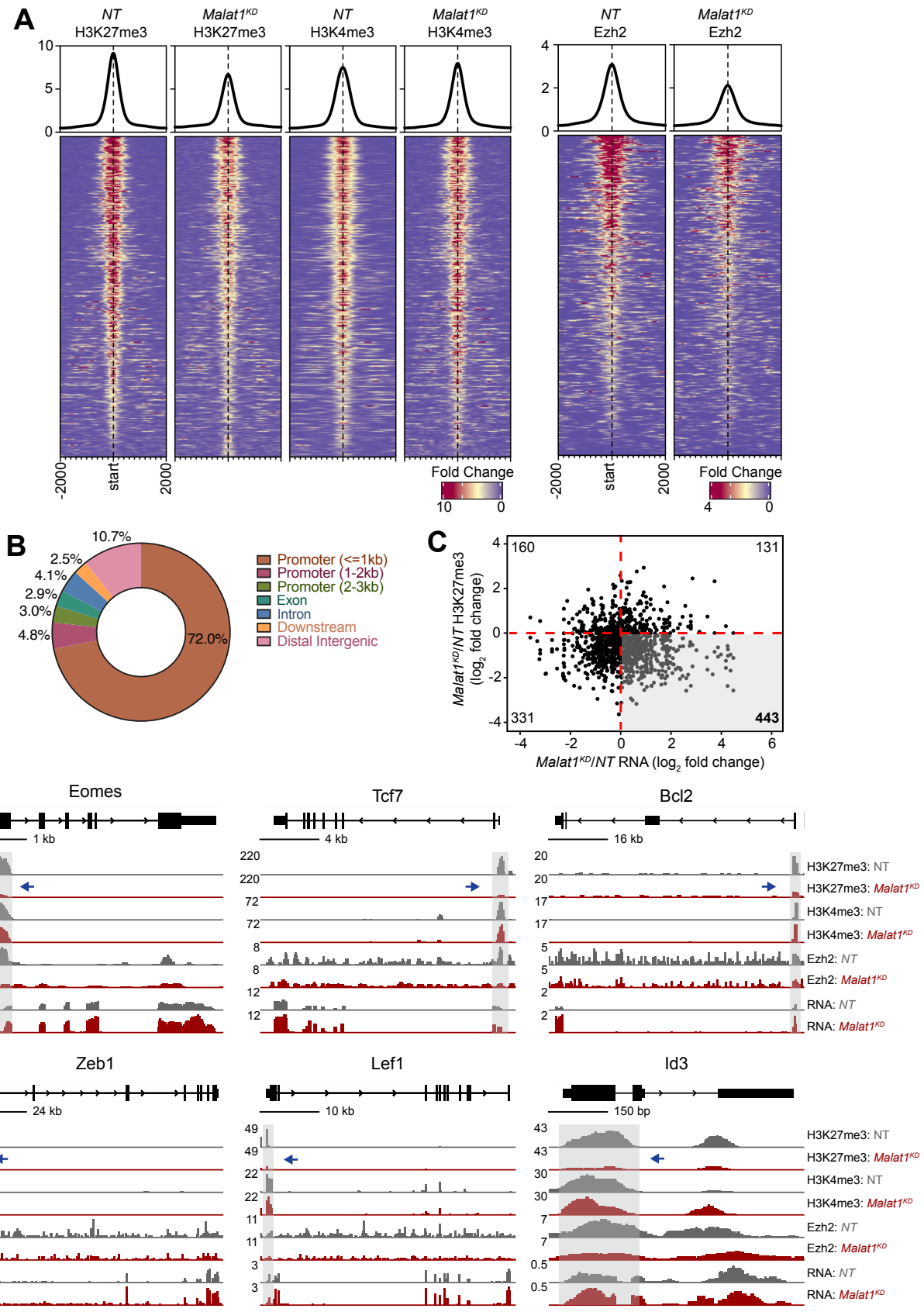
A
NT H3K27me3
Malat1KD H3K27me3
NT H3K4me3
Malat1KD H3K4me3
NT Ezh2
Malat1KD Ezh2
10
5
0
4
2
0
-2000
start
2000
Fold Change
10
0
4
0
B
10.7%
2.5%
4.1%
2.9%
3.0%
4.8%
72.0%
Promoter (<=1kb)
Promoter (1-2kb)
Promoter (2-3kb)
Exon
Intron
Downstream
Distal Intergenic
C
160
131
331
443
Malat1KD/NT H3K27me3 (log2 fold change)
Malat1KD/NT RNA (log2 fold change)
D
Eomes
Tcf7
Bcl2
1 kb
4 kb
16 kb
H3K27me3: NT
H3K27me3: Malat1KD
H3K4me3: NT
H3K4me3: Malat1KD
Ezh2: NT
Ezh2: Malat1KD
RNA: NT
RNA: Malat1KD
Zeb1
Lef1
Id3
24 kb
10 kb
150 bp

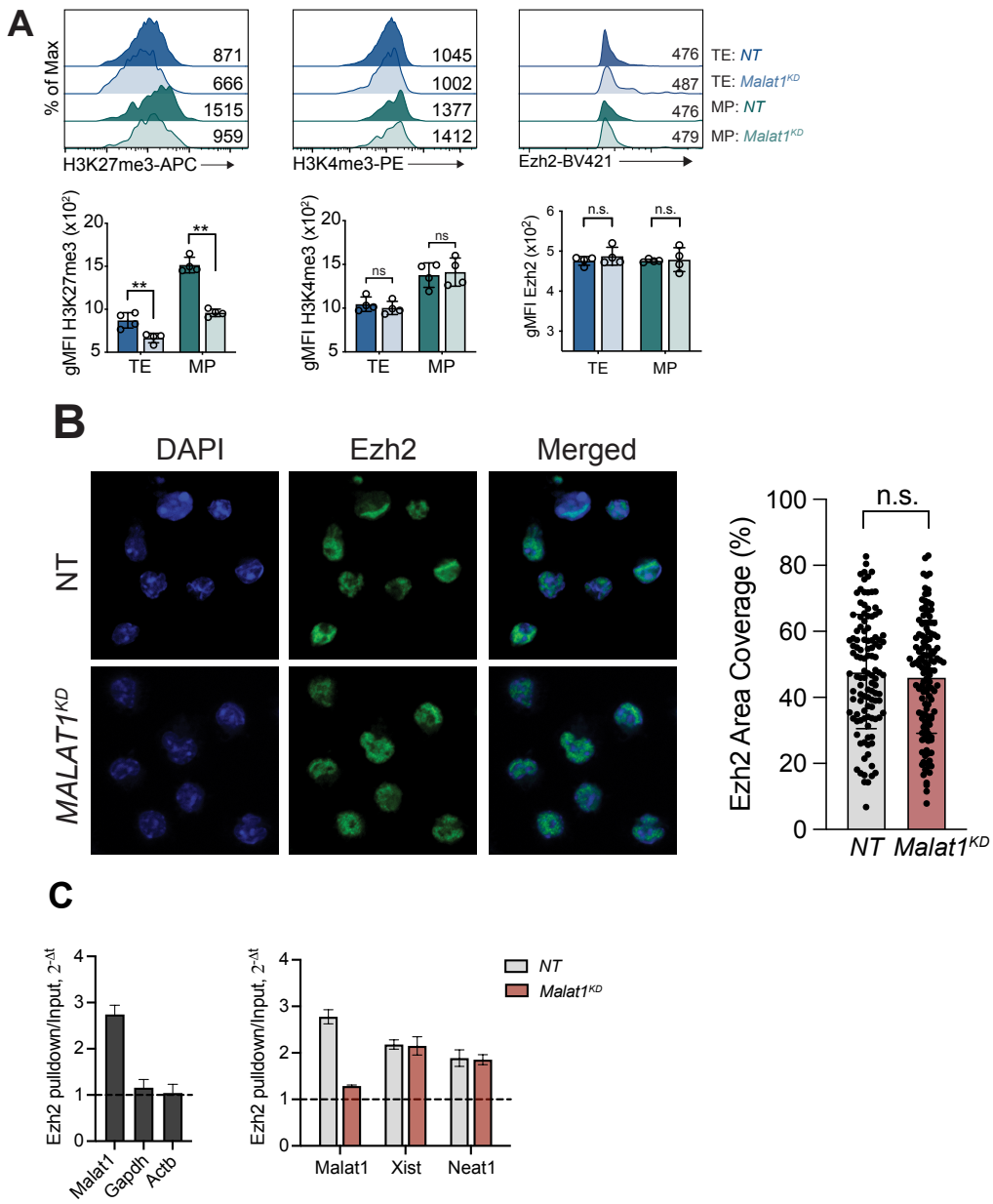

Figure 2.7. Malat1 interacts with Ezh2 to maintain H3K27me3 deposition. (A) Representative flow cytometry plots of H3K27me3, H3K4me3, and Ezh2 levels in *Malat1*^{KD} and *NT* TE and MP cells at day 7 after infection. **(B)** Ezh2 immunofluorescence in *Malat1*^{KD} and *NT* cells 5 days after *in vitro* transduction (left) and bar graph quantification of area coverage of Ezh2 within the nucleus (right). **(C)** Ezh2 pull-down RIP-qPCR analyses of Ezh2-bound RNA in wild-type CD8^{+} T cells (left) and Ezh2-bound lncRNA in *Malat1*^{KD} and *NT* cells (right). Flow cytometry data are from one representative experiment out of two independent experiments with n = 4 mice per group; *P < 0.05, ***P < 0.005, paired *t* test. Graphs indicate mean ± SEM, symbols represent individual mice (A). Statistical significance was determined in by Student's *t* test (B).

CHAPTER 3: CONCLUSION

The molecular regulation of memory $CD8^+$ T cell differentiation has been an area of intense investigation. Recent work has highlighted cell type specific expression patterns of lncRNAs in $CD8^+$ T cells, providing incentive to study this class of molecules and mechanisms of action. This dissertation aimed to explore lncRNA Malat1 and characterize its role in regulating the differentiation of $CD8^+$ T cells in response to microbial infection. Using an shRNA knockdown approach, we demonstrated that Malat1 has a critical role promoting terminal effector differentiation while suppressing memory differentiation. We found that early defects in terminal effector differentiation led to subsequent reduction of t-T_{EM} cells. Additionally, memory-associated transcription factors in $KLRG1^{hi}$ effector cells were consistently upregulated upon Malat1 depletion, further indicating a suppressive role for Malat1 in $CD8^+$ T cells.

Recent work has shown $KLRG1^{hi}$ effector cells can differentiation towards T_{EM} and T_{CM} cells suggesting the overall pool of T_{EM} and T_{CM} cells are seeded by a heterogeneous population of $KLRG1^{hi}$ and $KLRG1^{lo}$ (Herndler-Brandstetter et al., 2018, Renkema et al., 2020). This has impactions in our Malat1 knockdown data where we observe a dramatic loss of $KLRG1^{hi}$ which would in turn reduces the contribution to the overall T_{EM} and T_{CM} pool. Despite this possibility, *Malat1*^{KD} T_{EM} and T_{CM} cells persist at equivalent numbers to *NT* cells demonstrating that Malat1 has a selective effect in promoting certain circulating memory cell subsets (t-T_{EM}) but not others (T_{EM} and T_{CM}). Interestingly Malat1 did not play a critical role in the ability of primary t-T_{EM} cells to give rise to secondary t-T_{EM} cells upon infectious rechallenge, in contrast to primary T_{EM} and T_{CM} cells, which were dependent on Malat1 to give rise to secondary t-T_{EM} cells. This

suggests that Malat1 impacts multipotent cells to greater effect than cells are more terminally differentiated or have low proliferative potential as in the case of t-T_{EM} cells. Indeed, primary T_{EM}, and T_{CM} cells gave rise to a robust amount of secondary T_{EM}, important findings with regards to understanding recall response to infection.

Our single cell data generated three clusters, where two (Clusters 0 and 2) enriched for a TE signature with elevated KLRG1 expression, and one cluster (Cluster 1) that enriched for the MP gene signature. Interestingly, these KLRG1^{hi} Clusters 0 and 2 were sensitive to loss of Malat1, leading to subsequent enrichment of MP genes. Cluster 0 *Malat1*^{KD} cells were particularly sensitive to this effect resulting in upregulation of many key memory-associated genes including *Eomes*, *Tcf7*, *Zeb1*, *Lef1*, and *Bcl2*. Most *Malat1*^{KD} cells grouped with Cluster 0 suggesting the transcriptional consequence of Malat1 depletion is reflected largely in these cells. This led us to perform WGCNA analysis to find gene modules of co-expressed genes that may be regulated by Malat1. Three gene modules were differentially expressed between *Malat1*^{KD} and *NT* cells, with Module 3 expressing the highest frequency of differential expressed genes (728 of 1,856 genes; 39.2%). Module 3 annotated to T lymphocyte differentiation and activation. Cluster 0 *Malat1*^{KD} cells upregulated many of these Module 3 memory-associated genes, once again providing further evidence that Malat1 may act as a transcriptional repressor.

A prior report using a germline deletion model demonstrated that Malat1 was dispensable for CD8^{+} T cell responses in LCMV infection (Yao et al., 2018), in contrast to the defects we observed in the current study using acute knockdown approaches. A possible explanation for these disparate results is that germline deletion models may

have led to compensatory effects, as has been previously observed in T cells (El-Brolosy and Stainier, 2017). For example, deletion of the DNA epigenetic modifier *Tet2* did not lead to any obvious defects in T cell development, but deletion of both *Tet2* and *Tet3* led to a massive lymphoproliferative phenotype (Tsagaratou et al., 2017; Lio and Rao, 2019), suggesting that Tet2 and Tet3 may be able to compensate for each other. As another example, T lymphocyte proliferation and immune function was unaffected by the deletion of *Rbl2*, a recruiter of histone methyltransferases, likely due to compensation by *Rbl1* (Mulligan et al., 1998). Since lncRNAs represent a substantial fraction of chromatin-enriched RNAs, future studies elucidating chromatin-enriched lncRNAs in a Malat1 knockout model may reveal which lncRNA interactions are upregulated at sites normally occupied by Malat1.

In this dissertation we utilized GRID-seq to evaluate unique features of Malat1 chromatin interaction patterns relative all other lncRNAs in activated $CD8^+$ T cells. Interestingly, unsupervised k-means clustering found three clusters of lncRNAs based on their chromatin interaction patterns. Two of these clusters contained highly *trans* interacting lncRNAs with high coverage of the genome. What was striking was even though both clusters were highly *trans*, they had unique genomic interaction features. Malat1 grouped with a cluster of lncRNAs with preferential interaction at gene bodies and promoter regions. This finding lends to the hypothesis that Malat1 may be involved in transcriptional regulation. Indeed, we found high correlation of Malat1 interaction regions and coverage of the histone repressive mark H3K27me3. Furthermore, Malat1 interaction was significantly higher on gene bodies of MP-associated genes relative to TE-associated genes indicating preferential interaction at genes that Malat1 may

repress. We tested this hypothesis by performing H3K27me3 ChIP-seq in *Malat1*^{KD} cells demonstrating reduction of H3K27me3 was concentrated mostly at promoter sites which is in support of our GRID-seq data suggesting preferential interaction of Malat1 at gene bodies and promoters. Importantly H3K27me3 reduction was coupled with increased expression including key memory-associated genes.

We note that *Malat1*^{KD} cells exhibited upregulation of memory-associated genes along with downregulation of genes associated with terminal effector differentiation. Since we did not observe changes in the epigenetic activation mark H3K4me3 upon Malat1 depletion, it remains possible that Malat1 depletion promotes the activity of another epigenetic repressor acting on genes associated with terminal effector cell differentiation. One such mechanism may be through DNA methylation, which is often associated with gene silencing. Indeed, previous work has shown that naive cell activation led to DNA demethylation of many effector cell-associated loci including *Prf1*, *IFN*γ and *Gzmk* (Youngblood et al., 2017). Taken together, this dissertation demonstrates that Malat1 may promote terminal effector and t-T_{EM} cell formation by epigenetically repressing a transcriptional program that promotes memory differentiation and advances our understanding of the functional role and underlying mechanisms by which lncRNAs may influence $CD8^+$ T cell memory differentiation.

APPENDIX A: MATERIALS AND METHODS

Mice

All mice were housed under specific pathogen–free conditions in an American Association of Laboratory Animal Care–approved facility at UCSD, and all procedures were approved by the UCSD Institutional Animal Care and Use Committee. C57BL6/J ($CD45.1.2^+$ or $CD45.2^+$) and P14 TCR transgenic ($CD45.1^+$ or $CD45.1.2^+$, maintained on a C57BL6/J background) mice were bred at UCSD or purchased from the Jackson Laboratories. Recipient male and donor female mice used in adoptive transfer experiments were all 6 to 9 weeks of age. No randomization of blinding was used in infection experiments and only mice that had rejected adoptively transferred P14 $CD8^+$ T cells were excluded.

$CD8^+$ *T cell isolation*

For isolation of $CD8^+$ T cells from spleen and peripheral lymph nodes, tissues were dissociated through 70 μm cell strainers. Cells were then treated with Red Blood Cell Lysis Buffer for 5 minutes. $CD8^+$ T cells were then enriched using the $CD8a^+$ T Cell Isolation Kit and LS MACS Columns (Miltenyi Biotec, Catalog number: 130-104-075) according to the manufacturers protocol. For $CD8^+$ T cells isolated from tissues, small intestines were resected, Peyer's patches removed, and washed with phosphate-buffered saline (PBS). Tissues were then cut into 1 cm and incubated in DTE buffer [dithioerythritol (1 μg/ml; Thermo Fisher Scientific) in 10% Hanks' balanced salt solution and 10% Hepes bicarbonate] at 37°C for 30 min. Lymphocytes were then enriched using a 44/67% Percoll density gradient. $CD8^+$ T cells were maintained in T cell media

(TCM) [Iscove's Modification of DMEM (Catalog number: 10-016-CV) supplemented with 10% fetal bovine serum (v/v), 2 mM L-Glutamine (Catalog number: 25030149), 100 U/mL Penicillin-Streptomycin (Catalog number: 15140122), and 55 mM μl 2-Mercaptoethanol (Catalog number: 21985023)] at 37°C.

Antibodies and flow cytometry

Surface proteins were stained for 10 minutes on ice in Hank's Balanced Salt Solution (Catalog number: 21-021-CV) with the following antibodies: Vα2 (B20.1), CD8α (53-6.7), CD45.1 (A20), CD44 (), CD45.2 (104), KLRG1 (2F1/KLRG1), CD127 (A7R34), CD27 (LG.3A10), CX3CR1 (SA011F11), CD62L (MEL-14), CD69 (H1.2F3), CD103 (2E7), all purchased from BioLegend. For intracellular protein staining, samples were fixed in 2% paraformaldehyde (Electron Microscopy Services, Catalog number: 15710) at room temperature for 45 minutes. Cells were then permeabilized using the FoxP3/Transcription Factor Staining Buffer Kit (ThermoFisher, Catalog number: 00-5523-00) and stained for 8 hours at 4°C with the following antibodies: Tcf7 (C63D9), Eomes (Dan11mag), Bcl2 (BCL/1064), Ezh2 (11/EZH2), Ki67 (B56), Zeb1 (E2G6Y), Lef1 (C12A5), Id2 (ILCID2), Gzma (GzA-3G8.5), Gzmb(GB11), T-bet (4B10), H3K27me3 (C36B11), and K3K4me3 (C42D8), purchased from BioLegend, Cell Signaling, BD Biosciences, and ThermoFisher.

shRNA CD8$^+$ *T cell transfers, infection and treatments*

shERWOOD-designed UltramiR sequences targeting Malat1 (*Malat1*^{KD}, *Malat1*$^{KD\ \#2}$, *Malat1*$^{KD\ \#3}$) and Nontarget Control (*NT*) in an LMP-d Ametrine vector backbone were

purchased from transOMIC technologies (Table S1). To generate retroviral particles, platinum E cells were grown in 10 cm plates with full selection media [DMEM (Catalog number: 11965-118), 10% FBS (v/v), 2 mM L-Glutamine (Catalog number: 25030149), 100 U/mL Penicillin-Streptomycin (Catalog number: 15140122), 1 μg/mL puromycin and 10 μg/mL blasticidin]. Eighteen hours before transfection, selection media was replaced with antibiotic-free media (DMEM, 10% FBS (v/v), 2 mM L-Glutamine). For each 10 cm plate, 10 μg of each shRNA and 5 μg pCL-Eco helper plasmids were mixed in Opti-MEM (catalog number: 31985062) to a volume of 700 μl. This was combined with 45 ul *Trans*IT-LT1 Reagent and 655 μl Opti-MEM for 20 minutes at room temperature. The mixture was then added dropwise to each 10 cm plate. Twelve hours later, media was replaced with fresh antibiotic-free media and supernatant was subsequently harvested at 24 and 48 hours. Retroviral supernatant was filtered through a 0.45 μm syringe filter and stored at -80C.

Naive WT or P14 $CD8^+$ T cells were plated at a density of 1×10^6 cells/mL in 24 well plates precoated with 100 μg/ml goat anti-hamster IgG (Catalog number: 31115), followed by 5 μg/ml each of anti-CD3 (clone 3C11) and anti-CD28 (clone 37.51). Eighteen hours after activation, media was removed and replaced with 1 mL of retrovirus supplemented with 8 μg/mL polybrene followed by centrifugation for 90 minutes at 2000 rpm. Retroviral supernatant was removed and replaced with fresh TCM media allowing cells to rest 37°C for 2 hours.

For co-transfer experiments, *Malat1*^{KD} and *NT* P14 cells were mixed at a 1:1 ratio and a total of 5×10^5 donor cells/mouse was adoptively transferred into $CD45.2^+$ male recipient mice. One hour later, mice were infected with 2×10^5 PFU LCMV-Armstrong.

Seven and 35 days after infection, mice were euthanized and spleens and small intestine intraepithelial compartments were harvested and cells analyzed by flow cytometry to determine ratio of *Malat1*^{KD}/*NT* cells. For cell cycle analysis, 4.5 days after infection, 1 mg/mouse of BRDU was injected and mice euthanized 5 hours later. Staining for BRDU incorporation and 7-AAD was performed according to the manufacturer's protocol (BD Biosciences, Catalog number: 552598).

For rechallenge assays, 35 days after infection, *Malat1*^{KD} and *NT* P14 cells were FACS-sorted into three populations: CD127^{lo}CD62^{lo} t-T_{EM}, CD127^{hi}CD62l^{lo} T_{EM}, and CD127^{hi}CD62L^{hi} T_{CM}, constituting the donor populations. Donor *Malat1*^{KD} and *NT* cells from each memory population were mixed at a 1:1 ratio for a total of 10,000 donor cells/mouse and adoptively transferred into naive male CD45.2^{+} recipient mice and infected with 2×10^5 PFU LCMV. Thrifty-five days after secondary rechallenge infection, mice were euthanized to determine *Malat1*^{KD}/*NT* ratio.

For *ex vivo* restimulation to assess cytokine production, P14 CD8^{+} T cells were plated in a 96 well at 5x10^6 cells/well in the presence of 1 ng/μl LCMV GP33–41 peptide (Genscript, Catalog number: RP20257) and 1X Brefeldin A Solution (BioLegend, Catalog number: 420601) for 6 hours at 37°C. Cells were then fixed and permeabilized using BD Cytofix/Cytoperm (Catalog number: 554714) and stained for IFN-γ (XMG1.2), TNF-α (MP6-XT22), and IL-2 (JES6-5H4) antibodies all purchased from BioLegend for 30 minutes on ice. Flow cytometry of all samples were run on a LSRFortessa X-20 (BD Biosciences) or Novocyte (ACEA Biosciences). FACS sorting of cells was done on a FACSAria Fusion or FACSAria2 (BD Biosciences). FlowJo software (BD Biosciences) was used for analysis of flow cytometry data.

Pooled shRNA screen and validation of individual Malat1 constructs

A pooled LMP-d Ametrine plasmid library consisting of 375 shRNA constructs with replicates for 103 genes and 5 nontarget controls was purchased from transOMIC technologies (Table S1). Retroviral particles were made and stored as described above. Multiplicity of infection was determined by serially diluting the retroviral supernatant two-fold and performing activation and transfection as described above. Twenty-four hours after transfection, a dilution factor which yielded a 15-25% of Ametrine^{+} cells was determined. Next, 5x10^{5} transfected P14 cells were adoptively transferred into naive CD45.2^{+} recipient mice and infected with LCMV. To determine the baseline distribution of all shRNAs in the plasmid pool, part of the adoptive transfer mixture was grown for 24 hours in IL-2 (100 U/mL), and Ametrine^{+} cells were sorted and genomic DNAs were extracted (ThermoFisher, Catalog number: K182001). Seven days after infection, 20 mice were euthanized, spleens extracted, and Amtetrine^{+} CD8^{+} T cells were sorted into KLRG1^{hi}CD127^{lo} terminal effector (TE) and KLRG1^{lo}CD127^{hi} memory precursor (MP) populations. Genomic DNA was extracted and integrated shRNA constructs were amplified with two rounds of PCR, adding TruSeq indexed barcodes for shotgun sequencing (transOMIC technologies, Catalog numbers: TRP0001, TRP0002). Libraries were sequenced on a HiSeq 4000. Sequencing reads were mapped to the reference plasmid library. TE and MP reads were normalized to the input reads followed by taking the log2 ratio of TE/MP for every unique shRNA in the library. Z-score values for all shRNAs were calculated as follows:

$$Z(shRNA) = \frac{log2_2\left(\frac{MP_{KD}}{TE_{KD}}\right) - mean\left(log_2\left(\frac{MP_{NT}}{TE_{NT}}\right)\right)}{mean\left(SD\left(\frac{MP_{NT}}{TE_{NT}}\right)\right)}$$

Individual Malat1 shRNA constructs were validated for knockdown efficiency by sorting WT CD8$^+$ T cells 5 days after *in vitro* transduction. Total RNA was extracted using a Qiagen miRNeasy Micro Kit according to the manufacturer's protocol (Catalog number: 217084). Two-hundred nanograms of RNA was converted to cDNA using the Bio-Rad Script cDNA Synthesis Kit according to manufacturer's protocol (Catalog number: 1708890) and diluted with water for a final 1:5 dilution. Quantitative PCR was performed with 1 ng template per reaction using the Bio-Rad SsoAdvanced Universal SYBR Green Supermix according to manufacturer's protocol (Catalog number: 1725270) on a BioRad CFX. Three primer sets tiling the Malat1 locus [base pair (bp) position 2670-2885: GGGTGGGGGTGTTAGGTAAT, GGCAGAGGAACCAACCTTC. bp position 3143-3279: TGATTTTCCTTGTGACTAAACAAGA, AAGCCCACCCTCTAAAAGACA. bp position 4546-4741: AGGTGGGAGATGATGGTCAG, ACTCGTGGCTCAAGTGAGGT] and one primer set to RPL13a [bp position 41-257: GGGCAGGTTCTGGTATTGGAT, GGCTCGGAAATGGTAGGGG] as a control were used. Knockdown efficiency was quantified using the $2^{-\Delta\Delta C_T}$ method, $2^{-([MALAT1-RPL13a]_{KD} - [MALAT1-RPL13a]_{NT})}$.

Bulk RNA-seq library generation and analysis

Malat1^{KD} and *NT* P14 CD8$^+$ T cells were sorted 7 days after LCMV infection and total RNA extracted using a Qiagen miRNeasy Micro Kit. RNA quality was evaluated

using the Agilent TapeStation, confirming samples all with RIN scores >9.8. Samples were submitted to the UCSD Institute for Genomic Medicine (IGM) for TruSeq V2 mRNA library prep. Libraries were then sequenced on a HiSeq 4000. Sequencing reads were mapped to mm10 reference genome using STAR aligner (v2.7.6a) with default parameters. Mapped reads to genes were summarized using featureCounts (v1.5.3) with default parameters. This table was used as input for differential gene analysis using DeSeq2 (v1.32.0).

Bulk RNA-seq terminal effector and memory precursor datasets (GSE157072) were used in single cell gene enrichment analysis and mapped as described above. DeSeq2 (v1.32.0) was used to determine differentially expressed TE and MP genes keeping that demonstrated fold-change >1.5.

Single-Cell RNA-seq library generation and analysis

Malat1^{KD} and *NT* P14 CD8^{+} T cells were sorted 7 days after LCMV infection and resuspended in phosphate-buffered saline (PBS) + 0.04% (w/v) bovine serum albumin. 10,000 cells per sample were loaded into Single Cell A chips and partitioned into Gel Bead In-Emulsions in a Chromium Controller (10x Genomics). Single-cell RNA (scRNAseq) libraries were prepared with 10x Genomics Chromium Single Cell 3′ Reagent Kits v2 according to the manufacturer's protocol. Libraries were sequencing on a HiSeq 4000.

Reads from scRNA-seq were aligned to mm10 using the 10x Genomics Cell Ranger software (v 2.1.0). Reads were collapsed into unique molecular identifier counts. All samples had >2000 cells detected with >1000 genes per cells with >70% of

the coding genome covered. Genes that were not expressed in at least 5% of all cells were excluded. As previously described (Boland et al., 2020), replicates single cell libraries were normalized removing batch effects using RUVnormalize (v1.15.0). The raw UMI matrix was scaled and input to the naiveRandRUV function with parameters coeff=1e-3 and k=10. Fifty negative control genes were taken from a list of housekeeping genes (Eisenberg and Levanon, 2013) with least variability in all datasets. Seurat (v3.0.1) functions were used on the normalized matrix to calculate top variable genes, principal components analysis (PCA), and tSNE with FindVariableGenes, RunPCA, and RunTSNE. The top 5000 genes were considered as input for the PCA calculation, and only the top 25 principal components (PCs) were used in tSNE. Louvain clustering was performed by Seurat's FindClusters function based on the top 25 PCs, with resolution set to 0.9. Differentially expressed genes was performed between clusters or within clusters comparing *Malat1*^{KD} and *NT* cells using two-sided Wilcox test and threshold of $p < 0.05$. The AddModuleScore function was used gene enrichment analysis using TE and MP gene sets (GSE157072) as described above.

Weighted gene co-expression network analyses (WGCNA V1.63) was performed on a supercell matrix using the RUV normalized matrix to determine nearest neighbor cells to average as previously described (Kurd et al., 2020, https://github.com/Arthurhe/Lightbulb). The supercell matrix merged created an averaging expression of 50 nearest neighbor with seed single cells taken at random. Each cell was covered 10 fold creating 2,329 supercells. All genes were used in WGNA using Softpower set to 8 and gene module classification was calculated from the signed

adjacency matrix. Average hierarchical clustering using the hclust function was used for Genetree and eigengene clustering with a module cut height of 0.1. We performed GO analysis using compareCluster (clusterProfiler v3.0.14) and mouse reference database (org.Mm.eg.db v3.14.0) with parameters fun = ”enrichGO”, pAdjustMethod = "fdr", pvalueCutoff = 0.01 and qvalueCutoff = 0.05).

ChIP-seq library generation and analysis

Malat1^{KD} and *NT* P14 CD8^{+} T cells were sorted 7 days after LCMV infection and fixed in 1% fresh formaldehyde. Chromatin was then prepared using the EMD Millipore Magna ChIP A/G Chromatin Immunoprecipitation Kit according to manufactures protocol (Catalog Number: 1710085) and flash frozen in liquid nitrogen. Nuclei were sheared in Covaris microTUBES (Catalog number: 520045) using the Covaris E220 (Peak Incident Power 175W, Duty Factor 10%, Cycles per Burst 200, Treatment Time 600 seconds). For each immunoprecipitation (IP), 3 μg antibody per 1×10^6 cell equivalents were used for overnight incubation at 4°C. Antibodies used for IPs were as follows: anti-H3K27me3 (07-449, EMD Millipore) and anti-H3K4me3 (ab8580, abcam), anti-Ezh2 (AC22, 07-449, EMD Millipore). Five percent of each sample was kept as input control. Samples were then submitted for KAPA DNA Library Preparation and sequencing on a HiSeq400.

Libraries were filtered and mapped to the mm10 genome using ENCODE Transcription Factor and Histone ChIP-Seq processing pipeline with default parameters for histone marks (github.com/ENCODE-DCC/chip-seq-pipeline2). Final pooled bigwig files were used for visualization. Mapped non-duplicate read bam files for each

biological replicate and overlapped optimal Irreproducible Discovery Rate (IDR) peaks were used as inputs for DiffBind (v4.1.0). Differentially modified regions (DMRs) between *Malat1*^{KD} and *NT* were determined with a False Discovery Rate of less than 0.1. DMRs were annotated to their closest gene using CheapAnnoseak (v3.20.0) and genomic annotations using ChiPseeker (v1.22.0).

H3K27me3 (GSE111902, TE and MP), H3K4me3 (GSE95238, TE), H3K27ac (GSE111902, TE), and K3K4me1 (GSE95238, TE) and input ChIP-seq libraries were mapped to the mm10 genome using ENCODE Transcription Factor and Histone ChIP-Seq processing pipeline with default parameters for histone marks. Optimal IDR peaks for each histone mark were used as peak calls and coverage quantification in GRID-seq analysis.

GRID-seq library generation and analysis

Spleens from P14 mice were homogenized, and 1x10^6 cells/mL in TCM were pulsed with 1 ng/μl LCMV GP$_{33–41}$ peptide for 1 hour at 37°C. Cells were washed once with equal volume of warm TCM, then plated in a 96 well-plate at 5x10^4 cells/well. Cells were harvested 4.5 days later and dead cells removed using the Dead Cell Removal kit according to the manufacturer's protocol (Miltenyi Biotec, Catalog number: 130-010-101). CD8$^+$ T cells were then enriched using the CD8a$^+$ T Cell Isolation Kit. Cells were then cross-linked, nuclei isolated and GRID-seq libraries prepared as described previously (Li et al., 2017; Zhou et al., 2019). Final libraries were sequenced on HiSeq4000.

Reads were trimmed with cutadapt -l 86 --max-n 5 -o (v1.18), mapped to RNA-Linker-DNA (GTTGGATTCNNNGACACAGCTCACTCCCACACACCGAACTCCAAC) with bwa mem -k 5 -L 4 -B 2 -O 4 (v0.7.15) and sorted with samtools sort (v1.7). RNA and DNA reads were separated with GridTools matefq (https://github.com/biz007/gridtools). Reads were then mapped to the mm10 genome with bwa mem -k 17 -w 1 -T 1. GridTools evaluate was then used to correct against background and RNA-DNA mate read pair quality and quantity with bin size of 1 kb and moving windows of 10. GridTools RNA was used to identify expression levels of chromatin-enriched RNA. GridTools matrix was used to construct an interaction contact matrix of chromatin-associated RNA within specified genomic bin sizes of 1 kb or 100 kb. All lncRNAs with reads per kilobase DNA read density ≥10 on any genomic region were filtered from the interaction contact matrix. A 1 kb interaction matrix was directly visualized on a heatmap using the ComplexHeatmap package (v2.2.0). PCA, k-means clustering set to 3 clusters, and pearson correlation analysis were performed on the interaction matrix with the R stats package (v3.6.2). The correlation matrix was visualized with corrplot package (v0.89) and circos plots with the circlize package (v0.42). Differential RNA chromatin interaction regions were determined by taking the average RNA interaction level of each genomic bin for all lncRNAs in a cluster. These averaged genomic bins were annotated to the transcription start site of the nearest gene using the ChIPpeakAnno. Consecutive genomic bins annotated to a single gene with greater RNA interaction for each genomic bin in one cluster relative to another cluster were considered differentially interacting. Differential RNA chromatin interaction regions were annotated with ChiPseeker.

Bedtools coverage (v2.29) was used to calculated coverage of histone marks, H3K27me3, H3K27ac, H3K4me3, H3K4me1, on Malat1 interacting chromatin regions Malat1 interaction level was averaged over the gene body of terminal effector genes, memory precursor genes, and scRNAseq cluster 0 and 2 differentially expressed genes.

RIP preparation and analysis

Ten million *Malat1^{KD}* and *NT* P14 CD8^{+} T cells were sorted 5.5 days after transduction, washed twice in cold PBS, and lysed with the EMD Millipore Magna RIP RNA-Binding Protein Immunoprecipitation Kit according to the manufacturer's protocol (Catalog number: 17-700). Lysates were then flash frozen in liquid nitrogen. Ten percent of each lysate was removed as input control while the remaining lysates of each sample was immunoprecipitated with 5 μg of anti-Ezh2 (AC22) overnight at 4°C. Final bound RNA was quantified with Qubit HS RNA (Catalog number: Q32852) and 200 ng of each pull down sample with matched input were converted into cDNA (Catalog number: 1708890). Quantitative PCR was performed with a primer sets against Malat1 (bp position 3143-3279), Gapdh [bp position 683-925: AGAGAGGGAGGAGGGGAAAT, GATTTTCACCTGGCACTGCA] and Actb [bp position 1388-1602: ACTGGGACGACATGGAGAAG, ATGGGAGAACGGCAGAAGAA], with fold change calculated, $2^{-\Delta(KD-Input)}$.

Immunofluorescence and analysis

Malat1^{KD} and *NT* P14 CD8^{+} T cells were sorted 5.5 days after transduction. Cells were dried on a microscope coverslip at 37°C for 10 minutes, fixed in 3% PFA at room

temperature, then quenched for three washes with 50 mM NH_4Cl. Slides were then permeabilized with 0.3% Triton X-100 in PBS followed by 1X Block treatment (5X, 0.01% sap, 0.25% fish skin gelatin, 0.02% NaN_3 in PBS). Primary antibody staining anti-Ezh2 (AC22) was diluted 1:50 in PBS for 1 hour at room temperature followed by 5 washes with 1X Block. Secondary antibody staining was performed with Alexa Fluor 488 Donkey anti-rabbit IgG (Biolegend, Catalog number: 406417) diluted 1:200 in PBS for 1 hour at room temperature followed by 5 washes with 1X Block. Coverslips were mounted on glass slides with Prolong Glass Mounting Reagent containing DAPI (Thermo Fisher, Catalog Number: P36981) and left in the dark at room temperature overnight. Imaging was performed on a Leica SP8 Confocal with Lightning Deconvolution at 63X magnification. Minor adjustments of brightness and contrast were made equally to all images with ImageJ (v1.53a). Color channels were split and converted to grayscale 8-bit images. The DAPI channel was converted to a binary mask, edges of each nuclei found, then added as regions of interest (ROI). The Ezh2 channel was converted to a binary image, ROI overlayed, and percentage area was calculated to quantify coverage of Ezh2 within each nucleus.

APPENDIX B: SUPPLEMENTARY TABLES

Supplementary Table 1: Z-scores and shRNA Hairpin Sequences from the pooled screen results of all shRNAs.

Gene	MP/TE (Z-score)	shRNA Hairpin Sequence
Sept11	1.16140341	TGCTGTTGACAGTGAGCGAGTCAACAAATCCACTTCTCAATAGTG AAGCCACAGATGTATTGAGAAGTGGATTTGTTGACCTGCCTACTG CCTCGGA
Sept11	0.80304013	TGCTGTTGACAGTGAGCGCCGTACGGCTGAAGCTAACAAATAGTG AAGCCACAGATGTATTTGTTAGCTTCAGCCGTACGTTGCCTACTG CCTCGGA
Anp32b	1.74265287	TGCTGTTGACAGTGAGCGCACAGATGAATTTGTGAACTTATAGTG AAGCCACAGATGTATAAGTTCACAAATTCATCTGTTTGCCTACTGC CTCGGA
Anp32b	-2.4943198	TGCTGTTGACAGTGAGCGCGAAGACGAAGAAGATGAGGAATAGT GAAGCCACAGATGTATTCCTCATCTTCTTCGTCTTCATGCCTACTG CCTCGGA
Anp32b	7.35501007	TGCTGTTGACAGTGAGCGCGAAGGAGAAGATGATGAGGAATAGT GAAGCCACAGATGTATTCCTCATCATCTTCTCCTTCTTGCCTACTG CCTCGGA
Arid5a	1.10962721	TGCTGTTGACAGTGAGCGACCTCTACAAGTTCATGAAGGATAGTG AAGCCACAGATGTATCCTTCATGAACTTGTAGAGGCTGCCTACTG CCTCGGA
Arid5a	-0.054761	TGCTGTTGACAGTGAGCGCGCACAAGAAAAAGAAGTTTCATAGTG AAGCCACAGATGTATGAAACTTCTTTTTCTTGTGCTTGCCTACTGC CTCGGA
Arid5a	4.42987855	TGCTGTTGACAGTGAGCGAGCATGGCATCATGTCACCACATAGTG AAGCCACAGATGTATGTGGTGACATGATGCCATGCGTGCCTACTG CCTCGGA
Arid5a	3.79771229	TGCTGTTGACAGTGAGCGAGAGCCCCATCCCCTCATCCCATAGTG AAGCCACAGATGTATGGGATGAGGGGATGGGGCTCCTGCCTACT GCCTCGGA
Arpp19	3.37260599	TGCTGTTGACAGTGAGCGCCATGGCAAAAGCAAAGATGAATAGTG AAGCCACAGATGTATTCATCTTTGCTTTTGCCATGTTGCCTACTGC CTCGGA
Arpp19	-6.9494543	TGCTGTTGACAGTGAGCGCAAGCCTGGAGGGTCTGATTTTTAGTG AAGCCACAGATGTAAAAATCAGACCCTCCAGGCTTTTGCCTACTG CCTCGGA
Arpp19	1.09101486	TGCTGTTGACAGTGAGCGCGGGTCTGATTTTTTAAGGAAATAGTG AAGCCACAGATGTATTTCCTTAAAAAATCAGACCCTTGCCTACTGC CTCGGA
Arpp19	0.32589994	TGCTGTTGACAGTGAGCGCAAGGGCAAAAGTATTTTGATATAGTG AAGCCACAGATGTATATCAAAATACTTTTGCCCTTTTGCCTACTGC CTCGGA
Atp5g3	-2.8295012	TGCTGTTGACAGTGAGCGAAGCAGCTGTTCTCATATGCTATAGTG AAGCCACAGATGTATAGCATATGAGAACAGCTGCTGTGCCTACTG CCTCGGA

Atp5g3	-3.3487971	TGCTGTTGACAGTGAGCGCCCTGGGATTTGCCTTGTCTGATAGTG AAGCCACAGATGTATCAGACAAGGCAAATCCCAGGATGCCTACTG CCTCGGA
Atp5g3	3.03125668	TGCTGTTGACAGTGAGCGCGGAGAGGGCTCTACAGTTTTATAGTG AAGCCACAGATGTATAAAACTGTAGAGCCCTCTCCATGCCTACTG CCTCGGA
Atp5g3	-2.8298255	TGCTGTTGACAGTGAGCGCGAGGGCTCTACAGTTTTTAAATAGTG AAGCCACAGATGTATTTAAAAACTGTAGAGCCCTCTTGCCTACTG CCTCGGA
Atp5o	1.7976778	TGCTGTTGACAGTGAGCGACTCATGAATTTACTTGCTGAATAGTG AAGCCACAGATGTATTCAGCAAGTAAATTCATGAGGTGCCTACTG CCTCGGA
Atp5o	2.21387144	TGCTGTTGACAGTGAGCGACAGGGTATCATCTCTGCCTTATAGTG AAGCCACAGATGTATAAGGCAGAGATGATACCCTGGTGCCTACTG CCTCGGA
Atp5o	3.23759129	TGCTGTTGACAGTGAGCGCGACGCTGTTCTCTCTGAGTTATAGTG AAGCCACAGATGTATAACTCAGAGAGAACAGCGTCATGCCTACTG CCTCGGA
Atp5o	2.39693239	TGCTGTTGACAGTGAGCGACCTGTACTCTGCTGCATCTAATAGTG AAGCCACAGATGTATTAGATGCAGCAGAGTACAGGGTGCCTACTG CCTCGGA
Banf1	-1.5326588	TGCTGTTGACAGTGAGCGCTGGTGTGATGCCTTCTTGTAATAGTG AAGCCACAGATGTATTACAAGAAGGCATCACACCATTGCCTACTG CCTCGGA
Banf1	2.10199739	TGCTGTTGACAGTGAGCGCGGTGCTAAAGAAAGATGAAGATAGTG AAGCCACAGATGTATCTTCATCTTTCTTTAGCACCATGCCTACTGC CTCGGA
Banf1	0.79818764	TGCTGTTGACAGTGAGCGACCAGTTTCTGGTGCTAAAGAATAGTG AAGCCACAGATGTATTCTTTAGCACCAGAAACTGGCTGCCTACTG CCTCGGA
Banf1	-3.132715	TGCTGTTGACAGTGAGCGACAGTTTCTGGTGCTAAAGAAATAGTG AAGCCACAGATGTATTTCTTTAGCACCAGAAACTGGTGCCTACTG CCTCGGA
Btg1	2.75728195	TGCTGTTGACAGTGAGCGAGCAGAACAAGCCCTTCCAAAATAGTG AAGCCACAGATGTATTTTGGAAGGGCTTGTTCTGCCTGCCTACTG CCTCGGA
Btg1	-1.5586537	TGCTGTTGACAGTGAGCGCGGCAGAACATTACAAACATCATAGTG AAGCCACAGATGTATGATGTTTGTAATGTTCTGCCATGCCTACTGC CTCGGA
Btg1	-0.4633713	TGCTGTTGACAGTGAGCGCGCAAGGGATCAGGTTACCGTATAGT GAAGCCACAGATGTATACGGTAACCTGATCCCTTGCATGCCTACT GCCTCGGA
Btg1	2.50918847	TGCTGTTGACAGTGAGCGCCAAGCCCTTCCAAAAACTACATAGTG AAGCCACAGATGTATGTAGTTTTTGGAAGGGCTTGTTGCCTACTG CCTCGGA
Calm3	-0.8459915	TGCTGTTGACAGTGAGCGCCTTCCCAGAGTTCTTGACCAATAGTG AAGCCACAGATGTATTGGTCAAGAACTCTGGGAAGTTGCCTACTG CCTCGGA
Calm3	0.62273635	TGCTGTTGACAGTGAGCGCGACTGAGGAACAGATTGCAGATAGT GAAGCCACAGATGTATCTGCAATCTGTTCCTCAGTCATGCCTACT GCCTCGGA

Calm3	-4.476922	TGCTGTTGACAGTGAGCGAGAGAAGCTGACAGATGAGGAATAGT GAAGCCACAGATGTATTCCTCATCTGTCAGCTTCTCCTGCCTACT GCCTCGGA
Calm3	-1.0990868	TGCTGTTGACAGTGAGCGCCAGCGAGGAGGAGATACGAGATAGT GAAGCCACAGATGTATCTCGTATCTCCTCCTCGCTGTTGCCTACT GCCTCGGA
Capn12	-0.6130199	TGCTGTTGACAGTGAGCGCTGGAGCTTCAAGACTTTCTCATAGTG AAGCCACAGATGTATGAGAAAGTCTTGAAGCTCCATTGCCTACTG CCTCGGA
Capn12	-0.1680622	TGCTGTTGACAGTGAGCGAGCTGGTGAAGGGACATGCTTATAGT GAAGCCACAGATGTATAAGCATGTCCCTTCACCAGCCTGCCTACT GCCTCGGA
Capn12	0.53346719	TGCTGTTGACAGTGAGCGCGGAGTTGGCACAGCTATTTTATAGTG AAGCCACAGATGTATAAAATAGCTGTGCCAACTCCATGCCTACTG CCTCGGA
Cbx3	-1.3190596	TGCTGTTGACAGTGAGCGCAAGAGTAAAAAAGTTGAAGAATAGTG AAGCCACAGATGTATTCTTCAACTTTTTTACTCTTTTGCCTACTGC CTCGGA
Cbx3	2.27716874	TGCTGTTGACAGTGAGCGCCCAGAAGAAAATTTAGATTGATAGTG AAGCCACAGATGTATCAATCTAAATTTTCTTCTGGTTGCCTACTGC CTCGGA
Cbx3	1.50793362	TGCTGTTGACAGTGAGCGAAGAGTTAATGTTTCTCATGAATAGTG AAGCCACAGATGTATTCATGAGAAACATTAACTCTCTGCCTACTGC CTCGGA
Cbx3	-1.6132445	TGCTGTTGACAGTGAGCGCGAAGCATTTCTTAATTCTCAATAGTGA AGCCACAGATGTATTGAGAATTAAGAAATGCTTCATGCCTACTGC CTCGGA
Cd19	0.16518913	TGCTGTTGACAGTGAGCGATTCCTCCTCTTTCTTACCTTATAGTGA AGCCACAGATGTATAAGGTAAGAAAGAGGAGGAAGTGCCTACTG CCTCGGA
Cd19	-0.8923264	TGCTGTTGACAGTGAGCGCCCTAGGAGACCTAATGTTTCATAGTG AAGCCACAGATGTATGAAACATTAGGTCTCCTAGGATGCCTACTG CCTCGGA
Cd19	1.30759904	TGCTGTTGACAGTGAGCGAATCTTGCTAGTGATTGTCAAATAGTG AAGCCACAGATGTATTTGACAATCACTAGCAAGATGTGCCTACTG CCTCGGA
Cd4	0.17618694	TGCTGTTGACAGTGAGCGACAGGGTCTCTGAGGAGCAGAATAGT GAAGCCACAGATGTATTCTGCTCCTCAGAGACCCTGGTGCCTACT GCCTCGGA
Cd4	1.20326191	TGCTGTTGACAGTGAGCGAAAAGTGGCTCAGCTCAACAAATAGTG AAGCCACAGATGTATTTGTTGAGCTGAGCCACTTTCTGCCTACTG CCTCGGA
Cd4	-0.1232258	TGCTGTTGACAGTGAGCGACCAGAAGAAGATCACAGTCTATAGTG AAGCCACAGATGTATAGACTGTGATCTTCTTCTGGGTGCCTACTG CCTCGGA
Cenpw	1.34711225	TGCTGTTGACAGTGAGCGACGACCTCCTGATCCATTTGAATAGTG AAGCCACAGATGTATTCAAATGGATCAGGAGGTCGCTGCCTACTG CCTCGGA
Cenpw	1.10752864	TGCTGTTGACAGTGAGCGCGCCTACTTTTTATTCAGCGAATAGTG AAGCCACAGATGTATTCGCTGAATAAAAAGTAGGCATGCCTACTG CCTCGGA

Cenpw	2.43359516	TGCTGTTGACAGTGAGCGCGCTTGTGAAAGTAAATCTAGATAGTG AAGCCACAGATGTATCTAGATTTACTTTCACAAGCATGCCTACTGC CTCGGA
Cenpw	0.54174042	TGCTGTTGACAGTGAGCGCCCAGGACAAATGCTTGTGAAATAGTG AAGCCACAGATGTATTTCACAAGCATTTGTCCTGGATGCCTACTG CCTCGGA
Cisd1	2.84529368	TGCTGTTGACAGTGAGCGAACCTCTGATCATCAAGAAAAATAGTG AAGCCACAGATGTATTTTTCTTGATGATCAGAGGTCTGCCTACTGC CTCGGA
Cisd1	-2.6116137	TGCTGTTGACAGTGAGCGCTCTTCAGATCCAGAAAGACAATAGTG AAGCCACAGATGTATTGTCTTTCTGGATCTGAAGATTGCCTACTGC CTCGGA
Cisd1	0.08192982	TGCTGTTGACAGTGAGCGATAGGACCTCTGATCATCAAGATAGTG AAGCCACAGATGTATCTTGATGATCAGAGGTCCTACTGCCTACTG CCTCGGA
Cisd1	0.28897939	TGCTGTTGACAGTGAGCGCGAAGTTCTACGCTAAAGAGAATAGTG AAGCCACAGATGTATTCTCTTTAGCGTAGAACTTCTTGCCTACTGC CTCGGA
Cks1b	-0.8742808	TGCTGTTGACAGTGAGCGATCCCACAAACAAATCTACTAATAGTG AAGCCACAGATGTATTAGTAGATTTGTTTGTGGGACTGCCTACTG CCTCGGA
Cks1b	-0.5312375	TGCTGTTGACAGTGAGCGCCCCACAAACAAATCTACTATATAGTG AAGCCACAGATGTATATAGTAGATTTGTTTGTGGGATGCCTACTG CCTCGGA
Cks1b	-1.181978	TGCTGTTGACAGTGAGCGATGGTCCCGAAAACCCATCTGATAGTG AAGCCACAGATGTATCAGATGGGTTTTCGGGACCAGTGCCTACTG CCTCGGA
Cks1b	2.21675613	TGCTGTTGACAGTGAGCGCGAACCAGAACCTCACATCTTATAGTG AAGCCACAGATGTATAAGATGTGAGGTTCTGGTTCATGCCTACTG CCTCGGA
Cox5a	-6.0086249	TGCTGTTGACAGTGAGCGATCATAAGGAAATCTATCCCTATAGTG AAGCCACAGATGTATAGGGATAGATTTCCTTATGAGTGCCTACTG CCTCGGA
Cox5a	-7.3908281	TGCTGTTGACAGTGAGCGAAGGAACTTAGACCAACTTTAATAGTG AAGCCACAGATGTATTAAAGTTGGTCTAAGTTCCTGTGCCTACTG CCTCGGA
Cox5a	-0.9603375	TGCTGTTGACAGTGAGCGAAGCTGGGCCTTGACAAAGTGATAGT GAAGCCACAGATGTATCACTTTGTCAAGGCCCAGCTCTGCCTACT GCCTCGGA
Cox5b	0.40965252	TGCTGTTGACAGTGAGCGAGACAACTGTACTGTCATCTGATAGTG AAGCCACAGATGTATCAGATGACAGTACAGTTGTCCTGCCTACTG CCTCGGA
Cox5b	-0.7802906	TGCTGTTGACAGTGAGCGAACCCGCTCCATGGCTTCTGGATAGTG AAGCCACAGATGTATCCAGAAGCCATGGAGCGGGTCTGCCTACT GCCTCGGA
Cox5b	-1.8437696	TGCTGTTGACAGTGAGCGACGTCCATCAGCAACAAGAGAATAGTG AAGCCACAGATGTATTCTCTTGTTGCTGATGGACGGTGCCTACTG CCTCGGA
Cox5b	0.55509228	TGCTGTTGACAGTGAGCGAATCTGTGAAGAGGACAACTGATAGTG AAGCCACAGATGTATCAGTTGTCCTCTTCACAGATGTGCCTACTG CCTCGGA

Csda	-4.3076507	TGCTGTTGACAGTGAGCGAACGCGGAGAAGAAAGTTCTCATAGTG AAGCCACAGATGTATGAGAACTTTCTTCTCCGCGTCTGCCTACTG CCTCGGA
Csda	-0.925611	TGCTGTTGACAGTGAGCGCGAGTTTGATGTAGTTGAAGGATAGTG AAGCCACAGATGTATCCTTCAACTACATCAAACTCTTGCCTACTGC CTCGGA
Csda	-1.8833713	TGCTGTTGACAGTGAGCGCGACACCAAAGAAGATGTGTTATAGTG AAGCCACAGATGTATAACACATCTTCTTTGGTGTCATGCCTACTGC CTCGGA
Dcun1d5	1.27285106	TGCTGTTGACAGTGAGCGCGATCAGAGAAGCCTTGATATATAGTG AAGCCACAGATGTATATATCAAGGCTTCTCTGATCTTGCCTACTGC CTCGGA
Dcun1d5	0.44060447	TGCTGTTGACAGTGAGCGCACAGAGCAGGTTTGATTTTCATAGTG AAGCCACAGATGTATGAAAATCAAACCTGCTCTGTATGCCTACTG CCTCGGA
Dcun1d5	0.56166199	TGCTGTTGACAGTGAGCGACTGAATGACATCTCATCTTTATAGTGA AGCCACAGATGTATAAAGATGAGATGTCATTCAGCTGCCTACTGC CTCGGA
Dcun1d5	1.61258734	TGCTGTTGACAGTGAGCGCCATGGCCACTCTTTTCAGTAATAGTG AAGCCACAGATGTATTACTGAAAAGAGTGGCCATGTTGCCTACTG CCTCGGA
Ddx39	-4.0129096	TGCTGTTGACAGTGAGCGAGACATTGAGCGAGTCAACATATAGTG AAGCCACAGATGTATATGTTGACTCGCTCAATGTCCTGCCTACTG CCTCGGA
Ddx39	-1.9679668	TGCTGTTGACAGTGAGCGCGAGAGCTATAGTTGACTGTGATAGTG AAGCCACAGATGTATCACAGTCAACTATAGCTCTCATGCCTACTG CCTCGGA
Ddx39	-1.6264352	TGCTGTTGACAGTGAGCGACCCACGAGAAGCAGTGTATGATAGT GAAGCCACAGATGTATCATACACTGCTTCTCGTGGGGTGCCTACT GCCTCGGA
Ddx60	1.54888703	TGCTGTTGACAGTGAGCGATCTTGTTGAGAAGCTAAGGAATAGTG AAGCCACAGATGTATTCCTTAGCTTCTCAACAAGACTGCCTACTG CCTCGGA
Ddx60	2.14871661	TGCTGTTGACAGTGAGCGACTGCACTATTCTTTTTATTTATAGTGA AGCCACAGATGTATAAATAAAAAGAATAGTGCAGGTGCCTACTGC CTCGGA
Ddx60	2.83466579	TGCTGTTGACAGTGAGCGAAGACCTCTCAGTGATGATTAATAGTG AAGCCACAGATGTATTAATCATCACTGAGAGGTCTGTGCCTACTG CCTCGGA
Ddx60	-0.3565642	TGCTGTTGACAGTGAGCGCGAAACTGGAAGAGTTTTTGAATAGTG AAGCCACAGATGTATTCAAAAACTCTTCCAGTTTCTTGCCTACTGC CTCGGA
Dpy30	-0.6743052	TGCTGTTGACAGTGAGCGCTCCTAGCATCTTATCTTTTAATAGTGA AGCCACAGATGTATTAAAAGATAAGATGCTAGGAATGCCTACTGC CTCGGA
Dpy30	0.78714673	TGCTGTTGACAGTGAGCGAAGCGTTGAGAGAATAGTCGAATAGTG AAGCCACAGATGTATTCGACTATTCTCTCAACGCTGTGCCTACTG CCTCGGA
Dpy30	1.30398966	TGCTGTTGACAGTGAGCGCGACAGTTGTGCCTATCTTATATAGTG AAGCCACAGATGTATATAAGATAGGCACAACTGTCTTGCCTACTG CCTCGGA

Dut	-1.0236758	TGCTGTTGACAGTGAGCGCCGTTGGGGTCGTGCTGTTTAATAGTG AAGCCACAGATGTATTAAACAGCACGACCCCAACGTTGCCTACTG CCTCGGA
Dut	0.39438006	TGCTGTTGACAGTGAGCGATGAGCGGATTTCTTATCCAGATAGTG AAGCCACAGATGTATCTGGATAAGAAATCCGCTCACTGCCTACTG CCTCGGA
Dut	3.50458743	TGCTGTTGACAGTGAGCGACCATGGAGAAAGCCATCGTGATAGT GAAGCCACAGATGTATCACGATGGCTTTCTCCATGGGTGCCTACT GCCTCGGA
Dut	2.36993326	TGCTGTTGACAGTGAGCGACGGATTTCTTATCCAGACTTATAGTG AAGCCACAGATGTATAAGTCTGGATAAGAAATCCGCTGCCTACTG CCTCGGA
Erh	3.29646712	TGCTGTTGACAGTGAGCGCCAGACATACCAGCCGTATAACTAGTG AAGCCACAGATGTAGTTATACGGCTGGTATGTCTGTTGCCTACTG CCTCGGA
Erh	2.09607379	TGCTGTTGACAGTGAGCGCTCAGCCAGTTGTTTGATTTTATAGTG AAGCCACAGATGTATAAAATCAAACAACTGGCTGATTGCCTACTG CCTCGGA
Erh	-1.0930035	TGCTGTTGACAGTGAGCGCTGCTGACTATGAGTCTGTGAATAGTG AAGCCACAGATGTATTCACAGACTCATAGTCAGCATTGCCTACTG CCTCGGA
Erh	-1.0506129	TGCTGTTGACAGTGAGCGAAGCCAGTTGTTTGATTTTATATAGTGA AGCCACAGATGTATATAAAATCAAACAACTGGCTGTGCCTACTGC CTCGGA
Ezh2	0.86314753	TGCTGTTGACAGTGAGCGAGACCACAGTGTTACCAGCATATAGTG AAGCCACAGATGTATATGCTGGTAACACTGTGGTCCTGCCTACTG CCTCGGA
Ezh2	0.58300208	TGCTGTTGACAGTGAGCGCACTACGATAACTTTTGTGCCATAGTG AAGCCACAGATGTATGGCACAAAAGTTATCGTAGTATGCCTACTG CCTCGGA
Ezh2	-2.0295001	TGCTGTTGACAGTGAGCGAAAGAGGAAGACTTCCGAATAATAGTG AAGCCACAGATGTATTATTCGGAAGTCTTCCTCTTCTGCCTACTGC CTCGGA
Ezh2	-3.0693841	TGCTGTTGACAGTGAGCGCGCAGCTTTCTGTTCAACTTGATAGTG AAGCCACAGATGTATCAAGTTGAACAGAAAGCTGCATGCCTACTG CCTCGGA
Fam166a	0.85010478	TGCTGTTGACAGTGAGCGCTACCGTGATGGTGTCACACAATAGTG AAGCCACAGATGTATTGTGTGACACCATCACGGTAATGCCTACTG CCTCGGA
Fam166a	2.1108525	TGCTGTTGACAGTGAGCGAACACAAGCTATGGATGACTTATAGTG AAGCCACAGATGTATAAGTCATCCATAGCTTGTGTGTGCCTACTG CCTCGGA
Fam166a	0.57369183	TGCTGTTGACAGTGAGCGACTGCTCTGTTCTGTCACCTAATAGTG AAGCCACAGATGTATTAGGTGACAGAACAGAGCAGGTGCCTACTG CCTCGGA
Fau	3.54987198	TGCTGTTGACAGTGAGCGACATGCTGGGAGGTAAAGTTCATAGTG AAGCCACAGATGTATGAACTTTACCTCCCAGCATGCTGCCTACTG CCTCGGA
Fau	-2.1922592	TGCTGTTGACAGTGAGCGCCGCCCAGATCAAAGATCATGATAGTG AAGCCACAGATGTATCATGATCTTTGATCTGGGCGATGCCTACTG CCTCGGA

Fau	-1.290857	TGCTGTTGACAGTGAGCGCCCGGCGCTTTGTCAATGTTGATAGTG AAGCCACAGATGTATCAACATTGACAAAGCGCCGGTTGCCTACTG CCTCGGA
Fau	-1.3435195	TGCTGTTGACAGTGAGCGATGGGAGGTAAAGTTCACGGTATAGTG AAGCCACAGATGTATACCGTGAACTTTACCTCCCAGTGCCTACTG CCTCGGA
Fkbp2	0.81510754	TGCTGTTGACAGTGAGCGAAAGCTGCAGATTGGAGTGAAATAGTG AAGCCACAGATGTATTTCACTCCAATCTGCAGCTTCTGCCTACTG CCTCGGA
Fkbp2	0.82325969	TGCTGTTGACAGTGAGCGCCTGTCCTATCAAGTCTAGAAATAGTG AAGCCACAGATGTATTTCTAGACTTGATAGGACAGTTGCCTACTG CCTCGGA
Fkbp2	1.60675779	TGCTGTTGACAGTGAGCGACAGCCCTTTGTTTTCTCCCTATAGTG AAGCCACAGATGTATAGGGAGAAAACAAAGGGCTGGTGCCTACT GCCTCGGA
Fkbp2	4.40264935	TGCTGTTGACAGTGAGCGCGAGGTGGAGCTGCTCAAGATATAGT GAAGCCACAGATGTATATCTTGAGCAGCTCCACCTCATGCCTACT GCCTCGGA
Fmo1	2.32836396	TGCTGTTGACAGTGAGCGCCGCCCGGATTTTGCTGTCTCATAGTG AAGCCACAGATGTATGAGACAGCAAAATCCGGGCGTTGCCTACTG CCTCGGA
Fmo1	-1.138898	TGCTGTTGACAGTGAGCGCAGCTGTCTTCTTGATTTTCCATAGTG AAGCCACAGATGTATGGAAAATCAAGAAGACAGCTATGCCTACTG CCTCGGA
Fmo1	-1.2172117	TGCTGTTGACAGTGAGCGACTCGATGAATCCGTAGTGAAATAGTG AAGCCACAGATGTATTTCACTACGGATTCATCGAGGTGCCTACTG CCTCGGA
Fos	0.35822213	TGCTGTTGACAGTGAGCGCGAAGATGAGAAGTCTGCGTTATAGTG AAGCCACAGATGTATAACGCAGACTTCTCATCTTCATGCCTACTG CCTCGGA
Fos	2.72847176	TGCTGTTGACAGTGAGCGACAAAGTAGAGCAGCTATCTCATAGTG AAGCCACAGATGTATGAGATAGCTGCTCTACTTTGCTGCCTACTG CCTCGGA
Fos	2.10141947	TGCTGTTGACAGTGAGCGCAGCGGAGACAGATCAACTTGATAGT GAAGCCACAGATGTATCAAGTTGATCTGTCTCCGCTTTGCCTACT GCCTCGGA
Fos	2.54635238	TGCTGTTGACAGTGAGCGACACTACTTACACGTCTTCCTATAGTG AAGCCACAGATGTATAGGAAGACGTGTAAGTAGTGCTGCCTACTG CCTCGGA
Gapdh	1.06936272	TGCTGTTGACAGTGAGCGCCCACGAGAAATATGACAACTATAGTG AAGCCACAGATGTATAGTTGTCATATTTCTCGTGGTTGCCTACTGC CTCGGA
Gapdh	-0.5069568	TGCTGTTGACAGTGAGCGATGAACCACGAGAAATATGACATAGTG AAGCCACAGATGTATGTCATATTTCTCGTGGTTCACTGCCTACTGC CTCGGA
Gapdh	-1.204439	TGCTGTTGACAGTGAGCGAAAGGTCATCCATGACAACTTATAGTG AAGCCACAGATGTATAAGTTGTCATGGATGACCTTGTGCCTACTG CCTCGGA
Gm10094	-4.2299488	TGCTGTTGACAGTGAGCGCCACTTCAATTTTGCAATTGTATAGTGA AGCCACAGATGTATACAATTGCAAAATTGAAGTGTTGCCTACTGC CTCGGA

Gm10094	1.6177418	TGCTGTTGACAGTGAGCGCAGGGCACACACTTCAATTTTATAGTG AAGCCACAGATGTATAAAATTGAAGTGTGTGCCCTTTGCCTACTG CCTCGGA
Gm10094	-1.4389699	TGCTGTTGACAGTGAGCGAGCACACACTTCAATTTTGCAATAGTG AAGCCACAGATGTATTGCAAAATTGAAGTGTGTGCCTGCCTACTG CCTCGGA
Gm10094	4.91279505	TGCTGTTGACAGTGAGCGCGCAGTCACAGAAGTTCCAAAATAGTG AAGCCACAGATGTATTTTGGAACTTCTGTGACTGCATGCCTACTG CCTCGGA
Gzmb	-6.2401654	TGCTGTTGACAGTGAGCGCCCTCCACGTGCTTTCACCAAATAGTG AAGCCACAGATGTATTTGGTGAAAGCACGTGGAGGTTGCCTACTG CCTCGGA
Gzmb	-5.3611525	TGCTGTTGACAGTGAGCGAGGCAAATACTCAAACACGCTATAGTG AAGCCACAGATGTATAGCGTGTTTGAGTATTTGCCCTGCCTACTG CCTCGGA
Gzmb	-2.9357819	TGCTGTTGACAGTGAGCGCCACTGTGAAGGAAGTATAATATAGTG AAGCCACAGATGTATATTATACTTCCTTCACAGTGATGCCTACTGC CTCGGA
Ict1os	1.37037795	TGCTGTTGACAGTGAGCGACAGGCAGATTTCTGAGTTCAATAGTG AAGCCACAGATGTATTGAACTCAGAAATCTGCCTGCTGCCTACTG CCTCGGA
Kcnmb4	-3.8368873	TGCTGTTGACAGTGAGCGACAGTATTGGAAAGATGAGATATAGTG AAGCCACAGATGTATATCTCATCTTTCCAATACTGCTGCCTACTGC CTCGGA
Kcnmb4	1.5883364	TGCTGTTGACAGTGAGCGCGCCATTCACTTGCTATTTTAATAGTGA AGCCACAGATGTATTAAAATAGCAAGTGAATGGCTTGCCTACTGC CTCGGA
Kcnmb4	-2.2053528	TGCTGTTGACAGTGAGCGCCCCAGCCATTCACTTGCTATATAGTG AAGCCACAGATGTATATAGCAAGTGAATGGCTGGGATGCCTACTG CCTCGGA
Kcnmb4	-2.3266426	TGCTGTTGACAGTGAGCGAAGCCATTCACTTGCTATTTTATAGTGA AGCCACAGATGTATAAAATAGCAAGTGAATGGCTGTGCCTACTGC CTCGGA
Kmt2a	1.84737427	TGCTGTTGACAGTGAGCGCAGGTCTGATTCGCAAACCAATTAGTG AAGCCACAGATGTAATTGGTTTGCGAATCAGACCTTTGCCTACTG CCTCGGA
Kmt2a	2.09554112	TGCTGTTGACAGTGAGCGAAAGATAAACTCTTTCCTATTATAGTGA AGCCACAGATGTATAATAGGAAAGAGTTTATCTTCTGCCTACTGCC TCGGA
Lsm5	-2.5443606	TGCTGTTGACAGTGAGCGATGATGAAGAGTGATAAAGAAATAGTG AAGCCACAGATGTATTTCTTTATCACTCTTCATCACTGCCTACTGC CTCGGA
Lsm5	2.60903268	TGCTGTTGACAGTGAGCGAGAAGATGTCACAGAATTTGAATAGTG AAGCCACAGATGTATTCAAATTCTGTGACATCTTCCTGCCTACTGC CTCGGA
Lsm5	-0.8646672	TGCTGTTGACAGTGAGCGCCGGGACACTTCTAGGATTTGATAGTG AAGCCACAGATGTATCAAATCCTAGAAGTGTCCCGATGCCTACTG CCTCGGA
Lsm5	6.30671732	TGCTGTTGACAGTGAGCGCGGATTTGATGACTTTGTCAAATAGTG AAGCCACAGATGTATTTGACAAAGTCATCAAATCCTTGCCTACTGC CTCGGA

Lsm6	4.60504463	TGCTGTTGACAGTGAGCGATACGGAGATGCGTTCATCCGATAGTG AAGCCACAGATGTATCGGATGAACGCATCTCCGTACTGCCTACTG CCTCGGA
Lsm6	3.43184052	TGCTGTTGACAGTGAGCGAAACAGACAGAGGAGTATGTAATAGTG AAGCCACAGATGTATTACATACTCCTCTGTCTGTTCTGCCTACTGC CTCGGA
Lsm6	-2.5298547	TGCTGTTGACAGTGAGCGACTAGCGACTTCTTAAAGCAGATAGTG AAGCCACAGATGTATCTGCTTTAAGAAGTCGCTAGGTGCCTACTG CCTCGGA
Lsm7	-0.1859112	TGCTGTTGACAGTGAGCGCCCTCTCCAAGTACATCGATAATAGTG AAGCCACAGATGTATTATCGATGTACTTGGAGAGGTTGCCTACTG CCTCGGA
Lsm7	-1.7585074	TGCTGTTGACAGTGAGCGCGGACCTCTCCAAGTACATCGATAGTG AAGCCACAGATGTATCGATGTACTTGGAGAGGTCCATGCCTACTG CCTCGGA
Lsm7	-2.497064	TGCTGTTGACAGTGAGCGAAAGTACATCGATAAGACCATATAGTG AAGCCACAGATGTATATGGTCTTATCGATGTACTTGTGCCTACTGC CTCGGA
Lsm7	-0.8029229	TGCTGTTGACAGTGAGCGCTCGGGTGAAGTTCCAGGGTGATAGT GAAGCCACAGATGTATCACCCTGGAACTTCACCCGAATGCCTACT GCCTCGGA
Malat1	4.24814856	TGCTGTTGACAGTGAGCGCGCATTGTATACTTGTGTTTAATAGTGA AGCCACAGATGTATTAAACACAAGTATACAATGCATGCCTACTGC CTCGGA
Malat1	3.50458743	TGCTGTTGACAGTGAGCGCAGTTGGCAAGTAACTCCCAATTAGTG AAGCCACAGATGTAATTGGGAGTTACTTGCCAACTTTGCCTACTG CCTCGGA
Malat1	3.37260599	TGCTGTTGACAGTGAGCGCTACGATCATCTCATCCACTTATAGTG AAGCCACAGATGTATAAGTGGATGAGATGATCGTAATGCCTACTG CCTCGGA
Manf	2.07583243	TGCTGTTGACAGTGAGCGCGCAGATTGACCTGAGCACAGTTAGT GAAGCCACAGATGTAACTGTGCTCAGGTCAATCTGCTTGCCTACT GCCTCGGA
Manf	1.92545595	TGCTGTTGACAGTGAGCGCCCTGAGCACAGTGGACCTGAATAGT GAAGCCACAGATGTATTCAGGTCCACTGTGCTCAGGTTGCCTACT GCCTCGGA
Manf	0.07033502	TGCTGTTGACAGTGAGCGCGACTGTGAAGTTTGTATTTCATAGTG AAGCCACAGATGTATGAAATACAAACTTCACAGTCTTGCCTACTGC CTCGGA
Manf	1.38424562	TGCTGTTGACAGTGAGCGCCAGCCAGATCTGTGAACTAAATAGTG AAGCCACAGATGTATTTAGTTCACAGATCTGGCTGTTGCCTACTG CCTCGGA
Mcm3	0.68534171	TGCTGTTGACAGTGAGCGAAGCCTACATTGCAGAAGAATATAGTG AAGCCACAGATGTATATTCTTCTGCAATGTAGGCTGTGCCTACTG CCTCGGA
Mcm3	1.06624511	TGCTGTTGACAGTGAGCGATAATGTGAAGCAGATGAGTAATAGTG AAGCCACAGATGTATTACTCATCTGCTTCACATTACTGCCTACTGC CTCGGA
Mcm3	1.15544448	TGCTGTTGACAGTGAGCGAGGCATCGTCTTCCTTATCTGATAGTG AAGCCACAGATGTATCAGATAAGGAAGACGATGCCCTGCCTACTG CCTCGGA

Mcm3	-0.3071904	TGCTGTTGACAGTGAGCGAACTGGAAACTCTGATTCGACATAGTG AAGCCACAGATGTATGTCGAATCAGAGTTTCCAGTGTGCCTACTG CCTCGGA
Mcm6	0.97467741	TGCTGTTGACAGTGAGCGCCAGGACAAAAACCTGTACCAATAGTG AAGCCACAGATGTATTGGTACAGGTTTTTGTCCTGATGCCTACTG CCTCGGA
Mcm6	1.28230518	TGCTGTTGACAGTGAGCGAGGTAGTGATGGAGAAATTAAATAGTG AAGCCACAGATGTATTTAATTTCTCCATCACTACCCTGCCTACTGC CTCGGA
Mcm6	-1.9729998	TGCTGTTGACAGTGAGCGCCACTACGATCACGTTCTGATATAGTG AAGCCACAGATGTATATCAGAACGTGATCGTAGTGTTGCCTACTG CCTCGGA
Mcm6	0.48534553	TGCTGTTGACAGTGAGCGCCAGATCAAAATCTTTGAAACATAGTG AAGCCACAGATGTATGTTTCAAAGATTTTGATCTGTTGCCTACTGC CTCGGA
Mif	1.82324426	TGCTGTTGACAGTGAGCGAAGAACCGCAACTACAGTAAGATAGTG AAGCCACAGATGTATCTTACTGTAGTTGCGGTTCTGTGCCTACTG CCTCGGA
Mif	-3.1587389	TGCTGTTGACAGTGAGCGAACCGGGTCTACATCAACTATATAGTG AAGCCACAGATGTATATAGTTGATGTAGACCCGGTCTGCCTACTG CCTCGGA
Mif	-0.9809601	TGCTGTTGACAGTGAGCGAGGACCGGGTCTACATCAACTATAGTG AAGCCACAGATGTATAGTTGATGTAGACCCGGTCCGTGCCTACTG CCTCGGA
Mif	-0.386441	TGCTGTTGACAGTGAGCGCCCCGGACCAGCTCATGACTTATAGTG AAGCCACAGATGTATAAGTCATGAGCTGGTCCGGGATGCCTACTG CCTCGGA
Mrps21	2.99661669	TGCTGTTGACAGTGAGCGCTGCCGGAGGATCTACAACATATAGTG AAGCCACAGATGTATATGTTGTAGATCCTCCGGCATTGCCTACTG CCTCGGA
Mrps21	2.59880077	TGCTGTTGACAGTGAGCGCGGAAATGGCTCGAAAGATTAATAGTG AAGCCACAGATGTATTAATCTTTCGAGCCATTTCCATGCCTACTGC CTCGGA
Mrps21	0.2849574	TGCTGTTGACAGTGAGCGAACCACGGATGGGCTTACCGAATAGT GAAGCCACAGATGTATTCGGTAAGCCCATCCGTGGTGTGCCTACT GCCTCGGA
Mrps21	-0.8540583	TGCTGTTGACAGTGAGCGAGGACCCTGAACAGAATCCTCATAGTG AAGCCACAGATGTATGAGGATTCTGTTCAGGGTCCGTGCCTACTG CCTCGGA
Mrps36	-4.0735773	TGCTGTTGACAGTGAGCGAACCAGACACTGCAGAAATTAATAGTG AAGCCACAGATGTATTAATTTCTGCAGTGTCTGGTGTGCCTACTG CCTCGGA
Mrps36	3.85902577	TGCTGTTGACAGTGAGCGCCCAGACACTGCAGAAATTATATAGTG AAGCCACAGATGTATATAATTTCTGCAGTGTCTGGTTGCCTACTGC CTCGGA
Mrps36	-0.8985841	TGCTGTTGACAGTGAGCGCCAGAAGGAAACCTATGTCTCATAGTG AAGCCACAGATGTATGAGACATAGGTTTCCTTCTGTTGCCTACTG CCTCGGA
Ndufa1	5.2226896	TGCTGTTGACAGTGAGCGAGAGTCAATCGCTACTATGTGATAGTG AAGCCACAGATGTATCACATAGTAGCGATTGACTCCTGCCTACTG CCTCGGA

Ndufa1	1.84380208	TGCTGTTGACAGTGAGCGATCCAAGGGCCTGGAAAACATATAGTG AAGCCACAGATGTATATGTTTTCCAGGCCCTTGGACTGCCTACTG CCTCGGA
Ndufa1	-0.0867826	TGCTGTTGACAGTGAGCGAGAACGCGATAGACGTATCTCATAGTG AAGCCACAGATGTATGAGATACGTCTATCGCGTTCCTGCCTACTG CCTCGGA
Ndufa1	5.11284878	TGCTGTTGACAGTGAGCGCAGACGTATCTCTGGAGTCAATTAGTG AAGCCACAGATGTAATTGACTCCAGAGATACGTCTATGCCTACTG CCTCGGA
Ndufa12	-0.049676	TGCTGTTGACAGTGAGCGCACTACGAAGACAACAAGCAATTAGTG AAGCCACAGATGTAATTGCTTGTTGTCTTCGTAGTATGCCTACTGC CTCGGA
Ndufa12	6.66532252	TGCTGTTGACAGTGAGCGCACTACGAAGACAACAAGCAAATAGTG AAGCCACAGATGTATTTGCTTGTTGTCTTCGTAGTATGCCTACTGC CTCGGA
Ndufa12	2.20417376	TGCTGTTGACAGTGAGCGCCAAACCATAAATTCAATGTGATAGTG AAGCCACAGATGTATCACATTGAATTTATGGTTTGTTGCCTACTGC CTCGGA
Ndufa12	-3.6242714	TGCTGTTGACAGTGAGCGCACGAAGACAACAAGCAATTTATAGTG AAGCCACAGATGTATAAATTGCTTGTTGTCTTCGTATGCCTACTGC CTCGGA
Ndufa4	0.8110044	TGCTGTTGACAGTGAGCGCTGATTCCTCTCTTCGTATTTATAGTGA AGCCACAGATGTATAAATACGAAGAGAGGAATCAATGCCTACTGC CTCGGA
Ndufa4	3.49189811	TGCTGTTGACAGTGAGCGCGATGCGCTTGGCACTGTTTAATAGTG AAGCCACAGATGTATTAAACAGTGCCAAGCGCATCATGCCTACTG CCTCGGA
Ndufa4	1.89126006	TGCTGTTGACAGTGAGCGACCAATGAACAATATAAGTTCATAGTG AAGCCACAGATGTATGAACTTATATTGTTCATTGGGTGCCTACTGC CTCGGA
Ndufa4	-0.1891223	TGCTGTTGACAGTGAGCGCCTACAGCAAACTGAAGAAAGATAGTG AAGCCACAGATGTATCTTTCTTCAGTTTGCTGTAGTTGCCTACTGC CTCGGA
Ndufb6	-1.0383067	TGCTGTTGACAGTGAGCGATCCAGTCTCTTCGCTGTTTCATAGTG AAGCCACAGATGTATGAAACAGCGAAGAGACTGGAGTGCCTACT GCCTCGGA
Ndufb6	1.02502503	TGCTGTTGACAGTGAGCGAAGCGATTCTGGGATAACTTTATAGTG AAGCCACAGATGTATAAAGTTATCCCAGAATCGCTCTGCCTACTG CCTCGGA
Ndufb6	1.95906934	TGCTGTTGACAGTGAGCGATGGAGAAGTAATTCCACCAAATAGTG AAGCCACAGATGTATTTGGTGGAATTACTTCTCCAGTGCCTACTG CCTCGGA
Ndufb9	0.35067052	TGCTGTTGACAGTGAGCGCGCAGGAGGAAACATCACCTGATAGT GAAGCCACAGATGTATCAGGTGATGTTTCCTCCTGCATGCCTACT GCCTCGGA
Ndufb9	-1.8905075	TGCTGTTGACAGTGAGCGAGCATCCCTCTGAGAAAGCAAATAGTG AAGCCACAGATGTATTTGCTTTCTCAGAGGGATGCCTGCCTACTG CCTCGGA
Ndufc2	0.64152717	TGCTGTTGACAGTGAGCGCAAAACGTCAAAACTATTTGTATAGTG AAGCCACAGATGTATACAAATAGTTTTGACGTTTTATGCCTACTGC CTCGGA

Ndufc2	-2.2886362	TGCTGTTGACAGTGAGCGACCAGAAGATTTTCCTGAAAAATAGTG AAGCCACAGATGTATTTTTCAGGAAAATCTTCTGGGTGCCTACTG CCTCGGA
Ndufc2	-5.6119504	TGCTGTTGACAGTGAGCGCCCCAGAAGATTTTCCTGAAAATAGTG AAGCCACAGATGTATTTTCAGGAAAATCTTCTGGGTTGCCTACTG CCTCGGA
Non-targeting #2	1.15160951	TGCTGTTGACAGTGAGCGCCATGCACATGAAGCTGTACAATAGTG AAGCCACAGATGTATTGTACAGCTTCATGTGCATGTTGCCTACTG CCTCGGA
Non-targeting #3	-1.0651487	TGCTGTTGACAGTGAGCGCCGGGGTGAACTTCCCATCCAATAGT GAAGCCACAGATGTATTGGATGGGAAGTTCACCCCGTTGCCTACT GCCTCGGA
Non-targeting #4	-0.3293399	TGCTGTTGACAGTGAGCGaaggcagaagtatgcaaagcatTAGTGAAGCC ACAGATGTAatgctttgcatacttctgcctgTGCCTACTGCCTCGGA
Non-targeting #5	-1.1932008	TGCTGTTGACAGTGAGCGacacgtgttgacaattaatcatTAGTGAAGCCAC AGATGTAatgattaattgtcaacacgtgcTGCCTACTGCCTCGGA
Non-targeting #6	0.59523876	TGCTGTTGACAGTGAGCGCGGTAATGGTTCTTATAGGTTATAGTG AAGCCACAGATGTATAACCTATAAGAACCATTACCATGCCTACTGC CTCGGA
Oas2	0.88550747	TGCTGTTGACAGTGAGCGCACATGCGGAAGTTCCTACTGATAGTG AAGCCACAGATGTATCAGTAGGAACTTCCGCATGTATGCCTACTG CCTCGGA
Oas2	-4.5365264	TGCTGTTGACAGTGAGCGCCACTCCAAGCCACTTACTGAATAGTG AAGCCACAGATGTATTCAGTAAGTGGCTTGGAGTGATGCCTACTG CCTCGGA
Oas2	0.7341361	TGCTGTTGACAGTGAGCGCGGAGAGTTTTCTATCTGTTTATAGTG AAGCCACAGATGTATAAACAGATAGAAAACTCTCCTTGCCTACTG CCTCGGA
Ostc	0.50788813	TGCTGTTGACAGTGAGCGCCCGGAGGAATAATCTATGATATAGTG AAGCCACAGATGTATATCATAGATTATTCCTCCGGTTGCCTACTGC CTCGGA
Ostc	0.81618651	TGCTGTTGACAGTGAGCGATCAACAGGTTTCTTCTTCTGATAGTG AAGCCACAGATGTATCAGAAGAAGAAACCTGTTGAGTGCCTACTG CCTCGGA
Ostc	1.18498055	TGCTGTTGACAGTGAGCGCCAACAGGTTTCTTCTTCTGTATAGTG AAGCCACAGATGTATACAGAAGAAGAAACCTGTTGATGCCTACTG CCTCGGA
Plp2	2.1525016	TGCTGTTGACAGTGAGCGCAGCAACCATCCTGTACCTGAATAGTG AAGCCACAGATGTATTCAGGTACAGGATGGTTGCTATGCCTACTG CCTCGGA
Plp2	-2.0425262	TGCTGTTGACAGTGAGCGCGGCTACGATGCATACATCACATAGTG AAGCCACAGATGTATGTGATGTATGCATCGTAGCCATGCCTACTG CCTCGGA
Plp2	1.24474545	TGCTGTTGACAGTGAGCGACCTGGTGATCTTGATTTGCTATAGTG AAGCCACAGATGTATAGCAAATCAAGATCACCAGGCTGCCTACTG CCTCGGA
Plp2	2.76640151	TGCTGTTGACAGTGAGCGCCTGTGCTGCTGTCTTACTTGATAGTG AAGCCACAGATGTATCAAGTAAGACAGCAGCACAGATGCCTACTG CCTCGGA
Polr2k	-4.0160261	TGCTGTTGACAGTGAGCGAAAAGCAGCAGCCAATGATATATAGTG AAGCCACAGATGTATATATCATTGGCTGCTGCTTTGTGCCTACTG CCTCGGA

Polr2k	-1.994	TGCTGTTGACAGTGAGCGCCCAAAGCAGCAGCCAATGATATAGTG AAGCCACAGATGTATATCATTGGCTGCTGCTTTGGTTGCCTACTG CCTCGGA
Polr2k	-7.3775945	TGCTGTTGACAGTGAGCGACAGCAGCCAATGATATATATATAGTG AAGCCACAGATGTATATATATATCATTGGCTGCTGCTGCCTACTGC CTCGGA
Polr2k	1.19266528	TGCTGTTGACAGTGAGCGCTCCCATCAGATGCAGAGAATATAGTG AAGCCACAGATGTATATTCTCTGCATCTGATGGGATTGCCTACTG CCTCGGA
Pomp	3.72986895	TGCTGTTGACAGTGAGCGAAGTCACGATCTTCTCCGGAAATAGTG AAGCCACAGATGTATTTCCGGAGAAGATCGTGACTCTGCCTACTG CCTCGGA
Pomp	-2.7121245	TGCTGTTGACAGTGAGCGACCACGTGATGGTGGAACATAATAGTG AAGCCACAGATGTATTATGTTCCACCATCACGTGGGTGCCTACTG CCTCGGA
Pomp	-0.832884	TGCTGTTGACAGTGAGCGCGAGGATATTCTTAATGATCCATAGTG AAGCCACAGATGTATGGATCATTAAGAATATCCTCATGCCTACTGC CTCGGA
Ppia	0.50602766	TGCTGTTGACAGTGAGCGCGCAGACAAAGTTCCAAAGACATAGTG AAGCCACAGATGTATGTCTTTGGAACTTTGTCTGCATGCCTACTG CCTCGGA
Ppia	4.91879172	TGCTGTTGACAGTGAGCGCCCAAAGACAGCAGAAAACTTATAGTG AAGCCACAGATGTATAAGTTTTCTGCTGTCTTTGGATGCCTACTGC CTCGGA
Ppia	-0.9133698	TGCTGTTGACAGTGAGCGACTGGACCAAACACAAACGGTATAGTG AAGCCACAGATGTATACCGTTTGTGTTTGGTCCAGCTGCCTACTG CCTCGGA
Prdm1	1.00195994	TGCTGTTGACAGTGAGCGATCTGCCAGAAGACTTTTTGAATAGTG AAGCCACAGATGTATTCAAAAAGTCTTCTGGCAGAGTGCCTACTG CCTCGGA
Prdm1	0.20012251	TGCTGTTGACAGTGAGCGACAAGATCAAGTATGAGTGCAATAGTG AAGCCACAGATGTATTGCACTCATACTTGATCTTGCTGCCTACTGC CTCGGA
Prdm1	0.72859964	TGCTGTTGACAGTGAGCGCCCTACTCCTACTTGAATGTTATAGTG AAGCCACAGATGTATAACATTCAAGTAGGAGTAGGATGCCTACTG CCTCGGA
Prdm1	2.77051404	TGCTGTTGACAGTGAGCGAATCGGTGAAGTCTACACTAAATAGTG AAGCCACAGATGTATTTAGTGTAGACTTCACCGATGTGCCTACTG CCTCGGA
Prdx2	-2.4319503	TGCTGTTGACAGTGAGCGACTAGTCCAGGCCTTTCAGTAATAGTG AAGCCACAGATGTATTACTGAAAGGCCTGGACTAGGTGCCTACTG CCTCGGA
Prdx2	1.48057217	TGCTGTTGACAGTGAGCGACACTGGACTTCACTTTTGTTATAGTG AAGCCACAGATGTATAACAAAAGTGAAGTCCAGTGGTGCCTACTG CCTCGGA
Prdx2	5.65992331	TGCTGTTGACAGTGAGCGCCAGCAAGGAATACTTCTCCAATAGTG AAGCCACAGATGTATTGGAGAAGTATTCCTTGCTGTTGCCTACTG CCTCGGA
Prdx2	-2.2032464	TGCTGTTGACAGTGAGCGCGTACGTGGTCCTCTTTTTCTATAGTG AAGCCACAGATGTATAGAAAAAGAGGACCACGTACTTGCCTACTG CCTCGGA

Psma1	4.29341392	TGCTGTTGACAGTGAGCGCTGACTGCAGAGCTATGTCTAATAGTG AAGCCACAGATGTATTAGACATAGCTCTGCAGTCAATGCCTACTG CCTCGGA
Psma1	-0.8136728	TGCTGTTGACAGTGAGCGCCCAGAAGAAAATTCTCCATGATAGTG AAGCCACAGATGTATCATGGAGAATTTTCTTCTGGTTGCCTACTGC CTCGGA
Psma1	1.02439581	TGCTGTTGACAGTGAGCGCGGTTCAGCAACAGTTGGTCTATAGTG AAGCCACAGATGTATAGACCAACTGTTGCTGAACCTTGCCTACTG CCTCGGA
Psma1	0.44238152	TGCTGTTGACAGTGAGCGACAGTATGACAATGATGTCACATAGTG AAGCCACAGATGTATGTGACATCATTGTCATACTGGTGCCTACTG CCTCGGA
Psma3	-4.5764966	TGCTGTTGACAGTGAGCGCTGCCGTGATGTAGTTAAAGAATAGTG AAGCCACAGATGTATTCTTTAACTACATCACGGCAATGCCTACTGC CTCGGA
Psma3	6.59013383	TGCTGTTGACAGTGAGCGCTGCCAAGGAATCTTTGAAGGATAGTG AAGCCACAGATGTATCCTTCAAAGATTCCTTGGCATTGCCTACTG CCTCGGA
Psma3	2.31651926	TGCTGTTGACAGTGAGCGCCGACCCATCAGGTGTTTCATATAGTG AAGCCACAGATGTATATGAAACACCTGATGGGTCGATGCCTACTG CCTCGGA
Psma6	-2.966707	TGCTGTTGACAGTGAGCGCGTCGATTGACTTCAAACCTTATAGTG AAGCCACAGATGTATAAGGTTTGAAGTCAATCGACATGCCTACTG CCTCGGA
Psma6	1.96907559	TGCTGTTGACAGTGAGCGATGCAATTACATGCCTGTCTAATAGTG AAGCCACAGATGTATTAGACAGGCATGTAATTGCAGTGCCTACTG CCTCGGA
Psma6	1.87138933	TGCTGTTGACAGTGAGCGCGGTTACTACTGTGGCTTTAAATAGTG AAGCCACAGATGTATTTAAAGCCACAGTAGTAACCTTGCCTACTG CCTCGGA
Psma6	-2.0963872	TGCTGTTGACAGTGAGCGATGCAAAAGAATTGCTGATATATAGTG AAGCCACAGATGTATATATCAGCAATTCTTTTGCACTGCCTACTGC CTCGGA
Psmb2	1.09904147	TGCTGTTGACAGTGAGCGCCGATCATGACAAGATGTTTAATAGTG AAGCCACAGATGTATTAAACATCTTGTCATGATCGTTGCCTACTGC CTCGGA
Psmb2	1.39872454	TGCTGTTGACAGTGAGCGCAGATGGCATCCACAATCTGGATAGTG AAGCCACAGATGTATCCAGATTGTGGATGCCATCTTTGCCTACTG CCTCGGA
Psmb2	0.50075376	TGCTGTTGACAGTGAGCGCCCGGGTCATTGACAAAGATGATAGTG AAGCCACAGATGTATCATCTTTGTCAATGACCCGGATGCCTACTG CCTCGGA
Psmb3	-2.468096	TGCTGTTGACAGTGAGCGCCCAGAACACCTGTTTGAAACATAGTG AAGCCACAGATGTATGTTTCAAACAGGTGTTCTGGATGCCTACTG CCTCGGA
Psmb3	1.53919772	TGCTGTTGACAGTGAGCGCCCCATGGTGACTGATGACTTATAGTG AAGCCACAGATGTATAAGTCATCAGTCACCATGGGATGCCTACTG CCTCGGA
Psmb3	0.90525278	TGCTGTTGACAGTGAGCGCCCACGTCATTGAGAAAGACAATAGTG AAGCCACAGATGTATTGTCTTTCTCAATGACGTGGATGCCTACTG CCTCGGA

Psmb3	1.97707377	TGCTGTTGACAGTGAGCGAAACACCTGTTTGAAACCATTATAGTG AAGCCACAGATGTATAATGGTTTCAAACAGGTGTTCTGCCTACTG CCTCGGA
Psmb6	-0.721415	TGCTGTTGACAGTGAGCGACAGCTTGGTTTCCACAGTATATAGTG AAGCCACAGATGTATATACTGTGGAAACCAAGCTGGTGCCTACTG CCTCGGA
Psmb6	-0.0076722	TGCTGTTGACAGTGAGCGATCCGGGAGCTCGTACATCTAATAGTG AAGCCACAGATGTATTAGATGTACGAGCTCCCGGAGTGCCTACTG CCTCGGA
Psmb6	1.71566506	TGCTGTTGACAGTGAGCGACAAATCCCCAAGTTCACCATATAGTG AAGCCACAGATGTATATGGTGAACTTGGGGATTTGGTGCCTACTG CCTCGGA
Ptma	-1.5038763	TGCTGTTGACAGTGAGCGAGCTGACAATGAGGTAGATGAATAGTG AAGCCACAGATGTATTCATCTACCTCATTGTCAGCCTGCCTACTG CCTCGGA
Ptma	0.49698375	TGCTGTTGACAGTGAGCGAGATGGAGATGAAGATGAGGAATAGT GAAGCCACAGATGTATTCCTCATCTTCATCTCCATCCTGCCTACTG CCTCGGA
Ptma	2.15187511	TGCTGTTGACAGTGAGCGCCACCACCAAGGACTTGAAGGATAGT GAAGCCACAGATGTATCCTTCAAGTCCTTGGTGGTGATGCCTACT GCCTCGGA
Ptma	-4.0559326	TGCTGTTGACAGTGAGCGCGAGGTAGATGAAGAAGAGGAATAGT GAAGCCACAGATGTATTCCTCTTCTTCATCTACCTCATGCCTACTG CCTCGGA
Ran	1.71349367	TGCTGTTGACAGTGAGCGCGGCAACAAAGTGGATATTAAATAGTG AAGCCACAGATGTATTTAATATCCACTTTGTTGCCATGCCTACTGC CTCGGA
Ran	5.1524293	TGCTGTTGACAGTGAGCGAGAAAGTGAAGGCAAAATCTAATAGTG AAGCCACAGATGTATTAGATTTTGCCTTCACTTTCCTGCCTACTGC CTCGGA
Ran	3.48423669	TGCTGTTGACAGTGAGCGATACTATGACATTTCTGCCAAATAGTG AAGCCACAGATGTATTTGGCAGAAATGTCATAGTACTGCCTACTG CCTCGGA
Ran	-0.3332933	TGCTGTTGACAGTGAGCGCACAGAGGACCCATCAAGTTCATAGTG AAGCCACAGATGTATGAACTTGATGGGTCCTCTGTTTGCCTACTG CCTCGGA
Ranbp1	6.10890999	TGCTGTTGACAGTGAGCGAAAGATGAAGAGGAACTTTTTATAGTG AAGCCACAGATGTATAAAAAGTTCCTCTTCATCTTCTGCCTACTGC CTCGGA
Ranbp1	0.05327708	TGCTGTTGACAGTGAGCGAAGATGTCAAGCTTCTGAAGCATAGTG AAGCCACAGATGTATGCTTCAGAAGCTTGACATCTCTGCCTACTG CCTCGGA
Ranbp1	1.11840807	TGCTGTTGACAGTGAGCGCCAAAAGTTCAAAACAAAGTTATAGTG AAGCCACAGATGTATAACTTTGTTTTGAACTTTTGTTGCCTACTGC CTCGGA
Romo1	0.72963012	TGCTGTTGACAGTGAGCGAGAAAACCATGATGCAGAGTGATAGTG AAGCCACAGATGTATCACTCTGCATCATGGTTTTCCTGCCTACTG CCTCGGA
Romo1	-1.0107462	TGCTGTTGACAGTGAGCGCTCGGCACCTTCTCCTGTCTCATAGTG AAGCCACAGATGTATGAGACAGGAGAAGGTGCCGAATGCCTACT GCCTCGGA

Romo1	1.90230415	TGCTGTTGACAGTGAGCGAGCACCTTCTCCTGTCTCAGGATAGTG AAGCCACAGATGTATCCTGAGACAGGAGAAGGTGCCTGCCTACT GCCTCGGA
Romo1	1.70014502	TGCTGTTGACAGTGAGCGAGCGTGAAGATGGGCTTCGTCATAGT GAAGCCACAGATGTATGACGAAGCCCATCTTCACGCGTGCCTACT GCCTCGGA
Rpl27	2.96218754	TGCTGTTGACAGTGAGCGCTGTCAACAAGGATGTGTTCAATAGTG AAGCCACAGATGTATTGAACACATCCTTGTTGACAATGCCTACTG CCTCGGA
Rpl27	4.00096139	TGCTGTTGACAGTGAGCGCCAGCTGCCATGGGCAAGAAGATAGT GAAGCCACAGATGTATCTTCTTGCCCATGGCAGCTGTTGCCTACT GCCTCGGA
Rpl27	2.04636081	TGCTGTTGACAGTGAGCGCCAGGGAAGAACAAATGGTTTATAGTG AAGCCACAGATGTATAAACCATTTGTTCTTCCCTGTTGCCTACTGC CTCGGA
Rpl27	5.46662338	TGCTGTTGACAGTGAGCGAGGAGGCCAAGGTCAAGTTTGATAGT GAAGCCACAGATGTATCAAACTTGACCTTGGCCTCCCTGCCTACT GCCTCGGA
Rpl35a	1.95381414	TGCTGTTGACAGTGAGCGACCCACGGAAACAGCGGTATGATAGT GAAGCCACAGATGTATCATACCGCTGTTTCCGTGGGCTGCCTACT GCCTCGGA
Rpl35a	0.87356397	TGCTGTTGACAGTGAGCGAAAGAGATGTGCTTATGTGTAATAGTG AAGCCACAGATGTATTACACATAAGCACATCTCTTGTGCCTACTGC CTCGGA
Rpl35a	2.25047672	TGCTGTTGACAGTGAGCGCCACGGCTCTTCTTAAAATTGATAGTG AAGCCACAGATGTATCAATTTTAAGAAGAGCCGTGTTGCCTACTG CCTCGGA
Rpl35a	-0.737347	TGCTGTTGACAGTGAGCGACACACGGCTCTTCTTAAAATATAGTG AAGCCACAGATGTATATTTTAAGAAGAGCCGTGTGCTGCCTACTG CCTCGGA
Rpl41	2.24072468	TGCTGTTGACAGTGAGCGCGCGCAAGAGAAGAAAGATGAATAGT GAAGCCACAGATGTATTCATCTTTCTTCTCTTGCGCTTGCCTACTG CCTCGGA
Rpl41	3.42663412	TGCTGTTGACAGTGAGCGACAAGAGAAGAAAGATGAGGCATAGT GAAGCCACAGATGTATGCCTCATCTTTCTTCTCTTGCTGCCTACTG CCTCGGA
Rpl41	-1.4640993	TGCTGTTGACAGTGAGCGCAGCGCAAGAGAAGAAAGATGATAGT GAAGCCACAGATGTATCATCTTTCTTCTCTTGCGCTTTGCCTACTG CCTCGGA
Rpl41	0.45908084	TGCTGTTGACAGTGAGCGAATGAGGCAGAGGTCCAAGTAATAGT GAAGCCACAGATGTATTACTTGGACCTCTGCCTCATCTGCCTACT GCCTCGGA
Rps27l	-1.8156778	TGCTGTTGACAGTGAGCGCTGCTACAAGATTACTACAGTATAGTG AAGCCACAGATGTATACTGTAGTAATCTTGTAGCAATGCCTACTGC CTCGGA
Rps27l	2.31747135	TGCTGTTGACAGTGAGCGCCAGAAGGCTGTTCATTTAGAATAGTG AAGCCACAGATGTATTCTAAATGAACAGCCTTCTGTTGCCTACTGC CTCGGA
Rps27l	-5.7119849	TGCTGTTGACAGTGAGCGAACAGACTGTGGTTCTTTGTGATAGTG AAGCCACAGATGTATCACAAAGAACCACAGTCTGTGTGCCTACTG CCTCGGA

Rps27l	0.97139139	TGCTGTTGACAGTGAGCGACCCCTGGCTAGAGATCTGTTATAGTG AAGCCACAGATGTATAACAGATCTCTAGCCAGGGGCTGCCTACTG CCTCGGA
Sdf2l1	-0.5935017	TGCTGTTGACAGTGAGCGCCACTGGTGAACAGTATGGTAATAGTG AAGCCACAGATGTATTACCATACTGTTCACCAGTGATGCCTACTG CCTCGGA
Sdf2l1	-0.3688154	TGCTGTTGACAGTGAGCGAACGGGTCACGATGAACTCTGATAGTG AAGCCACAGATGTATCAGAGTTCATCGTGACCCGTGTGCCTACTG CCTCGGA
Sdf2l1	-3.237029	TGCTGTTGACAGTGAGCGCGCACTCACACGACATCAAATATAGTG AAGCCACAGATGTATATTTGATGTCGTGTGAGTGCATGCCTACTG CCTCGGA
Sdf2l1	-3.5179226	TGCTGTTGACAGTGAGCGATGCACTCACACGACATCAAAATAGTG AAGCCACAGATGTATTTTGATGTCGTGTGAGTGCAGTGCCTACTG CCTCGGA
Sdhb	-4.2579603	TGCTGTTGACAGTGAGCGCGGTGTTGGATGCTTTAATCAATAGTG AAGCCACAGATGTATTGATTAAAGCATCCAACACCATGCCTACTG CCTCGGA
Sdhb	-0.0672393	TGCTGTTGACAGTGAGCGCTCTACGCACAATACAAATCCATAGTG AAGCCACAGATGTATGGATTTGTATTGTGCGTAGAATGCCTACTG CCTCGGA
Sdhb	2.6611224	TGCTGTTGACAGTGAGCGCACCTTCCGAAGATCTTGTAGATAGTG AAGCCACAGATGTATCTACAAGATCTTCGGAAGGTTTGCCTACTG CCTCGGA
Serpinb9	0.49941949	TGCTGTTGACAGTGAGCGCCATCAGGCACAACAAAGCAAATAGTG AAGCCACAGATGTATTTGCTTTGTTGTGCCTGATGATGCCTACTG CCTCGGA
Serpinb9	2.46074789	TGCTGTTGACAGTGAGCGATGGCAGGTTCTCATCTCCATATAGTG AAGCCACAGATGTATATGGAGATGAGAACCTGCCACTGCCTACTG CCTCGGA
Serpinb9	0.67780317	TGCTGTTGACAGTGAGCGCCACCAGAGTGTAGTGGAGATATAGT GAAGCCACAGATGTATATCTCCACTACACTCTGGTGATGCCTACT GCCTCGGA
Serpinb9	2.88853711	TGCTGTTGACAGTGAGCGCTGAATACTCTGTCTGAAGGAATAGTG AAGCCACAGATGTATTCCTTCAGACAGAGTATTCATTGCCTACTGC CTCGGA
Slc25a5	-0.6889147	TGCTGTTGACAGTGAGCGCGGACGCAAAGGAACTGATATATAGTG AAGCCACAGATGTATATATCAGTTCCTTTGCGTCCATGCCTACTGC CTCGGA
Slc25a5	-0.0189525	TGCTGTTGACAGTGAGCGACCAAGAATACTCACATCTTCATAGTG AAGCCACAGATGTATGAAGATGTGAGTATTCTTGGGTGCCTACTG CCTCGGA
Slc25a5	-1.1039085	TGCTGTTGACAGTGAGCGCTGCTCCCAGATCCCAAGAATATAGTG AAGCCACAGATGTATATTCTTGGGATCTGGGAGCATTGCCTACTG CCTCGGA
Slc25a5	2.8335667	TGCTGTTGACAGTGAGCGCGCTGCCTACTTTGGTATCTAATAGTG AAGCCACAGATGTATTAGATACCAAAGTAGGCAGCTTGCCTACTG CCTCGGA
Smarca2	-0.067567	TGCTGTTGACAGTGAGCGCACGAAGCAGATGAACGCCATATAGT GAAGCCACAGATGTATATGGCGTTCATCTGCTTCGTTTGCCTACT GCCTCGGA

Smarca2	-0.9306415	TGCTGTTGACAGTGAGCGCGAACGCCATCATTGATACTGATAGTG AAGCCACAGATGTATCAGTATCAATGATGGCGTTCATGCCTACTG CCTCGGA
Smc2	3.89450895	TGCTGTTGACAGTGAGCGCCATTCTCAATTCATTGTGGTATAGTG AAGCCACAGATGTATACCACAATGAATTGAGAATGTTGCCTACTG CCTCGGA
Smc2	1.52300403	TGCTGTTGACAGTGAGCGATGGAATCGAAATTCTGTGAAATAGTG AAGCCACAGATGTATTTCACAGAATTTCGATTCCAGTGCCTACTGC CTCGGA
Smc2	1.51585102	TGCTGTTGACAGTGAGCGCGAAGAGATTACTCCAACGATATAGTG AAGCCACAGATGTATATCGTTGGAGTAATCTCTTCTTGCCTACTGC CTCGGA
Smc2	-0.7681841	TGCTGTTGACAGTGAGCGAGCTGAGGATTCTAAAGCATTATAGTG AAGCCACAGATGTATAATGCTTTAGAATCCTCAGCCTGCCTACTG CCTCGGA
Snrpa1	1.37704074	TGCTGTTGACAGTGAGCGCGCACAGCTTGCAAAGGATATATAGTG AAGCCACAGATGTATATATCCTTTGCAAGCTGTGCATGCCTACTG CCTCGGA
Snrpa1	1.81093175	TGCTGTTGACAGTGAGCGATGCCACCTTAGACCAGTTTGATAGTG AAGCCACAGATGTATCAAACTGGTCTAAGGTGGCACTGCCTACTG CCTCGGA
Snrpa1	-1.38069	TGCTGTTGACAGTGAGCGCGCTATTGATTTTTCTGACAAATAGTGA AGCCACAGATGTATTTGTCAGAAAAATCAATAGCATGCCTACTGC CTCGGA
Snrpa1	4.61927738	TGCTGTTGACAGTGAGCGATCAGAGTACTGGACTTTCAGATAGTG AAGCCACAGATGTATCTGAAAGTCCAGTACTCTGACTGCCTACTG CCTCGGA
Snrpb2	-0.6863009	TGCTGTTGACAGTGAGCGCAAAGACCATGAAGATGAGGGATAGT GAAGCCACAGATGTATCCCTCATCTTCATGGTCTTTATGCCTACTG CCTCGGA
Snrpb2	-4.4345821	TGCTGTTGACAGTGAGCGCGAGGAGACAAATGAGATGATATAGTG AAGCCACAGATGTATATCATCTCATTTGTCTCCTCTTGCCTACTGC CTCGGA
Snrpb2	2.30510769	TGCTGTTGACAGTGAGCGCCCCTGATTATCCTCCAAATTATAGTG AAGCCACAGATGTATAATTTGGAGGATAATCAGGGATGCCTACTG CCTCGGA
Snrpb2	3.02812394	TGCTGTTGACAGTGAGCGCCAACATGAATGACAAAATTAATAGTG AAGCCACAGATGTATTAATTTTGTCATTCATGTTGTTGCCTACTGC CTCGGA
Snrpd1	0.14179661	TGCTGTTGACAGTGAGCGCCAAGTCCATGGAACAATCACATAGTG AAGCCACAGATGTATGTGATTGTTCCATGGACTTGTTGCCTACTG CCTCGGA
Snrpd1	-0.1313249	TGCTGTTGACAGTGAGCGCTGAACCTAAGGTGAAGTCTAATAGTG AAGCCACAGATGTATTAGACTTCACCTTAGGTTCAATGCCTACTGC CTCGGA
Snrpe	2.53251879	TGCTGTTGACAGTGAGCGAGCTGTATGAACAAGTGAATATTAGTG AAGCCACAGATGTAATATTCACTTGTTCATACAGCCTGCCTACTGC CTCGGA
Snrpe	2.64656377	TGCTGTTGACAGTGAGCGCTGCAGAAGAGATTCATTCTAATAGTG AAGCCACAGATGTATTAGAATGAATCTCTTCTGCATTGCCTACTGC CTCGGA

Snrpe	2.40713876	TGCTGTTGACAGTGAGCGCACTTGCAAAATAGATCTCGAATAGTG AAGCCACAGATGTATTCGAGATCTATTTTGCAAGTATGCCTACTGC CTCGGA
Snrpe	2.50057243	TGCTGTTGACAGTGAGCGAAAGAGATTCATTCTAAAACAATAGTG AAGCCACAGATGTATTGTTTTAGAATGAATCTCTTCTGCCTACTGC CTCGGA
Snrpg	1.70690747	TGCTGTTGACAGTGAGCGAGGCTTTGATCCCTTTATGAAATAGTG AAGCCACAGATGTATTTCATAAAGGGATCAAAGCCCTGCCTACTG CCTCGGA
Snrpg	1.88159656	TGCTGTTGACAGTGAGCGCTGGACAAGAAGTTATCATTGATAGTG AAGCCACAGATGTATCAATGATAACTTCTTGTCCATTGCCTACTGC CTCGGA
Snrpg	0.07104982	TGCTGTTGACAGTGAGCGCGAAGTTATCATTGAAGTTAAATAGTG AAGCCACAGATGTATTTAACTTCAATGATAACTTCTTGCCTACTGC CTCGGA
Snrpg	-2.7043904	TGCTGTTGACAGTGAGCGCTATGGACAAGAAGTTATCATATAGTG AAGCCACAGATGTATATGATAACTTCTTGTCCATAATGCCTACTGC CTCGGA
Sumo2	-2.9799289	TGCTGTTGACAGTGAGCGCCAACGATCATATTAATTTGAATAGTGA AGCCACAGATGTATTCAAATTAATATGATCGTTGTTGCCTACTGCC TCGGA
Sumo2	3.8470282	TGCTGTTGACAGTGAGCGCCACACCTGCACAGTTGGAAAATAGTG AAGCCACAGATGTATTTTCCAACTGTGCAGGTGTGTTGCCTACTG CCTCGGA
Sumo2	4.80485773	TGCTGTTGACAGTGAGCGAACTGAGAACAACGATCATATATAGTG AAGCCACAGATGTATATATGATCGTTGTTCTCAGTCTGCCTACTGC CTCGGA
Tbx21	4.8805556	TGCTGTTGACAGTGAGCGAGACCAACAGCATCGTTTCTTATAGTG AAGCCACAGATGTATAAGAAACGATGCTGTTGGTCCTGCCTACTG CCTCGGA
Tbx21	3.07095826	TGCTGTTGACAGTGAGCGACAACAGCATCGTTTCTTCTAATAGTG AAGCCACAGATGTATTAGAAGAAACGATGCTGTTGGTGCCTACTG CCTCGGA
Tbx21	3.6902638	TGCTGTTGACAGTGAGCGCCACACACGTCTTTACTTTCCATAGTG AAGCCACAGATGTATGGAAAGTAAAGACGTGTGTGTTGCCTACTG CCTCGGA
Tmem14c	-0.8261301	TGCTGTTGACAGTGAGCGCCAGGATCCCAGGAATGTGTGATAGT GAAGCCACAGATGTATCACACATTCCTGGGATCCTGATGCCTACT GCCTCGGA
Tmem14c	-1.0162635	TGCTGTTGACAGTGAGCGCTGCCTTTACATTATTTTGGTATAGTGA AGCCACAGATGTATACCAAAATAATGTAAAGGCATTGCCTACTGC CTCGGA
Tmem14c	4.86546401	TGCTGTTGACAGTGAGCGCCAGTGGCCCATTGATGCCTTATAGTG AAGCCACAGATGTATAAGGCATCAATGGGCCACTGTTGCCTACTG CCTCGGA
Tmem14c	7.48313377	TGCTGTTGACAGTGAGCGACCCATTGATGCCTTTACATTATAGTG AAGCCACAGATGTATAATGTAAAGGCATCAATGGGCTGCCTACTG CCTCGGA
Tmem167	1.91339443	TGCTGTTGACAGTGAGCGCCAGCATCCTCTTCATACAGTATAGTG AAGCCACAGATGTATACTGTATGAAGAGGATGCTGATGCCTACTG CCTCGGA

Tmem167	2.64309438	TGCTGTTGACAGTGAGCGCTGACTGTAATCTTGCTGCTTATAGTG AAGCCACAGATGTATAAGCAGCAAGATTACAGTCAATGCCTACTG CCTCGGA
Tmem167	2.03109063	TGCTGTTGACAGTGAGCGCCAGAGTCTGTTGACTGTAATATAGTG AAGCCACAGATGTATATTACAGTCAACAGACTCTGATGCCTACTG CCTCGGA
Tuba1b	-0.1470921	TGCTGTTGACAGTGAGCGCGAGGCCATCTATGACATCTGATAGTG AAGCCACAGATGTATCAGATGTCATAGATGGCCTCATGCCTACTG CCTCGGA
Tuba1b	3.66053219	TGCTGTTGACAGTGAGCGAGCCCAACCTACACCAACCTTATAGTG AAGCCACAGATGTATAAGGTTGGTGTAGGTTGGGCGTGCCTACTG CCTCGGA
Tuba1b	4.63618601	TGCTGTTGACAGTGAGCGATAGATCACAAGTTTGATCTGATAGTG AAGCCACAGATGTATCAGATCAAACTTGTGATCTAGTGCCTACTG CCTCGGA
Tuba1b	2.00020409	TGCTGTTGACAGTGAGCGACGTGGTGATGTGGTTCCCAAATAGTG AAGCCACAGATGTATTTGGGAACCACATCACCACGGTGCCTACTG CCTCGGA
Txn1	-1.0857713	TGCTGTTGACAGTGAGCGAAAGCTGATCGAGAGCAAGGAATAGT GAAGCCACAGATGTATTCCTTGCTCTCGATCAGCTTCTGCCTACT GCCTCGGA
Txn1	3.65253049	TGCTGTTGACAGTGAGCGCGCATGCCGACCTTCCAGTTTATAGTG AAGCCACAGATGTATAAACTGGAAGGTCGGCATGCATGCCTACTG CCTCGGA
Txn1	0.57821228	TGCTGTTGACAGTGAGCGCGACTGTGAAGTCAAATGCATATAGTG AAGCCACAGATGTATATGCATTTGACTTCACAGTCTTGCCTACTGC CTCGGA
Txn1	4.67766483	TGCTGTTGACAGTGAGCGCCGAGAGCAAGGAAGCTTTTCATAGTG AAGCCACAGATGTATGAAAAGCTTCCTTGCTCTCGATGCCTACTG CCTCGGA
Ubl4	-0.1314866	TGCTGTTGACAGTGAGCGACAGCAACGTCTGCTGTTCAAGTAGTG AAGCCACAGATGTACTTGAACAGCAGACGTTGCTGGTGCCTACTG CCTCGGA
Ubl4	-1.7476875	TGCTGTTGACAGTGAGCGAAAGGCCCTAGCAGATGAAAAATAGTG AAGCCACAGATGTATTTTTCATCTGCTAGGGCCTTGTGCCTACTG CCTCGGA
Ubl4	1.59453059	TGCTGTTGACAGTGAGCGCCGACTGTCAGATTACAACATATAGTG AAGCCACAGATGTATATGTTGTAATCTGACAGTCGTTGCCTACTG CCTCGGA
Ubl4	0.11036603	TGCTGTTGACAGTGAGCGACAGCCGCTTTCTACACCCTGATAGTG AAGCCACAGATGTATCAGGGTGTAGAAAGCGGCTGGTGCCTACT GCCTCGGA
Uchl3	-1.4925677	TGCTGTTGACAGTGAGCGATGGAACGATTGGACTAATCCATAGTG AAGCCACAGATGTATGGATTAGTCCAATCGTTCCACTGCCTACTG CCTCGGA
Uchl3	2.18033868	TGCTGTTGACAGTGAGCGCCCCTATCACAGAAAAGTATGATAGTG AAGCCACAGATGTATCATACTTTTCTGTGATAGGGATGCCTACTG CCTCGGA
Uchl3	-0.9814839	TGCTGTTGACAGTGAGCGCCAGACTGAGGCACCAAGTATATAGTG AAGCCACAGATGTATATACTTGGTGCCTCAGTCTGATGCCTACTG CCTCGGA

Uchl3	1.07922659	TGCTGTTGACAGTGAGCGATGACATCATCAGTATATTTTATAGTGA AGCCACAGATGTATAAAATATACTGATGATGTCACTGCCTACTGCC TCGGA
Uhrf1	0.90361251	TGCTGTTGACAGTGAGCGATGGGATGATGTGCTAACTTCATAGTG AAGCCACAGATGTATGAAGTTAGCACATCATCCCACTGCCTACTG CCTCGGA
Uhrf1	-0.9469433	TGCTGTTGACAGTGAGCGACAACTACAGAGACTCTTTTAATAGTG AAGCCACAGATGTATTAAAAGAGTCTCTGTAGTTGGTGCCTACTG CCTCGGA
Uhrf1	-2.5775821	TGCTGTTGACAGTGAGCGAAGTGGACATTGTCAAAGCCAATAGTG AAGCCACAGATGTATTGGCTTTGACAATGTCCACTCTGCCTACTG CCTCGGA
Uhrf1	0.94876364	TGCTGTTGACAGTGAGCGATGACCAGAAGCTCACTAATAATAGTG AAGCCACAGATGTATTATTAGTGAGCTTCTGGTCAGTGCCTACTG CCTCGGA
Uqcc2	1.13462104	TGCTGTTGACAGTGAGCGCAGAGTACAAGCTGATCCTGTATAGTG AAGCCACAGATGTATACAGGATCAGCTTGTACTCTTTGCCTACTG CCTCGGA
Uqcc2	3.68454044	TGCTGTTGACAGTGAGCGCGCACGACTGCATTCAAACTAATAGTG AAGCCACAGATGTATTAGTTTGAATGCAGTCGTGCTTGCCTACTG CCTCGGA
Uqcc2	2.09978931	TGCTGTTGACAGTGAGCGACACAGACACTTTGGAAGAGTTTAGTG AAGCCACAGATGTAAACTCTTCCAAAGTGTCTGTGGTGCCTACTG CCTCGGA
Uqcr10	1.69738163	TGCTGTTGACAGTGAGCGACCTGTTCTTCGAGCGAGCCTATAGTG AAGCCACAGATGTATAGGCTCGCTCGAAGAACAGGGTGCCTACT GCCTCGGA
Uqcr10	-4.5625763	TGCTGTTGACAGTGAGCGCACGAGGGGAAACTGTGGAAACTAGT GAAGCCACAGATGTAGTTTCCACAGTTTCCCCTCGTTTGCCTACT GCCTCGGA
Uqcr10	-3.3741896	TGCTGTTGACAGTGAGCGATTCCGCAGAACTTCCACCTTATAGTG AAGCCACAGATGTATAAGGTGGAAGTTCTGCGGAACTGCCTACTG CCTCGGA
Uqcr10	0.74744654	TGCTGTTGACAGTGAGCGAGCGCCTGTACTCCTTGCTGTATAGTG AAGCCACAGATGTATACAGCAAGGAGTACAGGCGCGTGCCTACT GCCTCGGA
Uqcrq	1.43738453	TGCTGTTGACAGTGAGCGACCTTCCCAAGCTATTTCAGCATAGTG AAGCCACAGATGTATGCTGAAATAGCTTGGGAAGGCTGCCTACTG CCTCGGA
Uqcrq	-0.2466305	TGCTGTTGACAGTGAGCGCGGAGTTTGAGCAGTCGAAAAATAGTG AAGCCACAGATGTATTTTTCGACTGCTCAAACTCCTTGCCTACTGC CTCGGA
Uqcrq	2.92554664	TGCTGTTGACAGTGAGCGATGATCTCCTACAGCTTGTCGATAGTG AAGCCACAGATGTATCGACAAGCTGTAGGAGATCACTGCCTACTG CCTCGGA
Uqcrq	4.41219118	TGCTGTTGACAGTGAGCGACAGCCATGTATGAAAATGACATAGTG AAGCCACAGATGTATGTCATTTTCATACATGGCTGGTGCCTACTG CCTCGGA
Usp50	-1.6978395	TGCTGTTGACAGTGAGCGCCAGCCTATCTTCTGTTCTATATAGTG AAGCCACAGATGTATATAGAACAGAAGATAGGCTGTTGCCTACTG CCTCGGA

Usp50	0.21844611	TGCTGTTGACAGTGAGCGACGAAGAAGAGTGAATGAGAAATAGTG AAGCCACAGATGTATTTCTCATTCACTCTTCTTCGGTGCCTACTGC CTCGGA
Usp50	1.08937032	TGCTGTTGACAGTGAGCGCCAGTTACAGCATCACATGTTATAGTG AAGCCACAGATGTATAACATGTGATGCTGTAACTGATGCCTACTG CCTCGGA
Ybx1	4.3765135	TGCTGTTGACAGTGAGCGACAGCAGACCGTAACCATTATATAGTG AAGCCACAGATGTATATAATGGTTACGGTCTGCTGCTGCCTACTG CCTCGGA
Ybx1	2.05738686	TGCTGTTGACAGTGAGCGCACAGTCAAATGGTTCAATGTATAGTG AAGCCACAGATGTATACATTGAACCATTTGACTGTTTGCCTACTGC CTCGGA
Ybx1	1.97592911	TGCTGTTGACAGTGAGCGACCCAGAGAACCCTAAACCACATAGTG AAGCCACAGATGTATGTGGTTTAGGGTTCTCTGGGCTGCCTACTG CCTCGGA
Ybx1	2.41126099	TGCTGTTGACAGTGAGCGAGAGTTTGATGTTGTTGAAGGATAGTG AAGCCACAGATGTATCCTTCAACAACATCAAACTCCTGCCTACTG CCTCGGA
Zscan2	-2.1397561	TGCTGTTGACAGTGAGCGAGAGAACTCAAATGAAGACATATAGTG AAGCCACAGATGTATATGTCTTCATTTGAGTTCTCCTGCCTACTGC CTCGGA
Zscan2	-0.3804486	TGCTGTTGACAGTGAGCGAGTACCTCAAGAAGAAGATGAATAGTG AAGCCACAGATGTATTCATCTTCTTCTTGAGGTACCTGCCTACTGC CTCGGA
Zscan2	-8.0167501	TGCTGTTGACAGTGAGCGAACATGGGATGTTCTTGAACAATAGTG AAGCCACAGATGTATTGTTCAAGAACATCCCATGTGTGCCTACTG CCTCGGA
Zscan2	3.79698575	TGCTGTTGACAGTGAGCGCCAGCTCCAACTTCATCACACATAGTG AAGCCACAGATGTATGTGTGATGAAGTTGGAGCTGTTGCCTACTG CCTCGGA

REFERENCES

1. Arun, G., S.D. Diermeier, D.L. Spector, A. Zhang, M. Xu, Y. Mo, N. Amodio, L. Raimondi, G. Juli, M.A. Stamato, D. Caracciolo, P. Tagliaferri, P. Tassone, J. Xiang, S. Guo, S. Jiang, Y. Xu, J. Li, Q. Sun, Q. Hao, K. V. Prasanth, X. Zhang, M.H. Hamblin, and K.J. Yin. 2018. Nuclear Long Noncoding RNAs: Key Regulators of Gene Expression. *Trends in Molecular Medicine*. 24:1–19.

2. Banerjee, A., S.M. Gordon, A.M. Intlekofer, M.A. Paley, E.C. Mooney, T. Lindsten, E.J. Wherry, and S.L. Reiner. 2010. Cutting Edge: The Transcription Factor Eomesodermin Enables CD8+ T Cells To Compete for the Memory Cell Niche. *The Journal of Immunology*. 185:4988–4992.

3. Bernard, D., K. V. Prasanth, V. Tripathi, S. Colasse, T. Nakamura, Z. Xuan, M.Q. Zhang, F. Sedel, L. Jourdren, F. Coulpier, A. Triller, D.L. Spector, and A. Bessis. 2010. A long nuclear-retained non-coding RNA regulates synaptogenesis by modulating gene expression. *EMBO Journal*. 29:3082–3093.

4. Boland, B.S., Z. He, M.S. Tsai, J.G. Olvera, K.D. Omilusik, H.G. Duong, E.S. Kim, A.E. Limary, W. Jin, J. Justin Milner, B. Yu, S.A. Patel, T.L. Louis, T. Tysl, N.S. Kurd, A. Bortnick, L.K. Quezada, J.N. Kanbar, A. Miralles, D. Huylebroeck, M.A. Valasek, P.S. Dulai, S. Singh, L.F. Lu, J.D. Bui, C. Murre, W.J. Sandborn, A.W. Goldrath, G.W. Yeo, and J.T. Chang. 2020. Heterogeneity and clonal relationships of adaptive immune cells in ulcerative colitis revealed by single-cell analyses. *Science Immunology*. 5.

5. Chen, R., S. Bélanger, M.A. Frederick, B. Li, R.J. Johnston, N. Xiao, Y.C. Liu, S. Sharma, B. Peters, A. Rao, S. Crotty, and M.E. Pipkin. 2014. In vivo RNA interference screens identify regulators of antiviral CD4+ and CD8+ T cell differentiation. *Immunity*. 41:325–338.

6. Eisenberg, E., and E.Y. Levanon. 2013. Human housekeeping genes, revisited. *Trends in Genetics*. 29:569–574.

7. Eißmann, M., T. Gutschner, M. Hämmerle, S. Günther, M. Caudron-herger, M. Groß, K. Rippe, T. Braun, M. Zörnig, and S. Diederichs. 2012. Loss of the abundant nuclear non-coding RNA MALAT1 is compatible with life and development. *RNA Biology*. 9:1076–1087.

8. El-Brolosy, M.A., and D.Y.R. Stainier. 2017. Genetic compensation: A phenomenon in search of mechanisms. *PLoS Genetics*. 13:1–17.

9. Gomez, J.A., O.L. Wapinski, Y.W. Yang, J.F. Bureau, S. Gopinath, D.M. Monack, H.Y. Chang, M. Brahic, and K. Kirkegaard. 2013. The NeST long ncRNA controls microbial susceptibility and epigenetic activation of the interferon-γ locus. *Cell*. 152:743–754.

10. Gray, S.M., R.A. Amezquita, T. Guan, S.H. Kleinstein, S.M. Kaech, S.M. Gray, R.A. Amezquita, T. Guan, S.H. Kleinstein, and S.M. Kaech. 2017. Polycomb Repressive Complex 2-Mediated Chromatin Repression Guides Effector CD8 + T Cell Terminal Differentiation and Loss of Multipotency Article Polycomb Repressive Complex 2-Mediated Chromatin Repression Guides Effector CD8 + T Cell Terminal Differenti. *Immunity*. 46:596–608.

11. Gutschner, T., M. Hämmerle, and S. Diederichs. 2013a. MALAT1 — a paradigm for long noncoding RNA function in cancer. *J Mol Med*. 91:791–801.

12. Gutschner, T., M. Hämmerle, M. Eißmann, J. Hsu, Y. Kim, G. Hung, A. Revenko, G. Arun, M. Stentrup, M. Groß, M. Zörnig, A.R. MacLeod, D.L. Spector, and S. Diederichs. 2013b. The noncoding RNA MALAT1 is a critical regulator of the metastasis phenotype of lung cancer cells. *Cancer Research*. 73:1180–1189.

13. Hadjicharalambous, M.R., and M.A. Lindsay. 2019. Long non-coding RNAs and the innate immune response. *Non-coding RNA*. 5.

14. Herndler-Brandstetter, D., H. Ishigame, R. Shinnakasu, V. Plajer, C. Stecher, J. Zhao, M. Lietzenmayer, L. Kroehling, A. Takumi, K. Kometani, T. Inoue, Y. Kluger, S.M. Kaech, T. Kurosaki, T. Okada, and R.A. Flavell. 2018. KLRG1+Effector CD8+T Cells Lose KLRG1, Differentiate into All Memory T Cell Lineages, and Convey Enhanced Protective Immunity. *Immunity*. 48:716-729.

15. Hudson, W.H., N. Prokhnevska, J. Gensheimer, R. Akondy, D.J. McGuire, R. Ahmed, and H.T. Kissick. 2019a. Expression of novel long noncoding RNAs defines virus-specific effector and memory CD8 + T cells. *Nature Communications*. 10:1–11.

16. Ji, P., S. Diederichs, W. Wang, S. Bo, R. Metzger, M. Paul, N. Tidow, B. Brandt, H. Buerger, E. Bulk, M. Thomas, W.E. Berdel, H. Serve, and C. Mu. 2003. MALAT-1, a novel noncoding RNA , and thymosin b 4 predict metastasis and survival in early-stage non-small cell lung cancer. *Oncogene*. 22:8031–804.

17. Ji, Y., Z. Pos, M. Rao, C.A. Klebanoff, Z. Yu, M. Sukumar, R.N. Reger, D.C. Palmer, Z.A. Borman, P. Muranski, E. Wang, D.S. Schrump, F.M. Marincola, N.P. Restifo, and L. Gattinoni. 2011. Repression of the DNA-binding inhibitor Id3 by Blimp-1 limits the formation of memory CD8 + T cells. *Nature Immunology*. 12:1230–1237.

18. Joshi, N.S., W. Cui, A. Chandele, H.K. Lee, D.R. Urso, J. Hagman, L. Gapin, and S.M. Kaech. 2007a. Inflammation Directs Memory Precursor and Short-Lived Effector CD8+ T Cell Fates via the Graded Expression of T-bet Transcription Factor. *Immunity*. 27:281–295.

19. Kaech, S.M., and E.J. Wherry. 2007. Heterogeneity and Cell-Fate Decisions in Effector and Memory CD8 + T Cell Differentiation during Viral Infection. 393–405.

20. Kakaradov, B., J. Arsenio, C.E. Widjaja, Z. He, S. Aigner, P.J. Metz, B. Yu, E.J. Wehrens, J. Lopez, S.H. Kim, E.I. Zuniga, A.W. Goldrath, J.T. Chang, and G.W. Yeo. 2017. Early transcriptional and epigenetic regulation of CD8 + T cell differentiation revealed by single-cell RNA sequencing. *Nature Immunology*. 18:422–432.

21. Kallies, A., A. Xin, G.T. Belz, and S.L. Nutt. 2009. Blimp-1 Transcription Factor Is Required for the Differentiation of Effector CD8+ T Cells and Memory Responses. *Immunity*. 31:283–295.

22. Kim, J., H.L. Piao, B.J. Kim, F. Yao, Z. Han, Y. Wang, Z. Xiao, A.N. Siverly, S.E. Lawhon, B.N. Ton, H. Lee, Z. Zhou, B. Gan, S. Nakagawa, M.J. Ellis, H. Liang, M.C. Hung, M.J. You, Y. Sun, and L. Ma. 2018. Long noncoding RNA MALAT1 suppresses breast cancer metastasis. *Nature Genetics*. 50:1705–1715.

23. Klebanoff, C.A., L. Gattinoni, P. Torabi-Parizi, K. Kerstann, A.R. Cardones, S.E. Finkelstein, D.C. Palmer, P.A. Antony, S.T. Hwang, S.A. Rosenberg, T.A. Waldmann, and N.P. Restifo. 2005. Central memory self/tumor-reactive CD8+ T cells confer superior antitumor immunity compared with effector memory T cells. *Proceedings of the National Academy of Sciences of the United States of America*. 102:9571–9576.

24. Kopp, F., and J.T. Mendell. 2018. Functional Classification and Experimental Dissection of Long Noncoding RNAs. *Cell*. 172:393–407.

25. Kotzin, J.J., F. Iseka, J. Wright, M.G. Basavappa, M.L. Clark, M.A. Ali, M.S. Abdel-Hakeem, T.F. Robertson, W.K. Mowel, L. Joannas, V.D. Neal, S.P. Spencer, C.M. Syrett, M.C. Anguera, A. Williams, E.J. Wherry, and J. Henao-Mejia. 2019. The long noncoding RNA Morrbid regulates CD8 T cells in response to viral infection. *Proceedings of the National Academy of Sciences of the United States of America*. 116:11916–11925.

26. Kurd, N.S., Z. He, T.L. Louis, J.J. Milner, K.D. Omilusik, W. Jin, M.S. Tsai, C.E. Widjaja, J.N. Kanbar, J.G. Olvera, T. Tysl, L.K. Quezada, B.S. Boland, W.J. Huang, C. Murre, A.W. Goldrath, G.W. Yeo, and J.T. Chang. 2020. Early precursors and molecular determinants of tissue-resident memory CD8+ T lymphocytes revealed by single-cell RNA sequencing. *Science Immunology*. 5:16–19.

27. Li, X., B. Zhou, L. Chen, L.T. Gou, H. Li, and X.D. Fu. 2017. GRID-seq reveals the global RNA-chromatin interactome. *Nature Biotechnology*. 35:940–950.

28. Lio, C.W.J., and A. Rao. 2019. TET enzymes and 5hMC in adaptive and innate immune systems. *Frontiers in Immunology*. 10:1–13.

29. Mao, Y.S., B. Zhang, and D.L. Spector. 2011. Biogenesis and function of nuclear bodies. *Trends in Genetics*. 27:295–306.

30. Michelini, R.H., A.L. Doedens, A.W. Goldrath, and S.M. Hedrick. 2013. Differentiation of CD8 memory T cells depends on Foxo1. *Journal of Experimental Medicine*. 210:1189–1200.

31. Milner, J.J., H. Nguyen, K. Omilusik, M. Reina-Campos, M. Tsai, C. Toma, A. Delpoux, B.S. Boland, S.M. Hedrick, J.T. Chang, and A.W. Goldrath. 2020. Delineation of a molecularly distinct terminally differentiated memory CD8 T cell population. *Proceedings of the National Academy of Sciences of the United States of America*. 117:25667–25678.

32. Milner, J.J., C. Toma, B. Yu, K. Zhang, K. Omilusik, A.T. Phan, D. Wang, A.J. Getzler, T. Nguyen, S. Crotty, W. Wang, M.E. Pipkin, and A.W. Goldrath. 2017. Runx3 programs CD8+ T cell residency in non-lymphoid tissues and tumours. *Nature*. 552:253–257.

33. Morrison, T.A., W.H. Hudson, D.A. Chisolm, Y. Kanno, H.-Y. Shih, R. Ahmed, J. Henao-Mejia, M. Hafner, and J.J. O'Shea. 2021. Evolving Views of Long Noncoding RNAs and Epigenomic Control of Lymphocyte State and Memory. *Cold Spring Harbor Perspectives in Biology*. a037952.

34. Mueller, S.N., and L.K. Mackay. 2015. Tissue-resident memory T cells: local specialists in immune defence. *Nature Reviews Immunology*. 16:79–89.

35. Mulligan, G.J., J. Wong, and T. Jacks. 1998. p130 Is Dispensable in Peripheral T Lymphocytes: Evidence for Functional Compensation by p107 and pRB. *Molecular and Cellular Biology*. 18:206–220.

36. Nakagawa, S., J.Y. Ip, G.O. Shioi, V. Tripathi, X. Zong, T. Hirose, and K. V Prasanth. 2012. Malat1 is not an essential component of nuclear speckles in mice. *RNA*. 8:1487-1499.

37. Nolz, J.C., and J.T. Harty. 2011. Protective Capacity of Memory CD8+ T Cells Is Dictated by Antigen Exposure History and Nature of the Infection. *Immunity*. 34:781–793.

38. Omilusik, K.D., J. Adam Best, B. Yu, S. Goossens, A. Weidemann, J. V. Nguyen, E. Seuntjens, A. Stryjewska, C. Zweier, R. Roychoudhuri, L. Gattinoni, L.M. Bird, Y. Higashi, H. Kondoh, D. Huylebroeck, J. Haigh, and A.W. Goldrath. 2015. Transcriptional repressor ZEB2 promotes terminal differentiation of CD8+ effector and memory T cell populations during infection. *Journal of Experimental Medicine*. 212:2027–2039.

39. Omilusik, K.D., M.S. Nadjsombati, L.A. Shaw, B. Yu, J.J. Milner, and A.W. Goldrath. 2018. Sustained Id2 regulation of E proteins is required for terminal differentiation of effector CD8+ T cells. *The Journal of Experimental Medicine*. 215:773–783.

40. Plasek, L.M., and S. Valadkhan. 2021. lncRNAs in T lymphocytes: RNA regulation at the heart of the immune response. *American Journal of Physiology - Cell Physiology*. 320:C415–C427.

41. Quinodoz, S.A., N. Ollikainen, B. Tabak, A. Palla, J.M. Schmidt, E. Detmar, M.M. Lai, A.A. Shishkin, P. Bhat, Y. Takei, V. Trinh, E. Aznauryan, P. Russell, C. Cheng, M. Jovanovic, A. Chow, L. Cai, P. McDonel, M. Garber, and M. Guttman. 2018. Higher-Order Inter-chromosomal Hubs Shape 3D Genome Organization in the Nucleus. *Cell*. 174:744-757.

42. Ranzani, V., G. Rossetti, I. Panzeri, A. Arrigoni, R.J.P. Bonnal, S. Curti, P. Gruarin, E. Provasi, E. Sugliano, M. Marconi, R. de Francesco, J. Geginat, B. Bodega, S. Abrignani, and M. Pagani. 2015. The long intergenic noncoding RNA landscape of human lymphocytes highlights the regulation of T cell differentiation by linc-MAF-4. *Nature Immunology*. 16:318–325.

43. Renkema, K.R., M.A. Huggins, H. Borges da Silva, T.P. Knutson, C.M. Henzler, and S.E. Hamilton. 2020a. KLRG1 + Memory CD8 T Cells Combine Properties of Short-Lived Effectors and Long-Lived Memory . *The Journal of Immunology*. 205:1059–1069.

44. Rinn, J.L., H.Y. Chang, and H.Y. Chang. 2020. Long Noncoding RNAs: Molecular Modalities to Organismal Functions. *Annual Review of Biochemistry*. 89:283–308.

45. Sharma, S., G.M. Findlay, H.S. Bandukwala, S. Oberdoerffer, B. Baust, Z. Li, V. Schmidt, P.G. Hogan, D.B. Sacks, and A. Rao. 2011. Dephosphorylation of the nuclear factor of activated T cells (NFAT) transcription factor is regulated by an RNA-protein scaffold complex. *Proceedings of the National Academy of Sciences of the United States of America*. 108:17235.

46. Spector, D.L., and A.I. Lamond. 2011. Nuclear Speckles. *Cold Spring Harb Perspect Biol*. 1–13.

47. Tano, K., R. Mizuno, T. Okada, R. Rakwal, J. Shibato, Y. Masuo, K. Ijiri, and N. Akimitsu. 2010. MALAT-1 enhances cell motility of lung adenocarcinoma cells by influencing the expression of motility-related genes. *FEBS Letters*. 584:4575–4580.

48. Tripathi, V., J.D. Ellis, Z. Shen, D.Y. Song, Q. Pan, A.T. Watt, S.M. Freier, C.F. Bennett, A. Sharma, P.A. Bubulya, B.J. Blencowe, S.G. Prasanth, and K. V. Prasanth. 2010. The nuclear-retained noncoding RNA MALAT1 regulates alternative splicing by modulating SR splicing factor phosphorylation. *Molecular Cell*. 39:925–938.

49. Tsagaratou, A., E. González-Avalos, S. Rautio, J.P. Scott-Browne, S. Togher, W.A. Pastor, E. V. Rothenberg, L. Chavez, H. Lähdesmäki, and A. Rao. 2017. TET proteins regulate the lineage specification and TCR-mediated expansion of iNKT cells. *Nature Immunology*. 18:45–53.

50. Wang, Y., H. Zhong, X. Xie, C.Y. Chen, D. Huang, L. Shen, H. Zhang, Z.W. Chen, and G. Zeng. 2015. Long noncoding RNA derived from CD244 signaling epigenetically controls CD8+ T-cell immune responses in tuberculosis infection. *Proceedings of the National Academy of Sciences of the United States of America*. 112:E3883–E3892.

51. West, J.A., C.P. Davis, H. Sunwoo, M.D. Simon, R.I. Sadreyev, P.I. Wang, M.Y. Tolstorukov, and R.E. Kingston. 2014. The Long Noncoding RNAs NEAT1 and MALAT1 Bind Active Chromatin Sites. *Molecular Cell*. 55:791–802.

52. Wilusz, J.E., H. Sunwoo, and D.L. Spector. 2009. Long noncoding RNAs: Functional surprises from the RNA world. *Genes and Development*. 23:1494–1504.

53. Yao, Y., W. Guo, J. Chen, P. Guo, G. Yu, J. Liu, F. Wang, J. Liu, M. You, T. Zhao, Y. Kang, X. Ma, and S. Yu. 2018. Long noncoding RNA Malat1 is not essential for T cell development and response to LCMV infection. *RNA Biology*. 15:1477–1486.

54. Youngblood, B., J.S. Hale, H.T. Kissick, E. Ahn, X. Xu, A. Wieland, K. Araki, E.E. West, H.E. Ghoneim, Y. Fan, P. Dogra, C.W. Davis, B.T. Konieczny, R. Antia, X. Cheng, and R. Ahmed. 2017. Effector CD8 T cells dedifferentiate into long-lived memory cells. *Nature*. 552:404–409.

55. Yu, B., K. Zhang, J.J. Milner, C. Toma, R. Chen, J.P. Scott-Browne, R.M. Pereira, S. Crotty, J.T. Chang, M.E. Pipkin, W. Wang, and A.W. Goldrath. 2017. Epigenetic landscapes reveal transcription factors that regulate CD8+ T cell differentiation. *Nature Immunology*. 18:573–582.

56. Zhang, B., G. Arun, Y.S. Mao, Z. Lazar, G. Hung, G. Bhattacharjee, X. Xiao, C.J. Booth, J. Wu, C. Zhang, and D.L. Spector. 2012. The lncRNA malat1 is dispensable for mouse development but its transcription plays a cis-regulatory role in the adult. *Cell Reports*. 2:111–123.

57. Zhou, B., X. Li, D. Luo, D.H. Lim, Y. Zhou, and X.D. Fu. 2019. GRID-seq for comprehensive analysis of global RNA–chromatin interactions. *Nature Protocols*. 14:2036–2068.

58. Zhou, X., and H.-H. Xue. 2012. Cutting Edge: Generation of Memory Precursors and Functional Memory CD8+ T Cells Depends on T Cell Factor-1 and Lymphoid Enhancer-Binding Factor-1. *The Journal of Immunology*. 189:2722–2726.